Multi-body Simulation of Cervical Traction Therapy

WONG KIN FUNG LAWRENCE

(Degree)
博士（工学）

(Date of Degree)
2019-03-25

(Date of Publication)
2020-03-01

(Resource Type)
doctoral thesis

(Report Number)
甲第7518号

(URL)
https://hdl.handle.net/20.500.14094/D1007518

Doctoral Dissertation

Multi-body Simulation of Cervical Traction Therapy

頸椎牽引療法のマルチボディシミュレーション

Wong Kin Fung Lawrence

January 2019

Graduate School of System Informatics

Kobe University

Abstract

Cervical traction therapy has been widely employed in clinical situations and rehabilitation as a non-surgical treatment for the cervical spine. The basic principle of cervical traction therapy is to apply pulling force to the cervical spine at various angles away from the body. However, due to the complex structure of the cervical spine and the traction parameters, such as traction force, angle and position, involved in the treatment, the mechanism of cervical traction therapy has not been fully understood. Traction force and angle refer to the magnitude and the direction of the pulling force. Traction position refers to the posture of the subject during cervical traction, and it is one of the important mechanical factors (Harris 1977) that influence the result of the therapy. For instance, the sitting position is a common position used in the therapy. In this position, the subject is seated upright on a chair during traction. The inclined position is a new position proposed to improve therapy result, and the subject is seated on a motorized chair that rotates along the sagittal plane to control the traction angle. The motivation of this research is to evaluate the differences between the sitting and inclined positions, especially in their abilities to achieve separations at specific part of the cervical spine. We developed a multi-body simulation model that includes the cervical spine and two cervical traction devices which represent these two positions. By using the model, our objective is to compare the resulting intervertebral separations achieved by the two positions when different amount of traction force and traction angle are used. In order to achieve this objective, we performed the following three studies.

Firstly, a multi-body simulation model, namely Model 1, which includes the cervical spine and two traction devices was developed using a physics engine. In the cervical spine part of the model, each intervertebral vertebra was modeled as a rigid body. The intervertebral disc between two adjacent intervertebral vertebrae was modeled by a pair of translational and rotational joints using springs and dampers. The mechanical parameters, such as the range of motion, stiffness and damping coefficients, used to simulate the behavior of the cervical spine were referenced from published literatures (Jager 1996, Horst 2002, Lopik 2007). Model 1 was used to evaluate the inclined position and sitting position on how they affect the intervertebral separations during cervical

traction therapy. Traction forces ranged from 60N to 200N and traction angles at 10/20/30/40° were tested. The result showed that the movement of the cervical spine during traction was smaller using the inclined position, thus can potentially lead to more stable traction. Also, it was found that the inclined position created greater intervertebral separations than the sitting position in all four traction angles under the same amount of traction force.

Secondly, in order to validate the behaviour of Model 1, laboratory experiment was conducted to acquire radiographic images of the cervical spine from subjects receiving cervical traction in the inclined and sitting positions. Six male subjects were recruited for the experiment. Traction forces from 100N to 160N and traction angles at 10/20/30/40° were used. The result of the experiment showed that the movement of the cervical spine during traction was smaller in the inclined position. For the three subjects who received cervical traction in both positions, the inclined position was able to achieve greater separations than the sitting position in all four traction angles. Both findings agreed with the simulation result from the first study. The amount of change in posterior separations in response to traction angles was also examined. In the experimental result of the inclined position, we observed that increase in traction angle leads to larger posterior separations. The result of the sitting position showed similar but less consistent behavior. The experiment data suggested that using traction angle to control the amount of posterior separations becomes less reliable with the sitting position. In order to evaluate the behavior of Model 1, simulation result was re-generated based on the experiment setup conditions. The simulation result showed that the behavior of Model 1 was different from the ones in the experiment. While the posterior separations in the experiment increased with traction angles, posterior separations in Model 1 decreased with traction angles. In an attempt to modify the model to match with the experiment data, biomechanical parameters including the range of motion, stiffness and damping coefficients in the model were modified. Although the modified model was able to match the behavior of the experiment result, the values of the parameters did not match with the ones reported by the reference literatures. As a result, it indicated that Model 1 was insufficient to accurately simulate the behavior of the cervical spine during cervical traction therapy.

Finally, due to the difference between the behavior of Model 1 and the experiment result, Model 2 was developed. Anterior and posterior horizontal shear movement of the intervertebral discs were added to the model. Instead of using a single translational joint to represent the vertical movement of the discs, two translational joints were used to represent the anterior and posterior vertical movement separately, with the posterior vertical movement representing the resistance force of the posterior ligaments. The simulation result of Model 2 showed that the movement of the cervical spine is smaller in the inclined position. This result agreed with the experiment that the inclined position can achieve more stable traction than the sitting position. Also, the behavior of Model 2 was shown to match the overall behavior of the experiment result such that an increase in the traction angles leads to larger posterior separations. Next, the posterior separations in the upper and lower spine were compared between the two positions. In the experiment result of the inclined position, it was found that increase in traction angle leads to larger posterior separation only in the lower spine. The amount of posterior separations in the upper spine remains similar regardless of traction angle. This shows that when cervical traction is conducted in the inclined position, traction angle can be used to control the amount of posterior separations distributed between the upper and lower spine. On the other hand, such behavior was not observed in the sitting position. The behavior of the upper and lower spine in Model 1 and Model 2 were compared against the experiment result. While Model 1, even with the modified parameters, failed to match the behaviour, Model 2 was shown to match the behaviour of the upper and lower spine in the experiment.

Using Model 2, the behavior of cervical spine in relation to body parameter such as hip joint stiffness and the stiffness level at each cervical segment was investigated. By varying the stiffness parameters in the anterior/posterior shear, flexion/extension, and tension/compression, we found that the tension/compression stiffness parameter affects the resulting separations the most. The result also showed that the resulting separation of sitting position was more sensitive to variation in hip joint stiffness than the one of inclined position. The sitting position tends to cause the subject to lose balance during traction, thus leading to undesired changes at large traction angles. In contrast, for inclined position, the resulting separation was less sensitive to variations in hip joint

stiffness and the stiffness level at each cervical segment. This finding may help to explain the consistent results among subjects who used inclined traction in the experiment.

In summary, the study compared the inclined and sitting positions using two multi-body simulation models and data from a radiographic experiment. The inclined position was found to be able to achieve greater separations than sitting position. The movement of the cervical spine was smaller in the inclined position, making the traction process more stable. The result also suggested that traction angle could be used to influence the amount of intervertebral separations and such behavior was more consistent in the inclined position. In particular, with the inclined position, traction angle could be used to influence the amount of posterior separations in the lower spine, while keeping the separations constant in the upper spine. The study also investigated the inconsistent nature of the sitting position. Using the simulation model, the sitting position was shown to be more susceptible to variations in the subject's hip joint stiffness.

Future work of this study should focus on gathering more clinical data in the inclined and sitting positions. It would be important to capture radiographic videos of the cervical spine during traction to measure the transformation of each intervertebral discs, since such data will be necessary to validate the timing responses of our simulation model. The effects of body parameters, gender and age of cervical traction patients should be further investigated. By collecting more clinical data regarding the patients, the simulation model can be improved to estimate the intervertebral separations based on patient-specific data. It will help to identify the necessary traction parameters to achieve customized traction. We believe the present model can help clarify the mechanism of inclined and sitting traction positions, and to promote further research in studying the cervical traction technique.

Table of Contents

Chapter 1.
Introduction

Cervical traction therapy, also known as non-surgical spinal decompression therapy, is a common physical therapy used to retreat cervical spine related disorders and injuries. In recent years, cervical traction therapy has gained interest from researchers to study its mechanism, especially the relationship among the traction parameters, including the traction force, angle, position, and the resulting intervertebral separations. This section provides an overview of the cervical traction therapy and previously published cervical traction studies. A review of cervical spine simulation models is described in Section 1.2. The objectives of the study are described in Section 1.3. The outline of dissertation is presented in Section 1.4.

1.1 Cervical Traction Therapy

Cervical traction therapy has been widely employed in nonsurgical therapies and rehabilitation in treating herniated discs and other injuries at the cervical spine. The basic principle of cervical traction therapy is to apply pulling force to the cervical spine at various angles away from the body. In principle, the technique can produce a number of physiological effects. Since traction creates decompression at the spinal area, it can help to release pressure on compressed nerves, blood vessels and intervertebral discs and lead to temporary pain relief [1]. Traction also stretches the ligaments and muscles in the cervical spine area. This can reduce muscle tension and increase blood circulations in the area, leading to faster recovery. In addition, traction is also able to stimulate the large afferent fibers of muscles and joints that inhibit pain fiber transmission at the spinal cord level, thus reducing the feeling of pain [2].

1.1.1   Types of Cervical Traction Therapy

Cervical traction therapy can be mainly divided into two types: manual traction and mechanical traction. Manual cervical traction therapy is usually performed by a trained physical therapist or chiropractor. During the therapy, the subject lies on a flat surface, such as a bed or massage table. This position is also known as the supine position. At the beginning, the therapist gently applies a longitudinal force through the neck of the subject by holding the subject's occiput and over the forehead. The therapy can last for 10 to 30 minutes. Heat and muscle relaxants are sometimes used to reduce stiffness and improve traction result [1]. Since the traction force and angles in manual traction are completely controlled by therapist, previous research study has pointed out [3] that it is difficult to keep traction force uniform due to fluctuations in muscle activity, thus making it less effective than mechanical traction therapy. It is also difficult to reproduce the same effects consistently with different patients and therapists over a long period of time.

In mechanical traction therapy, the subject's head is attached to a head halter and a motorized traction machine pulls the halter at an angle, ranging from 0° to 40°. Unlike manual traction, since the pulling force of mechanical traction is generated by computer-controlled motors, it has the advantage of being able to accurately control the strength and frequency of the pulling force. By varying the amount of pulling force periodically, mechanical traction can provide constant traction and intermittent traction [4] during the therapy. With pulleys, cables and motorized chair, mechanical traction can be performed in various positions. Besides the supine position, the subject can also sit on a chair up right at 90°, also known as the sitting position [5]. In recent years, new traction positions, such as inclined position and anterior lean position, have also been proposed [6][7]. Examples of mechanical traction devices and traction positions are as shown in Figure 1.

Figure 1. Mechanical cervical traction devices (left: inclined position [6], right: sitting position [5])

1.1.2   Research Studies in Cervical Traction Therapy

Over the years, the efficacy of traction therapy was often studied by researchers. For instance, Heijden et al. [8] conducted a systematic analysis of literature with the aim to evaluate the efficacy of traction therapy for patients and argued that none of the studies showed favorable results for traction. In a more recent literature review, Daniel [9] argued that there was very limited evidence available to warrant the use of traction therapy, especially when there were other alternatives available. On the other hand, there are also many reports that supported the use of cervical traction therapies. In a randomized study that assigned patients to three types of traction, Zylbergold et al. [10] found that patients receiving traction had increased cervical spine mobility, decreased pain and less medication use compared to patients without traction therapy. Jellad et al. [4] conducted a randomized study with 39 patients involving intermittent mechanical traction and concluded that both manual and mechanical cervical traction appeared to be a major contribution in the rehabilitation of cervical radiculopathy. Savva et al. [11] also reported a case study that showed the application of cervical traction could produce significant improvements in terms of pain and disability in cervical radiculopathy when combined with neural mobilization.

Although cervical traction therapy is a widely used therapy technique in treating various types of cervical disorders, there are major differences in opinion regarding the optimal method in its application. With many variables involved in a cervical traction therapy, it can be difficult to evaluate its overall effectiveness. Traditional cervical traction guidelines [12] have stated that there are five mechanical factors relevant to the therapy: i) neck position, ii) traction force, iii) duration of traction, iv) traction angle, and v) position of the patient. With neck position being the only generally accepted factor, there are too many variables in the other factors such that therapists often can only rely on their clinical experiences to choose the appropriate parameters [13]. Traction force and angle refer to the magnitude and direction of the pulling force. Past studies have shown that traction angles can affect intervertebral space changes at different cervical segments in cervical traction [14][15]. Traction positions, refer to the posture of the subject during cervical traction, can also influence the intervertebral separations during cervical traction. For instance, the sitting and supine positions have been compared in past studies on their effectiveness in achieving greater intervertebral separations [16] or offering better pain relief [17]. The inclined position, as a new position, has not been thoroughly investigated yet. Thus, the present study aims to focus on evaluating the inclined and sitting positions to clarify their mechanism and the resulting intervertebral separations on the cervical spine.

1.2 Cervical Spine Simulation Models

As one of the most complex kinematic structures in the human body, many simulation models of the cervical spine have been developed by researchers. Panjabi [18] listed four techniques for modelling the cervical spine: 1) physical model, 2) *in vitro* model, 3) *in vivo* model and 4) mathematical computer model. Physical models are made of artificial materials such as plastic or glass and they are mainly used to demonstrate bone anatomy in the spine. Constructing *in vitro* model generally requires human cadaver or animal specimen, so they are mainly used to test for strength and stability of the spin structure. *In vivo* models require living animal or human volunteers. It can be costly but it is also useful, especially when researching living phenomena. Finally, computer models consist

of mathematical equations that are capable of simulating real-world phenomena but it can be difficult to validate its accuracy.

Along with advancement in modern computer technology, computer models have several advantages over the other three techniques. Since computer models can be easily modified, the simulation model, whether finished or in the process of being developed, can be placed in different environments and can also be improved when new data are gathered. As a result, simulation models allow for precise controlled experimentation, allowing researchers to vary input parameters to test the target system behavior under a variety of situations and conditions. Secondly, with the time constraint of real-life system, computer simulation model can lead to significant time-saving. Running operations of the target system in real-life can be affected by permitted operating hours and other external factors such as the environment and target conditions. With simulations running in controlled computer environment, many external factors can be eliminated. Also, with increasing processing power of computer, it is possible to simulate the result of long operations in mere minutes. Since the simulation model is separated from the actual target, it does not burden the target system, which may cause wear or damage to it. Moreover, researchers can share open source computer models with other researchers, thus it encourages reusability and efficiency [19]. Compared to other three techniques, the cost of building computer models is the lowest and simulations can be done repeatedly without significant additional running cost. It also has the lowest cost of maintenance as it does not degrade after repeated use.

Among the computer models used to simulate the behavior of cervical spine, physics-based multi-body simulation is particularly popular among researchers. Since multi-body simulation engines are capable of realistically simulating real world mechanical systems based on the laws of physics with high-degree of precision and flexibility [20], it enables researchers to interact with their cervical spine model in real-time, such as adjusting the stiffness and damping parameters that control the behaviors of the cervical spine. Multi-body simulation models have been developed to study the head-neck response to impact loading such as whiplash. Merrill et al. [21] was one of the early studies that developed a head-neck model to investigate the three-dimensional response due to impact and impulse

loading. In recent years, several head-neck simulation models were developed to investigate the effects of acceleration impact [22][23], or to evaluate artificial cervical disc designs [24]. However, the above head-neck models were designed and validated to simulate the behaviour of the neck in their specific applications. None of them investigated the mechanism of the cervical traction therapy and the effects of traction positions. Since many factors in their simulation models, such as time scale, amount of external force, and the neck positions, are different from the ones in cervical traction therapy, it deems necessary to develop a simulation model targeted for cervical traction therapy. By combining the cervical spine and the traction devices together, the present model can be used to investigate and compare the effects of the inclined and sitting positions during cervical traction.

1.3 Objectives of the study

Due to the complex structure of the cervical spine and the various traction parameters, such as traction force, angle and position, involved in the treatment, the mechanism of cervical traction therapy has not been fully understood. The motivation of this research is to evaluate the differences between the inclined and sitting traction positions, especially in their abilities to achieve separations at specific part of the cervical spine. While sitting position is a common traction position, inclined position is a new position proposed to improve the effectiveness of the cervical traction therapy. In order to better understand their mechanism, we developed a multi-body simulation model that includes the cervical spine and two cervical traction devices which represent the inclined and sitting positions. By using the model, our objective is to compare the intervertebral separations achieved by the two positions when different amount of traction force and traction angle are used. In order to achieve this objective, we performed the following three studies.

Firstly, a multi-body simulation model, namely Model 1, which includes the cervical spine and two traction devices was developed using a physics engine each intervertebral vertebra was modeled as a rigid body. The intervertebral disc between two adjacent intervertebral vertebrae was modeled by a pair of translational and rotational joints using

springs and dampers. The mechanical parameters, such as the range of motion, stiffness and damping coefficients, used to simulate the behavior of the cervical spine were referenced from published literatures [22][23][25]. Model 1 was used to evaluate the inclined position and sitting position, on how they affect the intervertebral separations during cervical traction therapy. Traction forces ranged from 60N to 200N and traction angles at 10/20/30/40˚ were tested.

Secondly, in order to validate the behaviour of Model 1, laboratory experiment was conducted to acquire radiographic images of the cervical spine from subjects receiving cervical traction in inclined and sitting positions. Six male subjects were recruited for the experiment. Traction forces from 100N to 160N and traction angles at 10/20/30/40˚ were used. The experiment result of the inclined and sitting positions were compared. The simulation result of Model 1 was also compared to the experiment data.

Finally, due to the difference between the behavior of Model 1 and the experiment data, Model 2 was developed. Anterior and posterior horizontal shear movement of the intervertebral discs were added to the model. Instead of using a single translational joint to represent the vertical movement of the discs, two translational joints were used to represent the anterior and posterior vertical movement separately, with the posterior vertical movement representing the resistance force of the posterior ligaments. The behavior of Model 2 was compared to the experiment data. Using Model 2, the behavior of the cervical spine in relation to body parameter such as hip joint stiffness and the stiffness level at each cervical segment was investigated.

We believe this study can provide insight on the benefits and drawbacks regarding the two traction positions. Traction equipment manufacturers will also benefit from this study since they can evaluate new traction technique and designs by using our simulation models.

1.4 Outline of Dissertation

The dissertation is organized into the following chapters:

Chapter 1: The current chapter provides an introduction of cervical traction therapy and an overview of multi-body simulation model of cervical spine. It also explains the objectives of the research.

Chapter 2: This chapter presents the research background of this study. It includes an overview of the cervical spine, intervertebral discs and the simulation engine used to construct the multi-body simulation model.

Chapter 3: This chapter describes how the simulation model, namely Model 1, was developed. The two traction positions and the simulation results are also presented. The details of Model 1 are also explained.

Chapter 4: This chapter describes the radiographic experiment to gather clinical data of cervical traction in the inclined and sitting traction positions, and how the collected data was analyzed. The experiment result then was used to compare with the simulation result from Model 1.

Chapter 5: This chapter describes the development of a new model, namely Model 2, and discusses its improvement over Model 1. The details of Model 2 are explained. The validation process using the experiment result are also described. Using Model 2, parametric study was conducted to further investigate the difference between the inclined and sitting positions.

Chapter 6: The final chapter gives conclusive discussion of the findings, and suggestions for future work.

Chapter 2.
Research Background

2.1   Human Cervical Spine

This section reviews the biomechanics of the cervical spine. Section 2.1.2 describes the basic structure of the human cervical spine. Section 2.1.2 describes definition of the coordinate system and the naming of the direction used in this study. Section 2.1.3 presents the structure of the intervertebral discs and discusses a cervical spine related disorder, namely the cervical radiculopathy and how it affects the human body. Section 2.1.4 discusses the functions of other soft tissues in the cervical spine.

2.1.1   Structure of Human Cervical Spine

The human cervical spine is composed of seven vertebrae, from C1 to C7. It provides support to the head and allow a wide range of possible movement, including flexion, extension, lateral bending and axial rotation. Figure 2 illustrates the human cervical spine. The bones colored in red in the figure indicate the cervical vertebrae. The cervical vertebrae are surrounded and joined by various types of soft tissues, in order to stabilize the head while providing maximum flexibility to the its movement. The soft tissues surrounding the cervical spine include the intervertebral discs, muscles, facet joint capsules and ligaments, such as the anterior/posterior longitudinal ligaments.
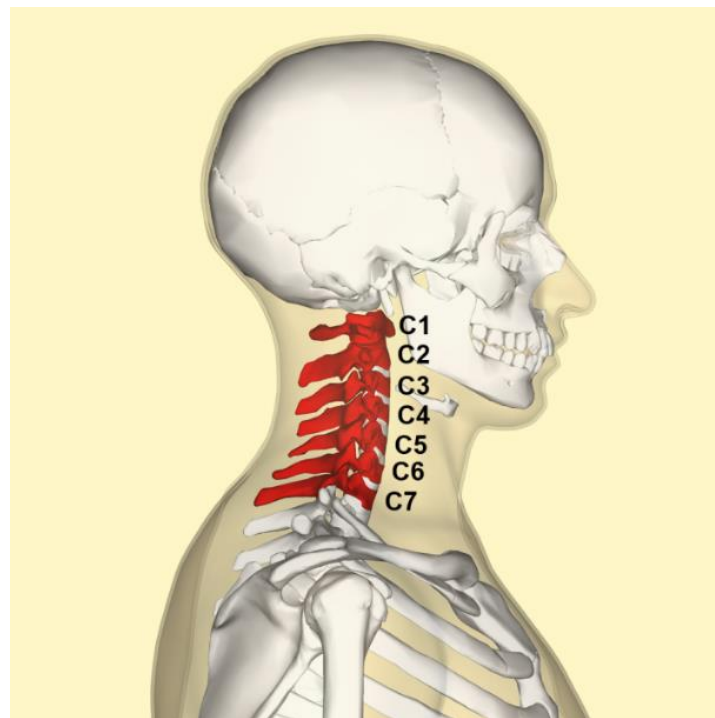
Figure 2. Cervical vertebrae C1 to C7 [29]

Among the seven pieces of cervical vertebrae, C1 and C2 have unique shapes while C3 to C7 shares a lot of similarity. Figure 3 and Figure 4 show the 3D rendering of C1 and C2. Being the topmost cervical vertebra, C1, also known as the atlas, resembles a thin ring and is directly connected to the base of the skull. There is no vertebral disc between the skull and C1. C1 has large concave superior articular facet for the base of the skull to be situated. C2, also known as the axis, has a unique shape and it is different from the rest of the cervical vertebrae. The most noticeable feature of C2 is the protruded dens at the anterior side. Under normal circumstances, the dens fit inside the thin ring of C1 and support the axial rotation between the two vertebrae. The bottom of C2 (the inferior side) is connected to the top of C3 by the C23 intervertebral disc, which is the first intervertebral disc in the cervical spine. C1 and C2 form a specialized structure to allow a large range of motion and are responsible for flexion, extension and rotational movement.
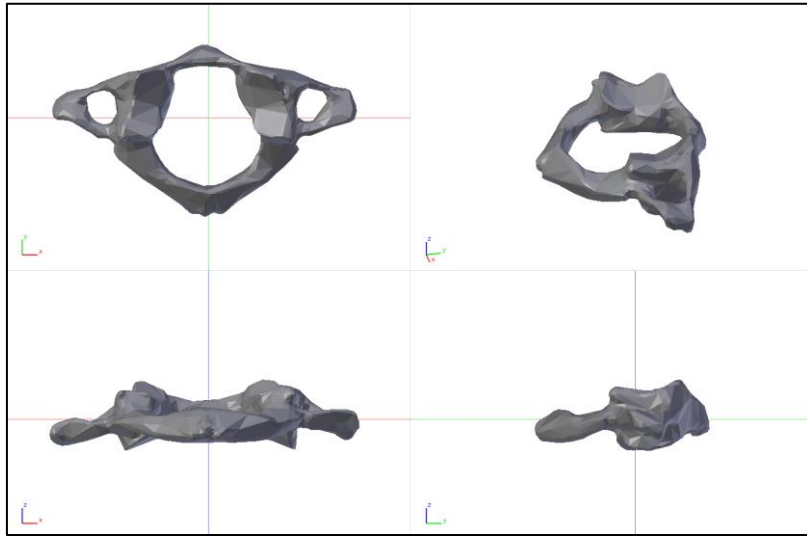
Figure 3. A 3D rendering of the C1 vertebra
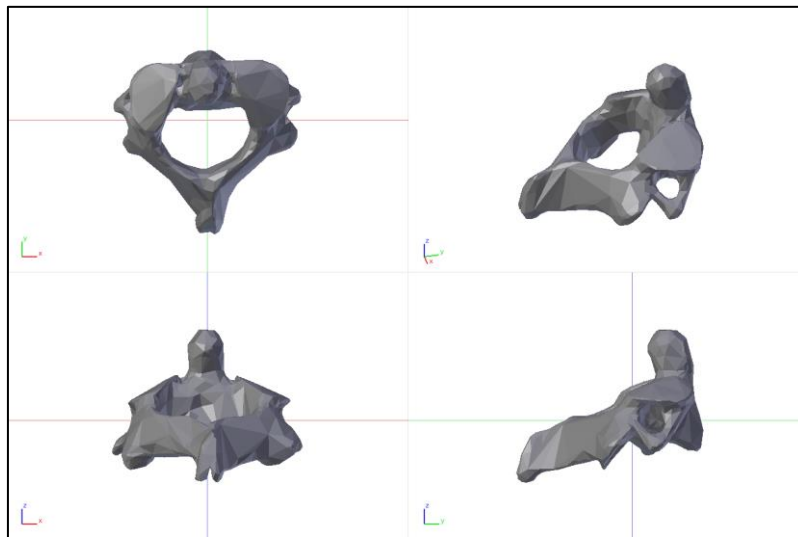
Figure 4. A 3D rendering of the C2 vertebra

The lower cervical spine composed of the C3-C7 vertebrae and these five vertebrae share very similar features. Figure 5 shows a 3D rendering of the C3 vertebra. The C3-C7 vertebrae each consists of a cylindrical body on the anterior side and an arch pointing to the posterior side. Each vertebra is connected to adjacent vertebrae by an intervertebral disc. The empty space in the center of vertebra is called the vertebral foramen and they exist in all the cervical vertebrae from C1 to C7.
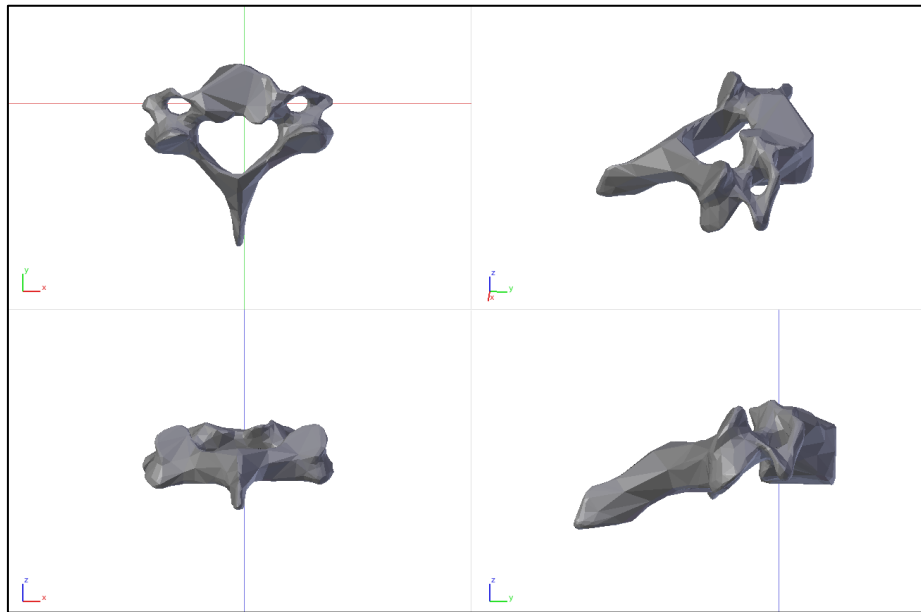
Figure 5. A 3D rendering of the C3 vertebra

2.1.2   Definition of Coordinate Systems

Before we proceed to describe the mechanical behavior of the cervical vertebrae and the rest of the cervical spine, it is essential to first define the coordinate systems used in this study. The coordinate system is illustrated in Figure 6. The movement of the vertebrae are defined as:

- X-axis
    - +/- displacement: lateral shear
    - + rotation: extension
    - - rotation: flexion
- Y-axis
    - + displacement: anterior shear
    - − displacement: posterior shear
    - +/- rotation: lateral bending
- Z-axis
    - + displacement: tension/separation
    - − displacement: compression
    - +/- rotation: axial rotation
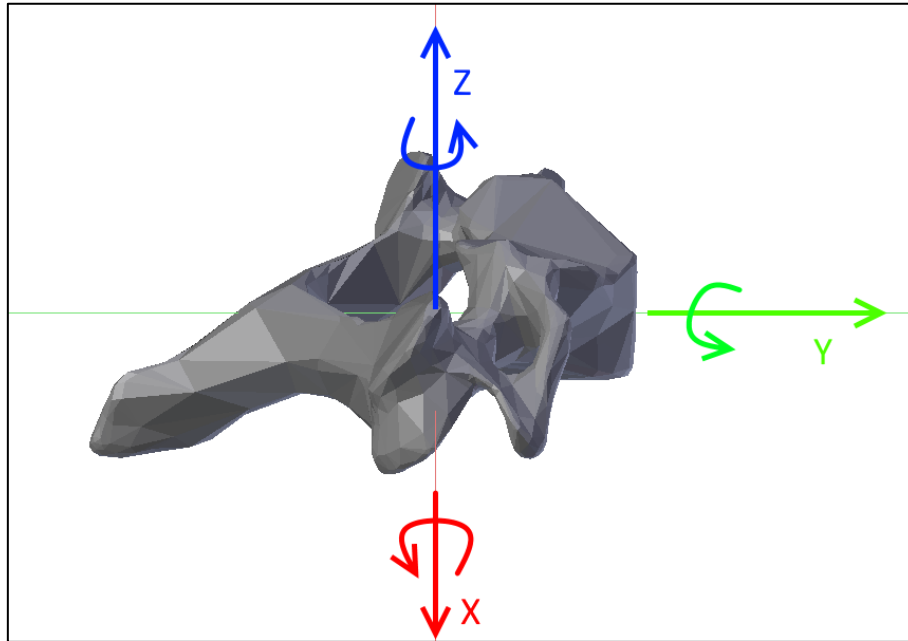
Figure 6. Definition of coordinate sytems

It is worth noting that in our cervical traction simulation model, the lateral shear, lateral bending and axial rotation are not included in the simulation, i.e. the translational or rotational joints are locked in these directions. This simplification was made because under normal circumstances, the cervical traction therapy performed in the inclined and sitting positions does not cause movement in lateral bending and axial rotation. As the traction force is applied symmetrically to the head, it is assumed that there is no force causing lateral shear. It is important to point out that this simplification can only be made to this study of mechanical traction therapy in these two positions. In manual cervical traction therapy, however, traction force from all directions can occur depending on the traction therapist's choice of method.

2.1.3   Intervertebral Discs

With the exception of the space between the atlas (C1) and axis (C2), there are five cervical intervertebral discs between C2 to C7 in the cervical spine region. Intervertebral discs are highly specialized structures that contribute up to one-third of the height of the vertebral column and they form specialized joints between the adjacent cervical vertebrae.

They can absorb shocks and compressive forces transmitted through the skeletal structures of the body. Under normal conditions, intervertebral discs are able to withstand greater than normal loads and exhibit viscoelastic properties and hysteresis [30].

However, many reasons can cause these discs to change shape and become herniated discs. For example, cervical spondylosis is a common age-related condition that develops from wear and tear of the cartilage and bones in the cervical spine and it can lead to bone spurs and herniated discs. Prolonged incorrect stance, such as the forward head posture [32], can apply long duration of pressure on the discs, causing the inside fluid to break through the disc wall and change the shape of the disc. Whiplash, a type of neck injury that occurs when a person's head moves backward and forward suddenly with great force, is also a common cause of herniated discs. As the herniated discs are surrounded by cervical nerve roots, the protruded portion of a damaged disc could result in compression of the nerve roots, and lead to neck pain. Figure 7 shows a radiographic image of a herniated disc.

Figure 7. A radiographic image of a herniated disc[31]

Cervical radiculopathy is caused by compression or irritation of a nerve in the cervical spine and can be a consequence of a herniated disc. When a nerve root is compressed, it can cause pain, weakness, and/or numbness in the corresponding body parts [30]. As illustrated in Figure 8, there are eight cervical nerve roots, named C1 to C8, in the cervical spine. These nerve roots are connected to different parts of the body, such as shoulders, arms, hands and fingers. For instance, it has been found that irritation at C5 nerve root (vertebral disc between C4-C5) can cause shoulder pain and weakness at the top of the upper arm. A herniated disc at C6 can cause weakness in biceps and wrist muscles. It can also cause numbness and tingling pain at the thumb. On the other hand, compression at C7 can lead to weakness with handgrip and numbness to the little finger. While these typical pain patterns associated with cervical radiculopathy may not apply to every patient, they can help doctors and therapists to determine the location of the herniated disc and the corresponding treatment.
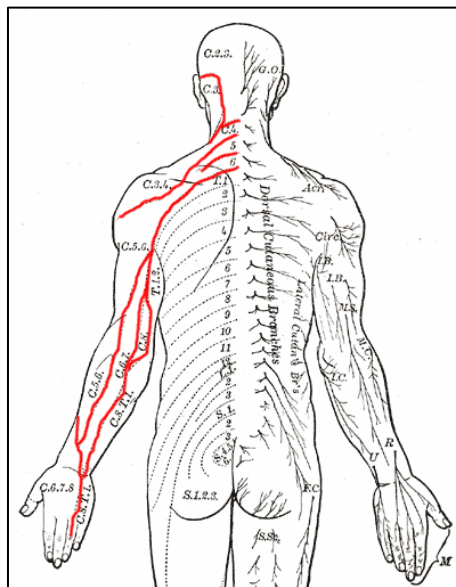
Figure 8. Cervical nerve roots and potentially affected areas in cervical radiculopathy [33]

Cervical radiculopathy and other related injuries can be treated by various methods, including resting, short-term immobilization, anti-inflammatory medications, cervical traction therapy, and surgery. In severe cases, surgeries such as cervical spinal fusion which joins the adjacent vertebrae together, or spinal decompression which removes part of the affected vertebra, or artificial disc replacement are required. For less severe cervical disorders, cervical traction therapy provides a conservative non-surgical alternative.

Since herniation can occur at any of the cervical discs, an effective cervical traction therapy should achieve intervertebral separations only at the target region of the cervical spine, in order to avoid applying unnecessary pressure to unaffected discs.

2.1.4   Facet joints, ligament, and muscles

Besides the intervertebral discs, soft tissues surrounding the cervical spine also include facet joints, ligaments and neck muscles. The facet joints located at the posterior vertebra and provide structural stability to the vertebral column. Each vertebra has two facet joints in each spinal motion segment. They are between the superior articular process of a vertebra and the inferior articular process of the vertebra directly above it. Ligaments connects the cervical vertebrae together and provide resistive force to limit spinal motion. There are short ligaments that connect adjacent vertebrae together, yet there are also long ligaments that extend over several vertebrae. Ligaments can be found in the anterior and posterior side of the vertebrae, such as the anterior/posterior longitudinal ligaments. They can also be found on the side of the vertebrae such as the capsular ligaments. It is important to point out that ligaments only provide resistive force when being stretched and does not generate any force under compression. Muscles are active components that are able to maintain and change the posture of the cervical spine. In the human cervical spine, the muscular anatomy is very complex. Neck muscles goes through the cervical spine in many places, and can be divided into superficial, intermediate and deep muscle. They are responsible for generating the internal force to cause translational and rotational spinal movement in all directions.

2.2 Physics-based Multi-body Simulation

This section discusses the multi-body simulation engines used in this research. Two physics-based simulation engines were used. The first engine was a commercial engine called Vortex and it was developed by CM Labs Simulations [37]. Vortex is capable of generating accurate mechanical simulation. Setting up joint constraints in the

environment were also straightforward. Using the Vortex library helped to reduce the time it took to develop the model that included the cervical spine and the two traction devices. The simulation model, namely Model 1, used in Chapter 3 was first constructed with the Vortex engine.

As the research continues, however, we decided to replace Vortex with another physics engine due to performance and licensing issue for the works in Chapter 4 and onwards. Since Vortex was installed on an old computer, it was no longer able to handle the processing load of the new simulation. Its license also did not allow us to transfer it to a new computer. As a result, the simulation was re-constructed using Bullet [34] in the second part of the research. Bullet is a free open source physics engine library that is popular among robotic researchers, filmmakers and game developers. It features rigid body and soft body simulation with discrete and continuous collision detection and supports importing 3D models constructed by software such as Blender [35]. Although it required a significant amount of time to rebuild Model 1 in Bullet, being able to run the simulation in a more powerful computer reduced development time and allowed the simulation to run faster. During the rebuilding process, basic rigid body motion tests and spring mechanism tests were conducted. These tests confirmed that both physics engines gave the same simulation results when given the same parameters.

2.2.1   Dynamic Equations in Simulation

Since all the parts in the simulation are modelled as rigid bodies, the equation of motion can be represented by the Newton's equation of motion and Euler's equation of motion. Newton's equation of motion can be used to describe translational motion, while Euler's equation can be used to describe rotational motions.
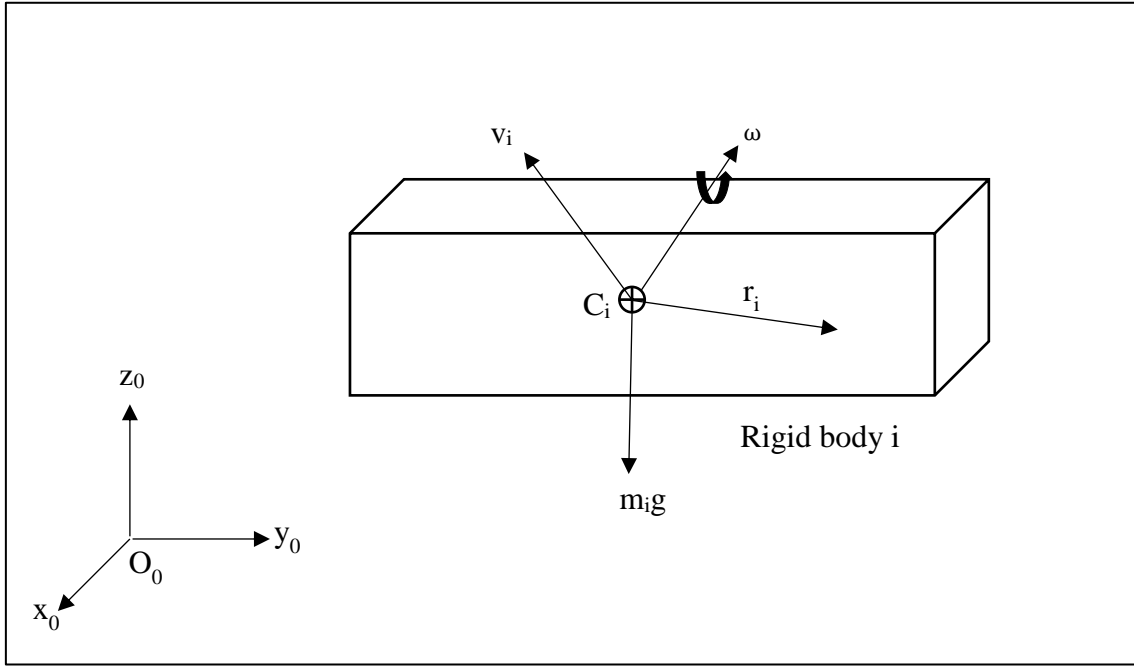
Figure 9. Free body diagram of a rigid body i

For a rigid body i with mass m_i in base coordinate frame $O_0 - x_0 y_0 z_0$, as shown in Figure 9, let v_{ci} be the linear velocity of the center of mass. The inertia force is then given by $-m_i \dot{v}_{ci}$. With gravity as g, the Newton's equation of motion then becomes

$$F_i + m_i g - m_i \dot{v}_{ci} = 0 \qquad i = 1, \dots, n$$

where F_i is the external force acting on the rigid body i.

The Euler's equation can be used to describe rotational motions of rigid body. Using the inertia tensor, I, a 3 x 3 symmetric matrix defined by

$$I = \begin{bmatrix} I_{xx} & I_{xy} & I_{xz} \\ I_{yx} & I_{yy} & I_{yz} \\ I_{zx} & I_{zy} & I_{zz} \end{bmatrix}$$

$$I_{xx} = \sum_{i=1,N} (y_i^2 + z_i^2) \, m_i = \int (y^2 + z^2) \, dm,$$

$$I_{yy} = \sum_{i=1,N} (x_i^2 + z_i^2) \, m_i = \int (x^2 + z^2) \, dm,$$

$$I_{zz} = \sum_{i=1,N} (x_i^2 + y_i^2) \, m_i = \int (x^2 + y^2) \, dm,$$

$$I_{xy} = I_{yx} = -\sum_{i=1,N} x_i y_i \, m_i = -\int xy \, dm,$$

$$I_{yz} = I_{zy} = -\sum_{i=1,N} y_i z_i \, m_i = -\int yz \, dm,$$

$$I_{xz} = I_{zx} = -\sum_{i=1,N} x_i z_i \, m_i = -\int xz \, dm.$$

and with dm $= p dV$ and p being the mass density, where x_i, y_i, z_i are the coordinates of the centroid of the rigid body and each integral is taken over the entire volume V of the rigid body. The inertia torque acting on rigid body i is given by the time rate of change of the angular momentum of the rigid body at that instant.

Referring to the same figure, let ω_i be the angular velocity vector, r_i be the position vector and I_i be the centroidal inertia tensor of rigid body i, then the angular momentum is given by $I_i \omega_i$. The angular acceleration is given by $I_i \dot{\omega}_i$ and the gyroscopic torque is given by $\omega_i \times (I_i \omega_i)$. Thus, the rotational motion can be described by the following equation:

$$N_i + r_i \times F_i - I_i \dot{\omega}_i - \omega_i \times (I_i \omega_i) = 0 \qquad i = 1, \dots, n$$

where F_i represents the external force and N_i represents the moment on the rigid body i.

Using the Newton-Euler equation of motion, one can describe the combined translation and rotational dynamics of an individual rigid body i. However, in order to calculate the

dynamic behavior in a simulation model, it requires the evaluations of the above equations for all the rigid bodies in the model simultaneously. By leveraging the computational power of modern computers, a physic engine is capable of doing such simulation. Thus, in present study, it is essential to construct our simulation models with a physics engine to evaluate the dynamic response of the cervical spine when external traction force is applied.

2.2.2   Numerical Integration Method and Constraint Solver

A stable and accurate integration of ordinary differential equations (ODE) is important for the solution of the equations of motion. In present study, the physics engine Bullet uses the semi-implicit Euler method for numerical integration. The dependent variables in the semi-implicit Euler method are defined by the following equations:

$$v_{n+1} = v_n + g(t_n, x_n)\Delta t \tag{Eq. 1}$$

$$x_{n+1} = x_n + f(t_n, v_{n+1})\Delta t \tag{Eq. 2}$$

where Δt represents the time step. $t_n = t_0 + n\Delta t$ defines the time after n steps. Implicit method is more suitable than explicit method for multi-body systems because the components in such systems can often have large differences in masses, stiffness and damping. In such cases, using an explicit method would require very small time step Δt to keep the error in result bounded, while an implicit method would allow a larger time step to achieve stability and accuracy with less computational time.

In multi-body systems, all rigid bodies are either controlled by constraints, or otherwise act as free bodies affected only by gravity. A free rigid body has 6 degrees of freedom, i.e. the 3 translational and 3 rotational DOF. When a rigid body is connected by a constraint, its DOF is reduced depending on the constraint type. There are many constraint types, such as collision contacts, springs, damper, hinges, and they all require constraint solver. Solving the constraint for each rigid body and calculate the motion in each simulation step is thus a crucial task for the simulation engine. In general, there are

two types of constraint solver, namely the direct solver and iterative solver. Direct solver has the benefits of producing exact results that satisfy all constraints and conditions in the system but generally have poorer time complexity than iterative solvers. On the other hand, iterative solver involved calculating the impulse or forces acting on each rigid body and apply them to the constrained body iteratively. While it is capable of generating close to real-time results, it also runs the risk of violating constraints when insufficient iteration count is set. The present study made use of two physics engines at different stages of the research due to technical and licensing issues. In Chapter 3, the physics engine Vortex was used. It uses the default iterative solver named "kStableStepper". In Chapter 4 and Chapter 5, the physics engine was changed to Bullet. The constraint solver was also changed to an iterative solver called "Sequential Impulse" [36]. The number of iteration count was set to 5000. The time step is set at 1/360th second to achieve the desired stability and accuracy of the simulation result.

Chapter 3.

The Effect of Traction Position in Cervical Traction Therapy Based on Multi-body Simulation Model

3.1   Introduction

In order to evaluate the effect of the inclined and sitting positions in cervical traction therapy, we developed a multi-body simulation model, named Model 1. It includes a skeleton body, a cervical spine and two mechanical cervical traction devices, representing the inclined and sitting positions respectively. Using this multi-body model, the objective of this chapter is to investigate the amount of intervertebral separations in cervical traction therapy in the two positions when different amount of traction force and angles are used. The chapter is divided into two parts. The first part describes the development process of Model 1. In the second part, cervical traction simulation is performed using the model and the resulting intervertebral separations in the two traction positions are compared.

3.2   Methods

3.2.1   Cervical Traction Simulation Model

The simulation model was built with the following design requirements.

- The simulation should be built with reasonable flexibility that allows easy manipulation of most of the testing parameters, such as the mass and bones of the vertebrae, the stiffness and damping of the joints, traction force and angle of the traction devices.

- The subject, the cervical spine and the traction devices should be built with reasonable accuracy, but with consideration that future revision may occur, such as changes in body dimensions and posture.

- The traction devices should be modeled with existing products in the market at to reduce development time and mimic actual experience received by patients.
- The model should be able to export the measurement data for further analysis.
- The model should be able to consistently reproduce similar measurement results within reasonable degree, when the same test parameters and setup were given.

3.2.2   Cervical Traction Devices

A typical set of traction equipment includes a head halter, a pelvic belt, a spreader bar, a rope and a weight. Depending on the design of the head halter, the direction of force varies. Thus, it is important to predefine the points of contact between the head and the halter in order to identify the final acting force vector on the head. In the current model, the chin and the back of the head were selected as two contact points for the pulling force to apply on. The top part of the back of the head does not come in contact with the halter when traction is applied during the therapy. It is only when there is no pulling force that the halter will rest on the head. Rendered images of the halter and the points of contact are illustrated in Figure 10.
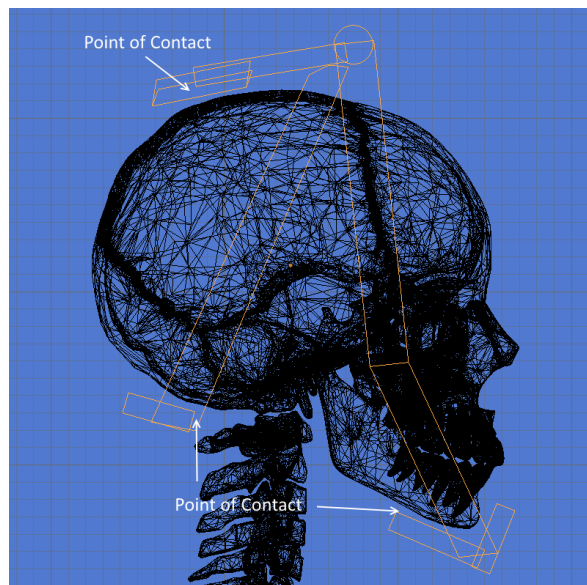

Figure 10. Head halter model

3.2.2.1   Inclined Traction Device Model

Figure 11. Inclined position traction device [5] and simulation model (Orange arrows indicate configuration of traction angle. Green arrow indicates traction direction)

Figure 12. Body diagram of the inclined position model (dotted block represents the cervical spine model)

Two types of traction device were developed and they represented the inclined and sitting positions respectively. The inclined position was modelled based on the Minato Tractizer TC-C1 [6] and is shown in Figure 11. The name "inclined" refers to the rotated seat, which looks like an incliner chair. This position aims to keep the subject remain in

the chair using gravity. In this position, the subject sits on a motorized chair that can rotate between 10° and 40° to determine the traction angle. In the simulation model, as shown in Figure 12, the chair was fixed to the ground and could not rotate. Four different chair models with preset traction angles were constructed and they were used to represent the four traction angles. Friction coefficient was set at surface of the chair, arm rest and the back of the chair to keep the body remain in the seat. The traction angle's vertex is at near the back of the subject's first thoracic vertebra (T1). Both models were constructed in Blender 3D, imported as Wavefront OBJ files into C++ and modelled using Vortex Dynamics 3.0 [37] in Microsoft Visual Studio 2015.

3.2.2.2   Sitting Traction Device Model

Figure 13. Sitting position traction device [5] and simulation model (Orange arrows indicate configuration of traction angle. Green arrow indicates traction direction)
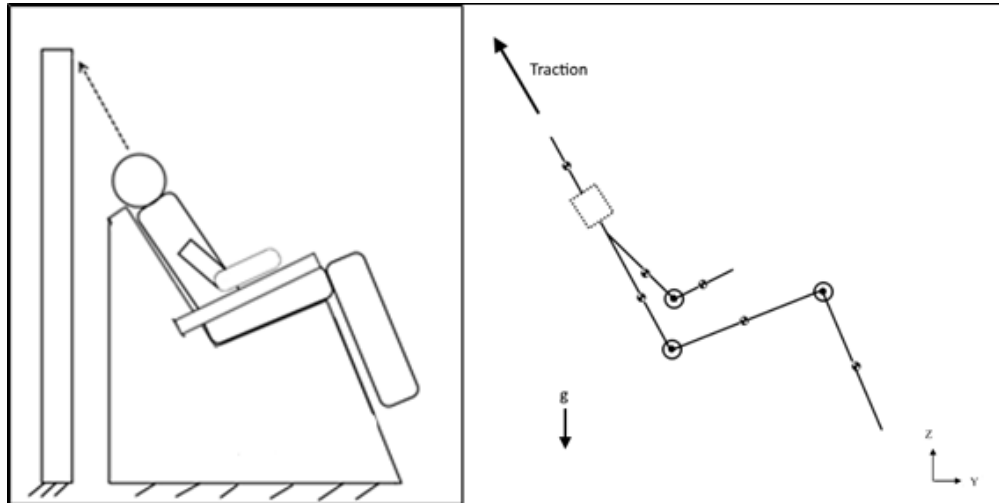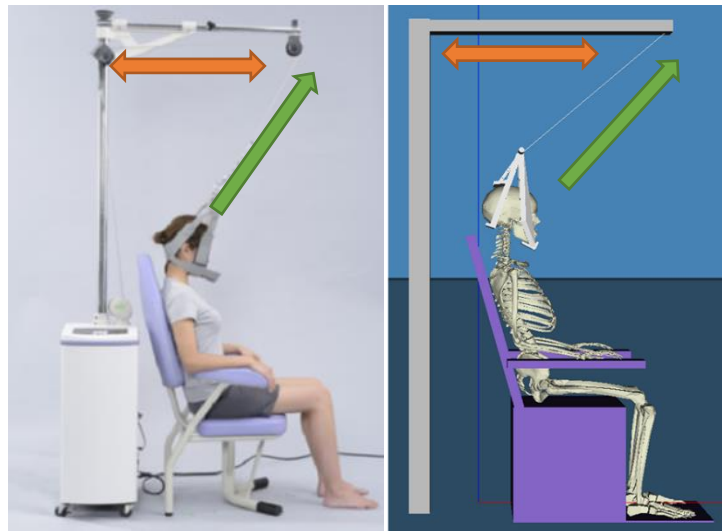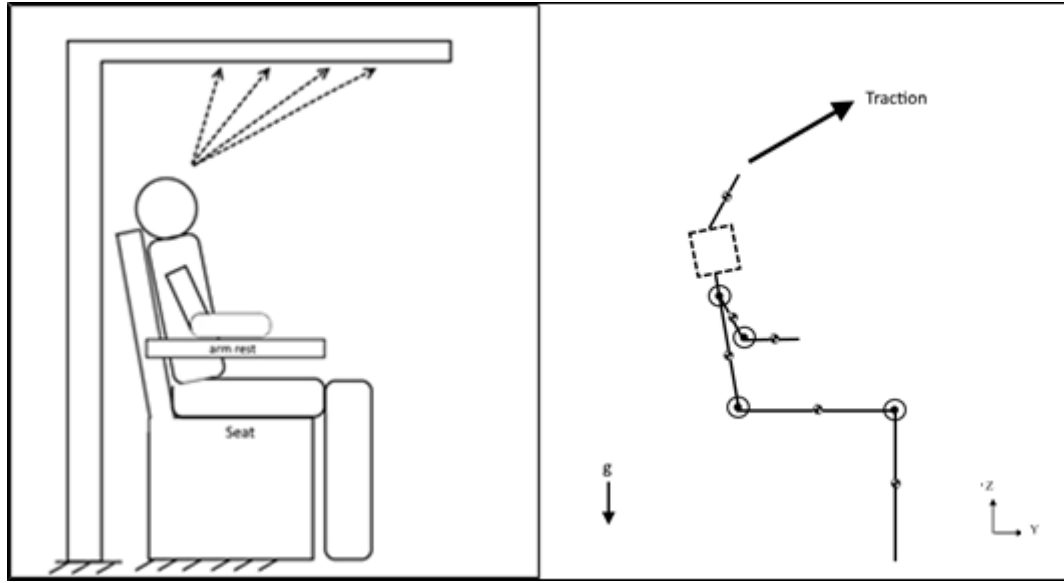
Figure 14. Body diagram of the sitting position model (dotted block represents the cervical spine model)

In the sitting position, the subject sits up right on a chair with the head attached to a head halter. The traction device applies a constant and continuous force to pull the halter upwards at an angle. The traction force can be set between 60N to 200N and the traction angle can be set at 10°/20°/30°/40° respectively. The sitting position was modelled based on the Minato Tractizer TC-30D [5]. A picture of the sitting position device and the corresponding simulation model are shown in Figure 13. The kinematic model of the sitting position is illustrated in Figure 14. The pulling device, which contains the motor and controller, is stationed on the ground in the actual device. In the simulation model, it was combined with the top pulling bar together and was modelled as one rigid body fixed to the ground. In the actual device, the length of the top bar can extend to various preset positions to set the traction angles. In the simulation model, the pulling force were set at different coordinates and direction to simulate the four traction angles from 10° to 40°. Bending behavior of the top bar was not included in the simulation model, since the traction force is relatively small compared to the mechanical strength of the top metal bar, thus it is safe to assume that there is very little bending movement of the top bar during traction. The arm rest and the seat were fixed to the ground as rigid body. In order to keep the subject in the chair during traction, the surface of the seat was set with a high fiction coefficient. Friction coefficient was not set for the arm rest and the back of the chair, since

in a typical user case the subject does not use the arm rest to resist the traction force. When simulation begins, traction force was applied to the halter and gradually pull in the direction of the designated angle.

It is worth noting that, unlike manual traction therapy that may contain axial rotation or lateral flexion stretching, both mechanical traction devices in present study do not involve translational forces along the X-axis and rotational forces along the Y and Z-axes. Since the physics engine support 2D and 3D simulation natively, and the unused loading directions were constrained for all rigid bodies, having a 3D simulation does not place excessive load in the calculation. Furthermore, future improvement of our model may include the currently unused directions, thus developing a 3D model can provide more flexibility in the future.

3.2.3   Human Skeleton Model

The human skeleton model was a full 3D human body retrieved from Anatomography/BodyParts3D [29], which is a research institute that provides 3D polygon data of anatomically-correct skeleton. The data was extracted from full-body MRI images of a male adult. Besides the head and the cervical spine, all the parts in the human skeleton model were modelled as separated rigid bodies. Each part was imported into a modelling software named Blender for scaling and re-positioning with the traction equipment. The topmost part of the trunk was cut off at the first vertebra of the lumbar spine (T1) and it served as a support for the lowest part of the cervical spine (C7). The left and right arms were attached to the trunk at the shoulders. The legs were separated into upper legs and lower legs. The upper legs (thighs) were attached to the pelvis at the hip and the lower legs (shanks) were attached to the upper legs at the knees. The coordinates of the center of mass of each part were calculated using Blender and were used as the origin of the rigid body in the simulation model. All the parts were connected with hinge joints that forced the attached parts to rotate along the X-axis as shown in Figure 15. Range of motion and rotational stiffness parameters of the hinge joints at the

arms and legs were set generously and relaxed such that they would not limit the movement of the body when traction applies.
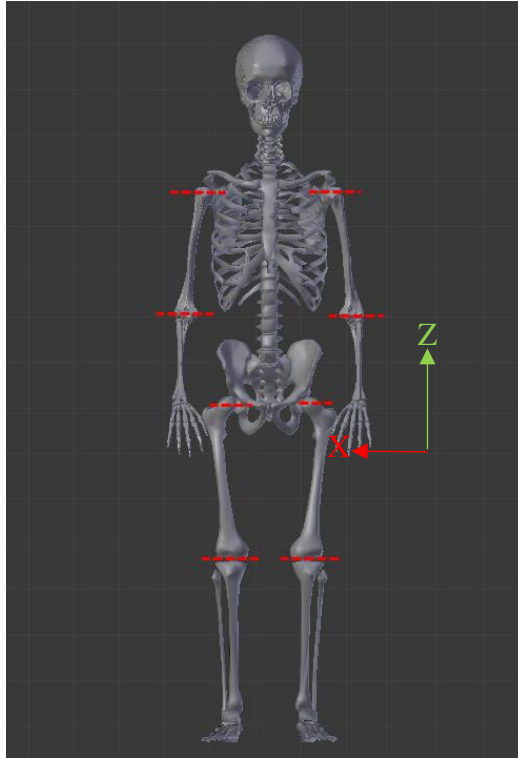

Figure 15. Human skeleton model (red dotted lines indicate hinge joints)

The body segment mass data was configured based on the data from Zatsiorsky et al. with adjustment made by DeLeva [38]. The human body model was 1.74m tall and weighted 73kg. The mass of each bone was calculated based on the percentage listed in the body segment parameter data and is shown in Table 1.

Table 1. Body Segment Mass

Group Names	Mass (% of body weight)	Mass (kg)
Head + Neck	6.94	5.07
Upper + Mid Trunk	32.29	23.57
Lower Trunk (pelvis)	11.17	8.15
Upper Arms	2.71 x 2	1.98 x 2
Forearms + Hands	2.23 x 2	1.63 x 2
Thighs	14.16 x 2	10.34 x 2
Shanks + Feet	5.70 x 2	4.16 x 2
Total	100%	73.00

3.2.4   Cervical Spine Model

Similar to the human skeleton model, the skull and the cervical spine components were also created based on the 3D models retrieved from Anatomography/BodyParts3D [29]. The model consisted of 8 rigid parts: a human skull and seven pieces of the cervical vertebrae as shown in Figure 16.
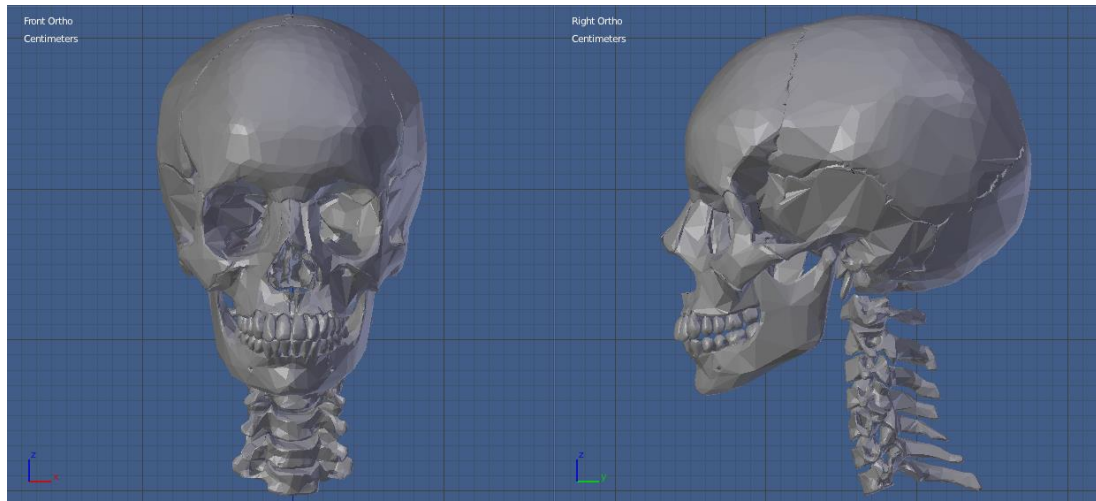
Figure 16. Skull and cervical spine 3D models

In order to minimize processing load in the simulation, all the bones that made up the cranium and the facial area were combined to form a single rigid body to represent the skull. The cervical vertebrae (C1-C7) were modeled separately. Previous study [39] stated that there is very little vertical and horizontal movement in the C0-C1-C2 joints. As a first step to create a simple cervical spine model, we decided to fix the translational and rotational movement of C0-C1-C2 for simplification, and only model the movement of the five links between C2 to C7. The C2-C7 cervical vertebrae were attached to adjacent vertebrae by a pair of translational and rotational joint with stiffness and damping parameters to control their movement. The C7-T1 joint was also fixed to secure the cervical spine to the upper body.
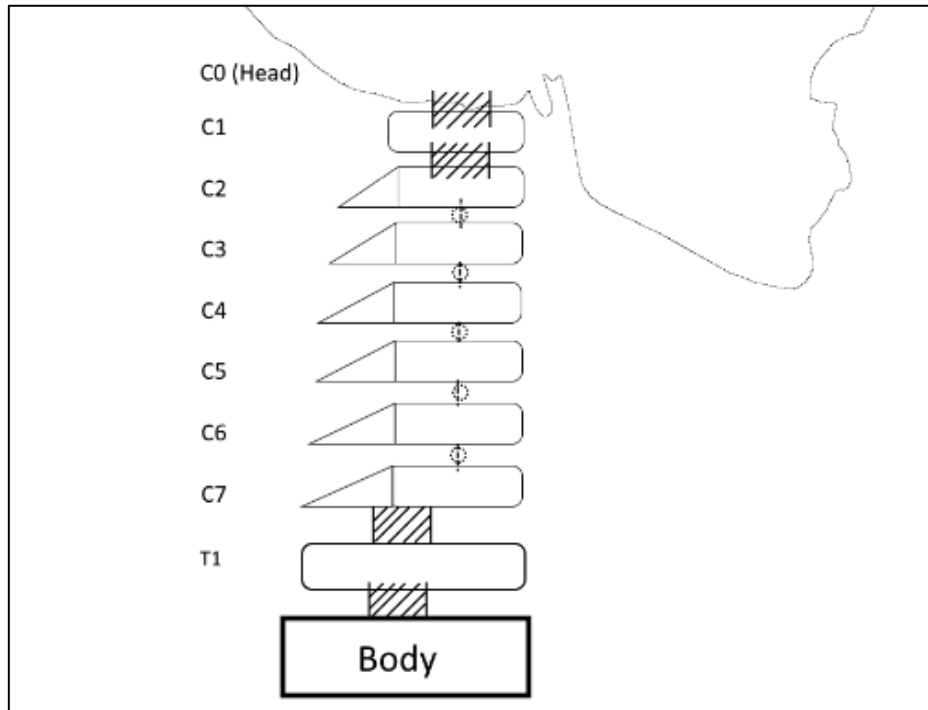
Figure 17. Translational and rotational joints in cervical spine
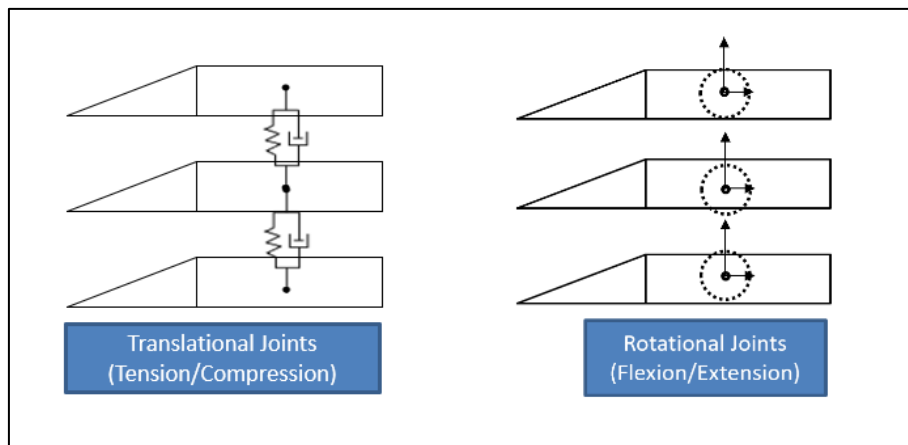
Figure 18. Intervertebral Joint Model

The vertebrae were connected together using translational and rotational joints with as shown in Figure 17 and Figure 18. As described in the section 3.2.2, cervical traction in inclined and sitting positions do not involve translation movement along the X-axis, and rotation along the Y and Z-axes. Thus, these three movement were constrained in the model. Only translation along the Y-axis and Z-axis, and rotation around the X-axis between vertebrae were allowed in the model.

Table 2. Mass of vertebrae [22]

Parts	C1	C2	C3	C4	C5	C6	C7
Mass (kg)	0.22	0.25	0.24	0.23	0.23	0.24	0.22

Table 3. Range of Motion of Cervical Spine Segment [22]

Loading direction	C2-C3	C3-C4	C4-C5	C5-C6	C6-C7
Flexion (Deg)	5.5	8.3	11.1	11.1	9.4
Extension (Deg)	4.5	6.7	8.9	8.9	7.6
Tension (mm)	1.1	1.1	1.1	1.1	1.1
Compression (mm)	0.7	0.7	0.7	0.7	0.7

The vertebrae, which are modelled as rigid bodies, are connected by the intervertebral joints that represent the combined behavior of the intervertebral disc, ligaments, facet joints and muscles. Due to the complexity of the muscle models and the nature of the cervical traction therapy, we assumed that the subject is relaxed enough that neck muscles has zero activation during traction. The mass and the range of motion of the cervical spine are listed in Table 2 and Table 3 and they are referenced from previous head-neck simulation model study [22]. The intervertebral joint is modeled as one vertical translational joint and one rotational joint, with separated stiffness and damper parameters. The starting values of the translational and rotational stiffness and damping coefficients were acquired from previous literatures [22][23] and are listed in Table 4. The center of rotation determines the rotational motion of a vertebra relative to its adjacent lower vertebra and it was set at the center of gravity of the vertebra.

Table 4. Stiffness and Damping Parameters of Cervical Spine Segment[22]

Parameters	Cervical Segment				
	C2-C3	C3-C4	C4-C5	C5-C6	C6-C7
Translational Stiffness (N/mm)	63.5	69.8	66.8	68	69
Rotational Stiffness (Nm/deg)	1.5	1.5	1.5	1.5	1.5
Translational Damping	1.0	1.0	1.0	1.0	1.0
Rotational Damping	0.026	0.026	0.026	0.026	0.026

3.2.5   Measuring the Intervertebral Space Changes

In previous literatures that evaluated the efficacy of cervical traction therapy [7][14], intervertebral separation was often used as an indicator to measure traction effectiveness. Intervertebral separation refers to the distance between the interior side of the upper vertebra and the superior side of the lower vertebra. Since this space is occupied by an intervertebral disc, it is also referred as the disc space or disc height. Rotational movement, such as flexion and extension of the cervical spine cause changes to the anterior and posterior separation. Figure 19 illustrates the anterior and posterior intervertebral separation between two adjacent vertebrae.
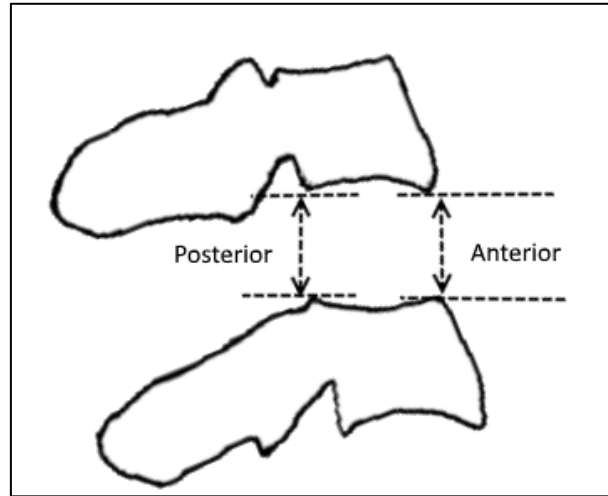
Figure 19. Intervertebral separation between adjacent vertebrae
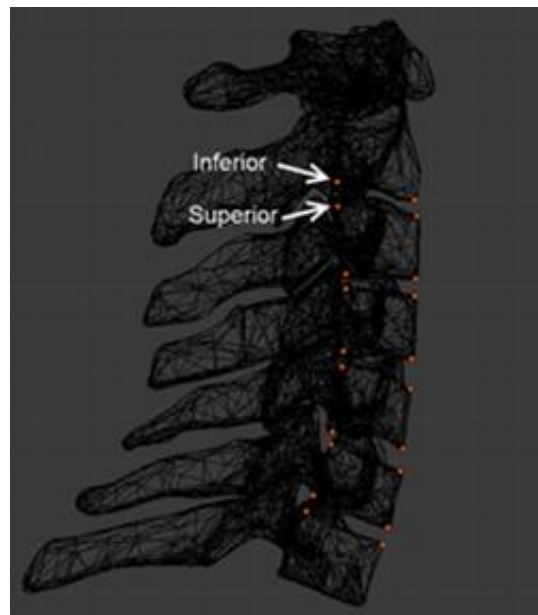
Figure 20. Sensors on the cervical spine

In order to measure the change of anterior and posterior separation, small sensors were attached to the C2 to C7 vertebrae. The sensors are weightless so they do not affect the movement of the spine. The sensors were attached to the C3, C4, C5 and C6 vertebrae in four positions, namely Anterior Superior, Anterior Inferior, Posterior Superior and Posterior Inferior. In C2, only the inferior side had sensors attached. In C7, only the superior side had sensors attached. The positions of the sensors are described in Figure

20. Since the sensors moved along with the vertebrae, the intervertebral space between each vertebra could be acquired by simply measuring the distance between the sensors.

3.2.6   Simulation Experiment

Simulation runs were performed using various traction angles, forces and positions. In each run, both the anterior and posterior separations between C2-C7 vertebrae were measured. Traction angle between $10°$ and $40°$ and traction force between 60N and 200N were used. The traction force was applied within the first 60 seconds of the simulation as a ramping function until it reached the target force and remain constant. Both positions were tested under the same environment, i.e. all the material properties, stiffness and damping parameters of the mechanical joints were the same for both positions.

The terms "intervertebral compression" and "intervertebral separation" represent the total amount of disc space changes in the intervertebral joint between C2 and C7, before and during traction. It does not represent the actual total disc space. In other words, $\Delta C27 = \Delta C23 + \Delta C34 + \Delta C45 + \Delta C56 + \Delta C67$. Positive amount of changes indicates separation and negative amount of changes indicates compression.

3.3 Results

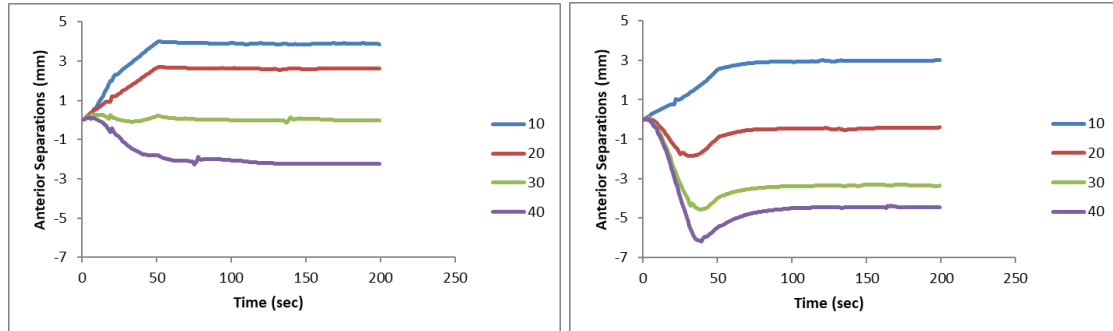### 3.3.1 Time responses of Intervertebral Separations

Figure 21. Changes of anterior separations at 160N in inclined (left) and sitting (right) positions
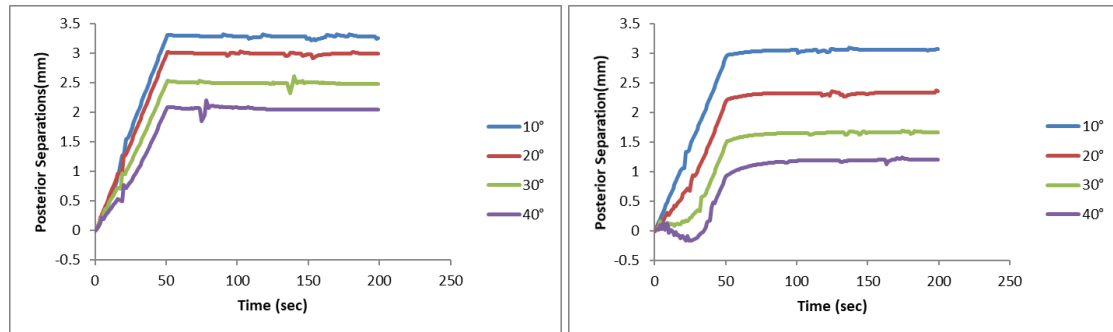

Figure 22. Changes of posterior separations at 160N in inclined (left) and sitting (right) positions

The changes of the anterior and posterior separations are shown in Figure 21 and Figure 22. Only the results from 160N are presented since the observed time response behaviors are similar with different traction forces. The measurement represents the overall combined disc space changes from C2 to C7. On the anterior side in Figure 21, negative separations occurred when traction angles increase. The negative dips were much more noticeable in the sitting position compared to the posterior case. Traction angle at 10° resulted in the largest separations while 40° traction angle resulted in compressed cervical spine. Similarly, the posterior side of the sitting position in Figure 22 also show small dips at the beginning of the test at the 30° and 40° lines. The dips become more apparent as the traction angle increases. When traction angle is at 40°, posterior compression was observed, indicating that the spine was in extension. Posterior Compression was not observed in the inclined position. The largest posterior separation was achieved at 10° and the smallest at 40°. The inclined position led to larger separations

in all traction angles when compared to the sitting position. The transformation of the cervical spine in inclined and sitting positions at 10° and 40° are shown in Figure 23 and Figure 24. Based on the figures, one can see that the cervical spine has a smaller movement in the inclined position than in the sitting position, thus may lead to a more stable traction.
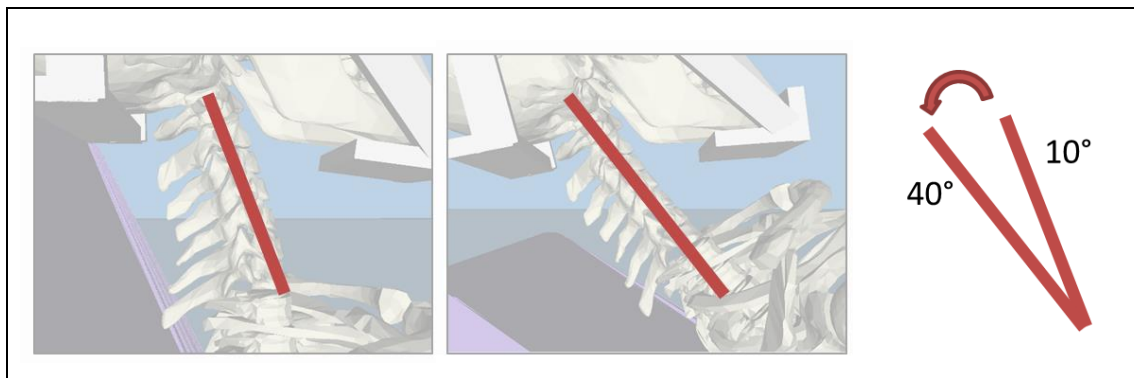
Figure 23. Inclined position at 10° (left) and 40° (right)
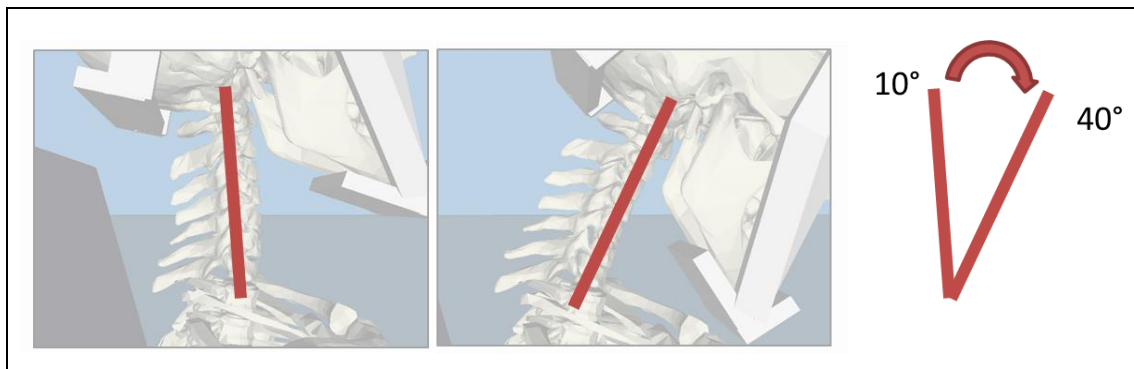
Figure 24. Sitting position at 10° (left) and 40° (right)

3.3.2 Change of Intervertebral Separations at Each Cervical Segment
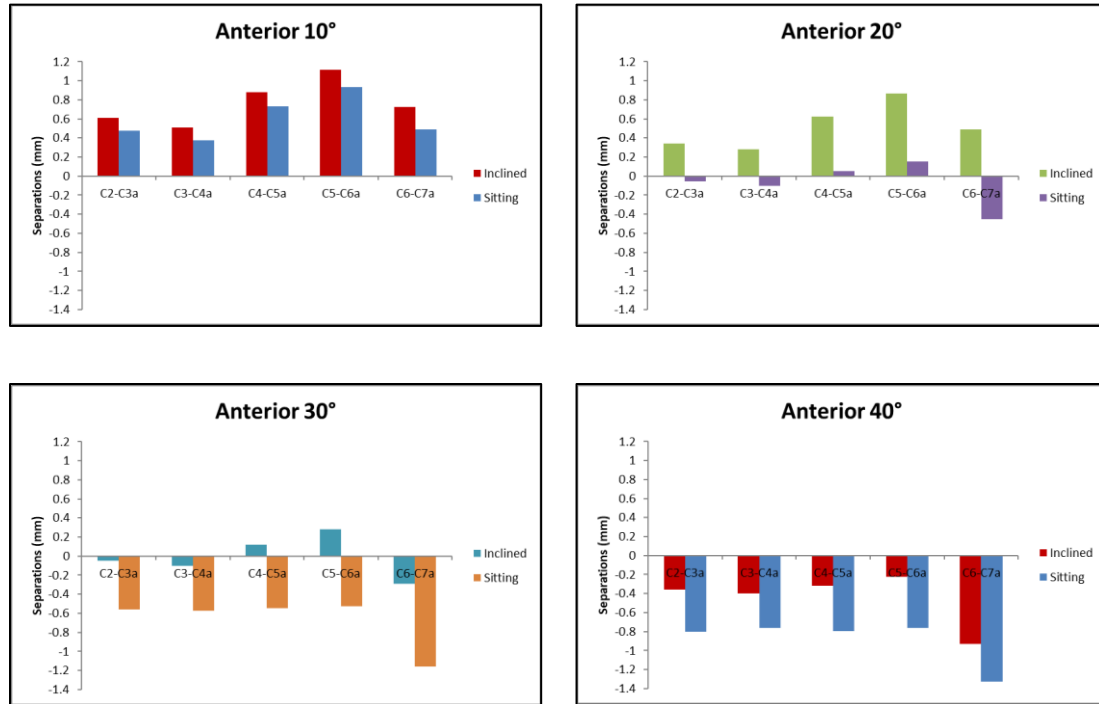
Figure 25. Changes of anterior separations at 10/20/30/40°

Figure 25 shows the changes of segment separations from C2 to C7 on the anterior side. The largest separations were at 10° and they gradually turned to negative as the traction angle increased. In all cases, the segment C5-C6 extended the most, followed by the segment C4-C5 and then C6-C7. The inclined position achieved larger separation and the sitting position achieved large compression.
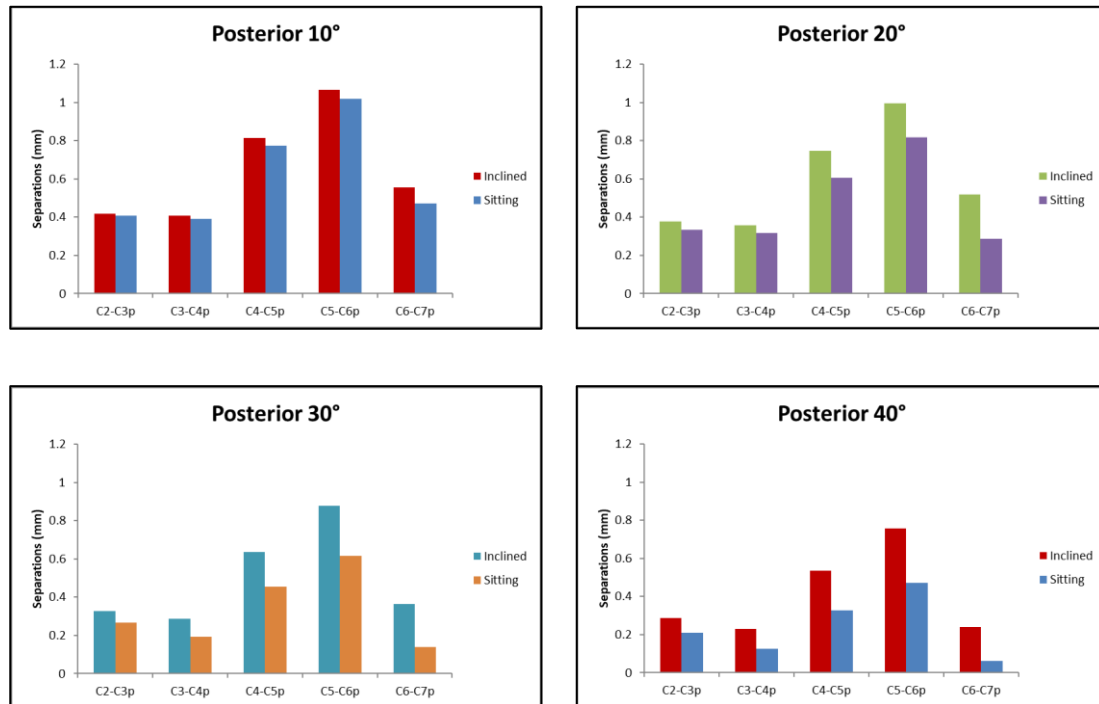
Figure 26. Changes of posterior separations at 10/20/30/40°

The posterior results are shown in Figure 26. Again, the segment C5-C6 achieved the highest separation, followed by C4-C5 and C6-C7. The inclined position was found to achieve larger separations than the sitting position. At 40°, the C6-C7 segment in the sitting position achieved the smallest separation.

3.3.3 Traction Angles and Traction Forces

The separations caused by combinations of traction angles and traction forces were compared. Figure 27 shows the anterior space changes in the inclined and sitting positions. Anterior compression can be found in both positions. The cervical spine was always compressed further in the sitting position in all combinations of angle and force when compared to the inclined position. Figure 28 shows the posterior separations. On the posterior side, the inclined position was able to achieve a larger separation than the sitting position. When the traction force was small, the sitting position recorded a negative separation in the 30° and 40° cases.
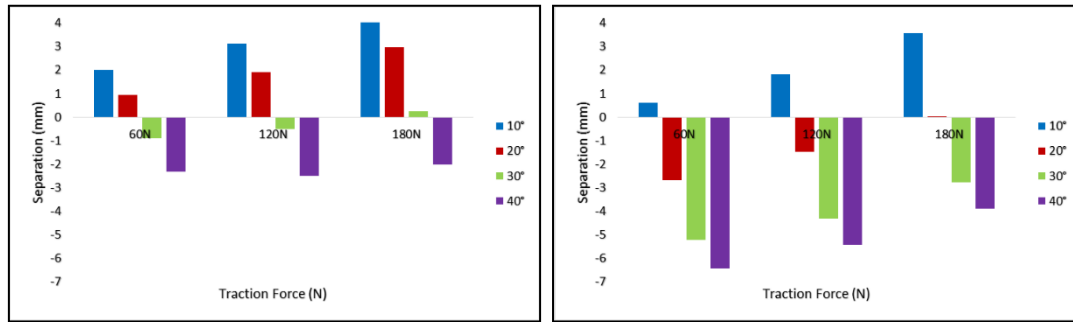
Figure 27. Traction angle vs force on anterior in inclined (left) and sitting (right) position
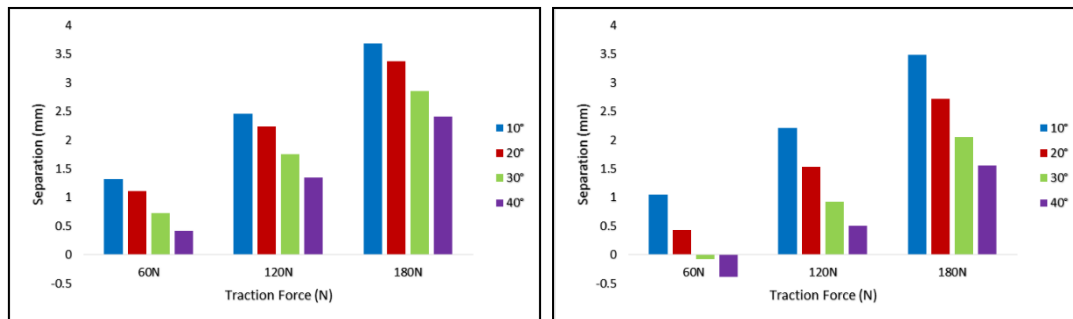
Figure 28. Traction angle vs force on posterior in inclined (left) and sitting (right) position

3.4 Discussion

The small dips in the sitting position measurements in Figure 21 and Figure 22 are likely related to the forward leaning motion of the body during the traction therapy. In the simulation when traction starts, the subject's lower body stays in the chair due to friction between the lower body and the chair. At this moment, the hip turns and the upper body gradually leans forward as the traction force increases. In the inclined position with the subject lying on a chair at an angle, gravity helps to keep the back of the body remain in contact with the chair. The hip does not turn and the neck did not over bend as in the sitting position. This observation agreed with Ito's study [15], which concluded that anterior separations become negative when traction angle goes beyond 20°.

Regarding the segmental separations in Figure 25 and Figure 26, the segment C5-C6 was extended the most, followed by the segment C4-C5 and then C6-C7. These results

also agreed with Ito's result [15]. However, since Ito's study was conducted in supine position, we cannot be certain if the behaviour of our cervical spine model is correct.

The weight of the head may contribute to the negative separation in the 60N case in Figure 27 and Figure 28. In the sitting position, the head exerts a constant downward force to the cervical spine due to gravity. Since the traction force is at only 60N, there is very little force to pull the head upward. As the body leans forward in the sitting position, both anterior and posterior sides become compressed. Another interesting observation was that the anterior separations reached -6mm in the sitting position at 40° in Figure 21, indicating a substantial anterior compression. In contrast, the inclined position only showed a 2 mm compression under the same condition. On the posterior side, the inclined position was able to achieve a larger separation in all combinations of angles and forces. This may be an indication that the sitting position was adding too much pressure on the anterior side and yet not able to achieve the posterior separations. Overall, the result suggested that using the inclined position provides a larger separation in both the anterior and posterior sides compared to the sitting position.

As a first step in building a multi-body simulation model for cervical traction therapy, Model 1 provided a straightforward comparison on how different traction angles, forces and traction positions affect the change in intervertebral space between each vertebra. However, there are several limitations in Model 1. First of all, the model used a simplified model to represent the combined behavior of the neck muscles, joint facets, ligaments and the intervertebral discs in the cervical spine. As a result, this model does not account for the overall anterior and posterior difference in stiffness in the whole cervical spine. Most importantly, due to the lack of experimental data in the sitting and inclined position, we could not validate the behavior and accuracy of the model. Model 1 also does not simulate the transient state of a stretched intervertebral disc resulted from traction therapy. Thus, it cannot compare the effect of continuous traction and intermittent traction.

3.5 Summary

In this chapter, we developed a multi-body simulation model to investigate the effects of the inclined and sitting positions on the intervertebral separations during cervical traction. Using Model 1, the anterior and posterior intervertebral separations were measured in a number of scenarios using different amount of traction forces and angles. In the simulation, we observed that the sitting position leads to excessive compression at the anterior side at large traction angles and unnecessary upper body forward movement. In contrast, the inclined position achieved larger intervertebral separations than the sitting position in all combinations of traction forces and angles. This suggests that the inclined position may be more effective in increasing intervertebral separations. Also, the overall transformation of the cervical spine was smaller in the inclined position, thus suggesting that the position can lead to more stable traction. Since the simulation model has not been validated with experimental data, we cannot be certain of the accuracy of the cervical spine behavior. The next chapter will describe the radiographic experiment that collects cervical traction clinical data to evaluate the behaviour of the Model 1.

Chapter 4.

Comparative Experiment and Multi-body Simulation of Cervical Traction Therapy in Inclined and Sitting Positions

4.1   Introduction

Although Model 1 was built based on biomechanical parameters referenced from published literatures, these parameters may not fully reflect the actual behavior of the cervical spine in the inclined and sitting positions. Thus, the objective of this chapter is to conduct a radiographic experiment and investigate the actual intervertebral separations during cervical traction therapy in inclined and sitting positions with human subjects. The acquired data will then be used to evaluate the behaviour of Model 1. The first part of the chapter describes the radiographic experiment setup and the findings of the experiment. In the second part, the collected data is used to evaluate the behaviour of Model 1.

4.2   Methods

4.2.1   Radiographic Experiment Setup

The radiographic experiment consisted of six asymptomatic Japanese male adults. The age groups (30s x 2, 50s x 2, 60s x 2) of the subjects were chosen as such to allow us to investigate the influence of age differences in cervical traction. All subjects reported that they did not have history of cervical-related injuries or related disorders. The experimental procedures and potential risks were explained to all subjects and signed consent forms were obtained before the experiment. Two mechanical traction devices [5][6] were set up in a laboratory for radiographic assessments, and they represented the inclined and sitting positions respectively.

Figure 29. Cervical traction in inclined position during radiographic experiment.

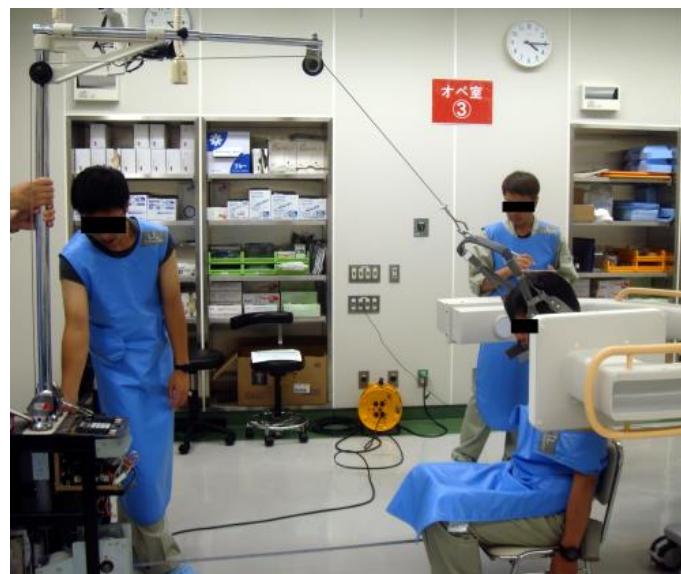**Figure 30. Cervical traction in sitting position during radiographic experiment.**

Figure 29 and Figure 30 show subjects in inclined and sitting positions during the experiment. The radiographic system (Model: Veradius Neo, Koninklijke Philips N.V.) used in the experiment consisted of a C-arc arm that takes radiographic images and videos of a subject who is seated on a traction device. The experiment was conducted in an X-

ray laboratory under the supervision of a medical doctor and a radiologist. The study was approved by an ethics research committee of Kobe University prior to data collection.

In the inclined position, the subject sits on a motorized seat with his head attached to the halter. By rotating the seat around the horizontal axis along the sagittal plane, traction angles between 10° and 40° can be achieved. In the sitting position, the subject sits up right on a fixed chair with his head attached to a head halter. Traction angles are adjusted by changing the length of the top metal bar. The head halter included two straps offering support to the chin and occiput during cervical traction. The mechanical movement of the two traction devices are illustrated in Figure 31. On both devices, the vertex of the traction angle was set at the base of the neck, near the position of the first thoracic vertebra (T1).
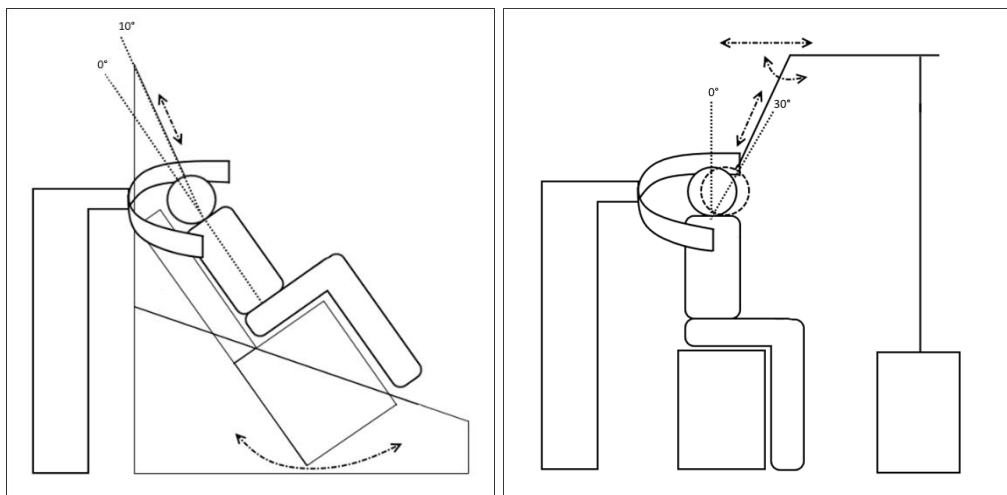
Figure 31. Experiment setup for inclined (left) and sitting (right) position. The C-arc arm system acquired image from the subject's cervical spine.

The experiment was completed in one day and was divided into nine sessions as shown in Table 5. Out of the six subjects, three were tested on both devices and they were given at least one hour to rest before they received the next round of traction. The traction force was set to 20% of the subject's body weight. Traction angles 10°/20°/30°/40° were used in the experiment.

Table 5. Experiment Setup for Each Subject

Subjects	Traction Positions		Traction Force	Traction Angle
	Inclined	**Sitting**		
30A	O	Not tested	100N	10°/20°/30°/40°
30B	Not tested	O	130N	10°/20°/30°/40°
50A	O	O	140N	10°/20°/30°/40°
50B	O	O	150N	10°/20°/30°/40°
60A	O	O	140N	10°/20°/30°/40°
60B	Not tested	O	160N	10°/20°/30°/40°

In each session, the subject sat in a traction machine for approximately 10 minutes. Each session contained four sets of traction. At the beginning of each traction, our team first adjusted the machine to reach the designated traction angle with the subject sitting in the traction machine. Then traction force is applied and maintained continuously. After around 10 seconds, the force is released and the subject is asked to rest and prepare for the next angle. The procedure repeats until all four sets of traction angles are tested. Figure 32 illustrates the experiment procedure in each traction. Radiographic images were taken before and during traction. No subject reported discomfort during and after the experiment.
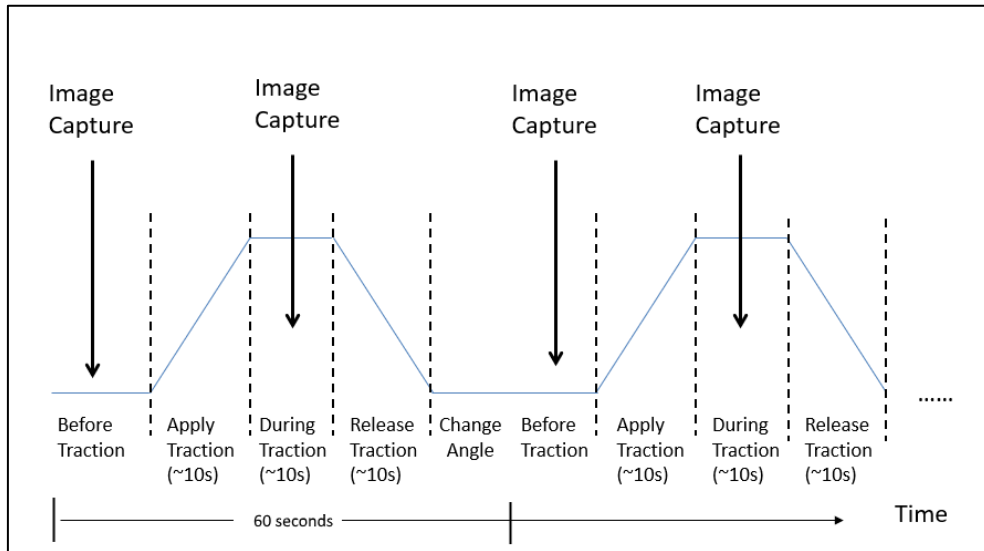
Figure 32. Experiment procedure in each traction

4.2.2   Radiographic Image Analysis

A total of 55 radiographic images were taken during the experiment. The digitalized images were in grayscale and had a resolution of 640 x 480. Some sample images are shown in Figure 33.
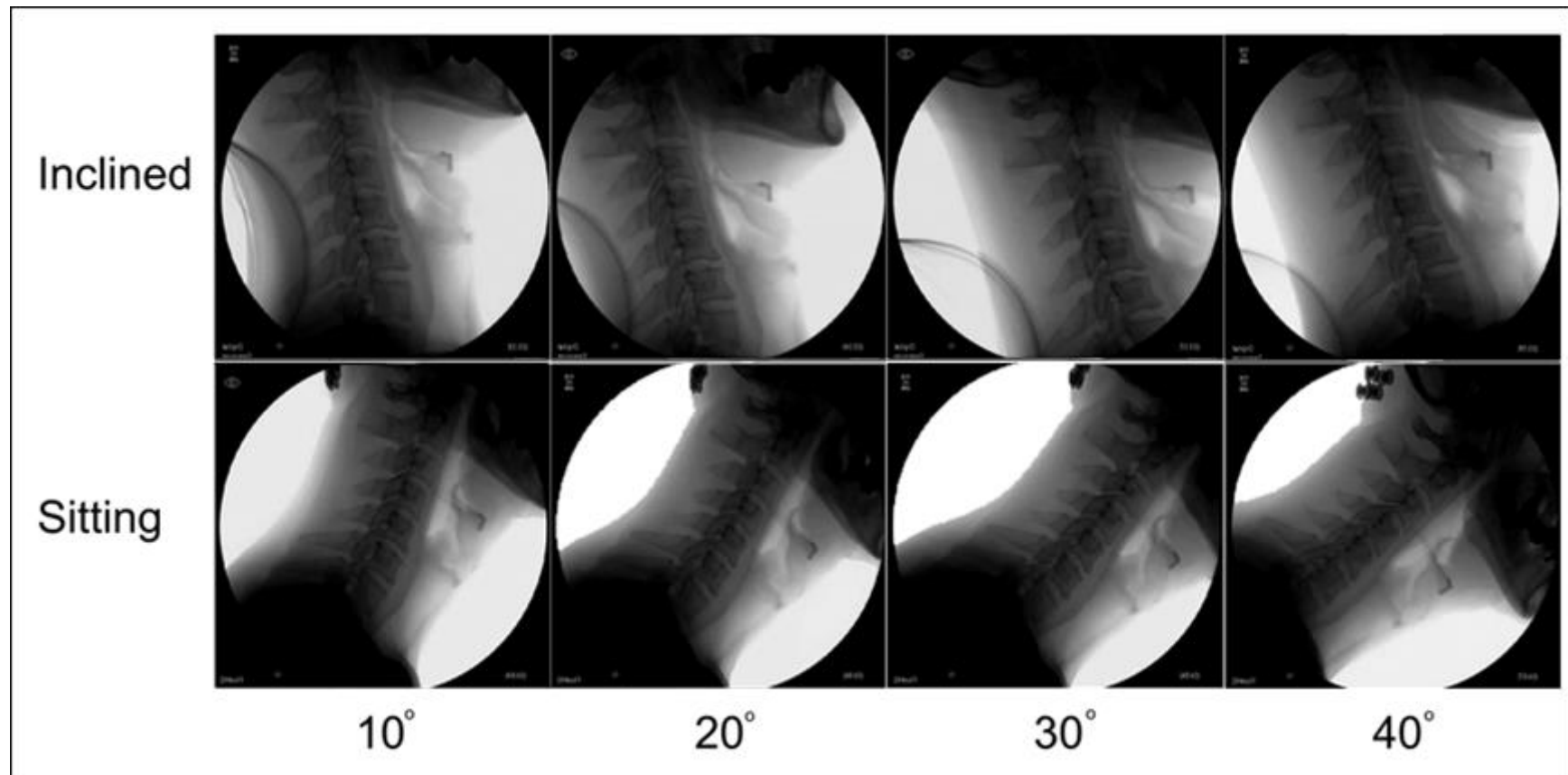
Figure 33. Radiographic images of the cervical spine taken during the experiment.

In order to improve the accuracy of the measurement, the low-resolution images were magnified using a technique called "image super-resolution" [43] to optimize picture quality. The anatomical identifications of the vertebral landmark were based on the method of Farfan et al. [44][45] as shown in Equation 2 and 3.

$$Anterior\ disc\ height = \frac{(A1+A2)}{2} \tag{2}$$

$$Posterior\ disc\ height = \frac{(P1+P2)}{2} \tag{3}$$

Figure 34 illustrates the modified Farfan's method used in the image analysis. A1/A2/P1/P2 are straight lines extended from point A/B/C/D and are perpendicular to the two horizontal lines joining the A-B and C-D points. The contrast and brightness level of the image were fine-tuned using ImageJ [46] and the vertebral landmarks were then manually traced using Inkscape [47]. All the images were measured three times digitally and the mean values of the three measurements were taken as the final result of each image.
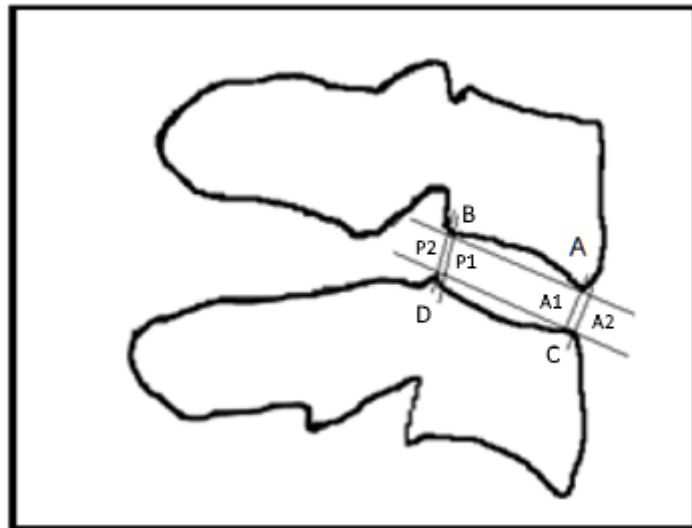
Figure 34. Measurement of disc space using a modified version of Farfan's method [44][45]

4.3   Results

4.3.1   Intervertebral Separations of Individual Subjects

This section describes the results of three test subjects (50A, 50B, 60A), who were all tested in both sitting and inclined positions.

Figure 35. C2-C7 disc spaces vs traction angles for 50A (left: inclined, right: sitting)

Figure 35 shows the anterior and posterior changes for subject 50A in both sitting and inclined positions. The measurement represents each disc space before and during traction at all the tested traction angles. In the inclined position, one can see that the increase of traction angle caused larger separation on the posterior side and compression in the anterior side. The overall change demonstrated an almost linear behaviour as traction angle increases. In the sitting position, the shortest disc space was at 20° anteriorly. For

the posterior side, the disc space at 20° was smaller than the ones at 10° and 30°. As a result, we failed to observe a consistent linear behavior in the sitting position.

Figure 36. C2-C7 disc spaces vs traction angles for 50B (left: inclined, right: sitting)

Figure 36 shows the result for subject 50B. Similar to the result of 50A, the result of the inclined position in 50B also demonstrated a linear change in relation to the traction angles. On the anterior side, the disc space reduced as traction angle increased. On the posterior side, the disc spaces increased along with traction angles. However, at 40°, the posterior side was slightly shorter than the one at 30°. For the sitting position, both the anterior and posterior disc spaces decreased at 30°.
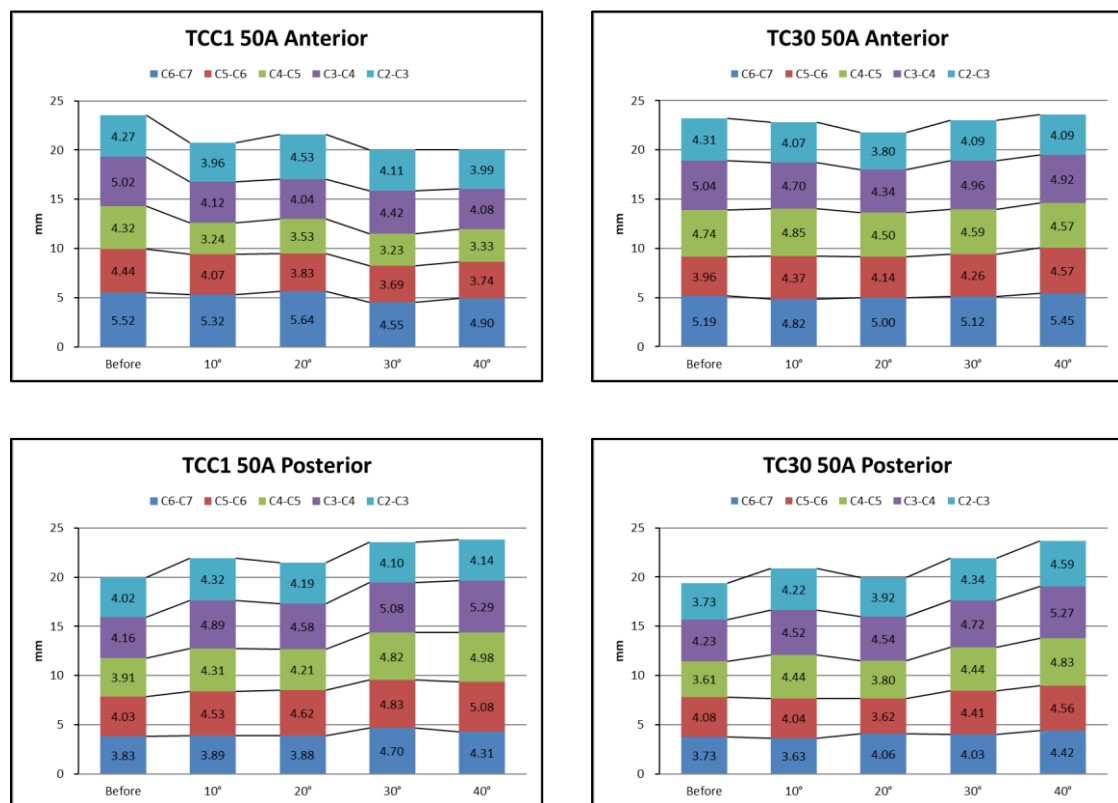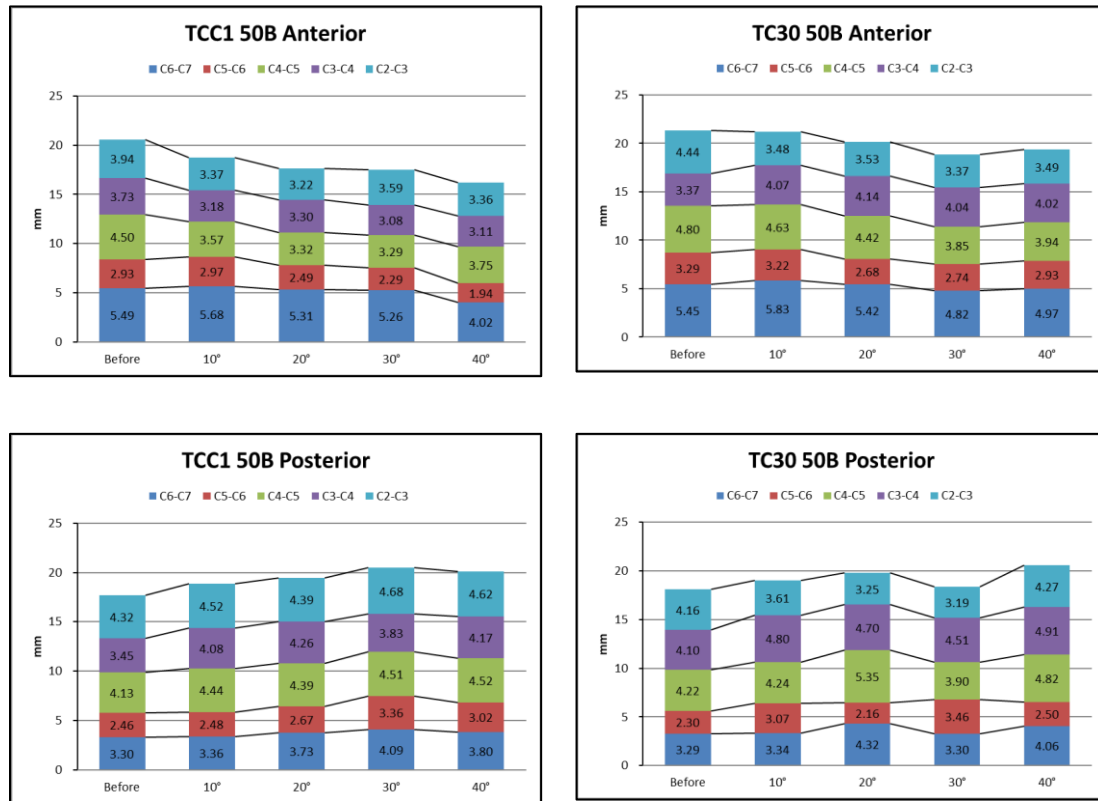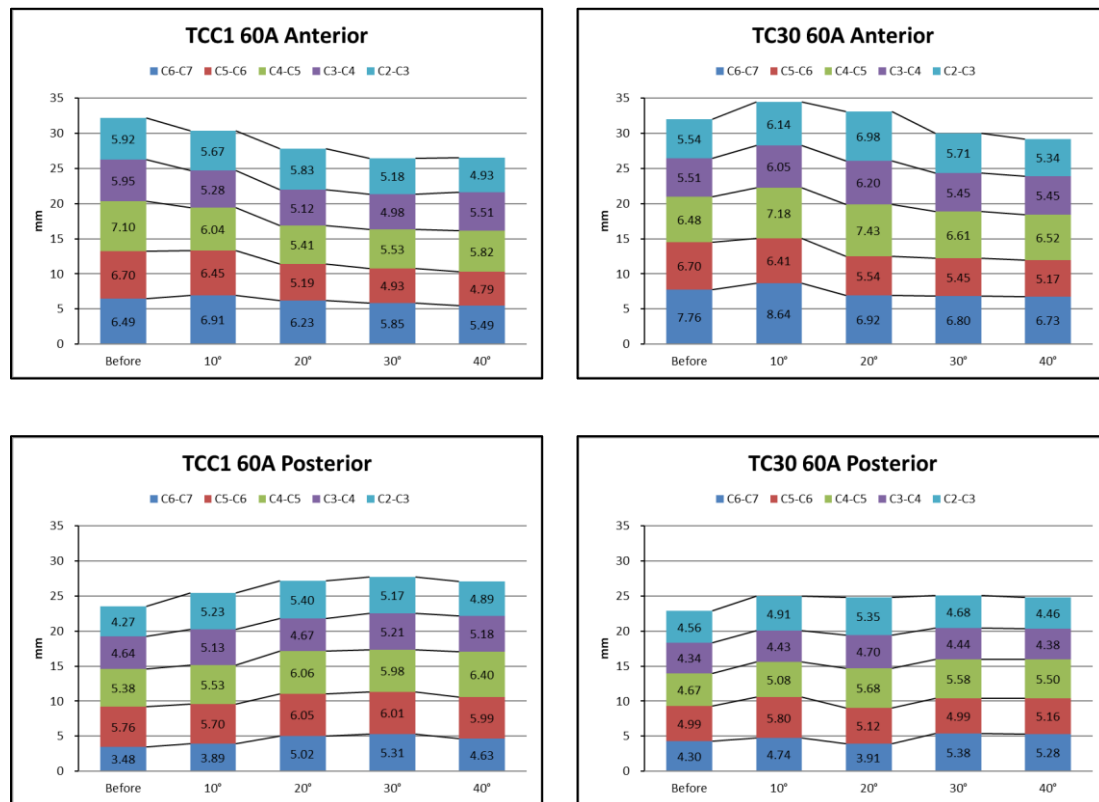
Figure 37. C2-C7 discs spaces vs traction angles for 60A (left: inclined, right: sitting)

Figure 37 shows the result for subject 60A. For the sitting position, the anterior disc spaces at 10° and 20° was actually larger than the one before traction. The spaces then decreased linearly as traction angle increased. However, the posterior result shows that there were almost no changes in separations when traction angles varied for this subject. Similar to previous two subjects, the anterior disc spaces at the inclined position demonstrated consistent and linear behavior. The posterior disc spaces also behaved linearly until traction angle reached 40°.

The mean values of anterior and posterior intervertebral disc space changes for the three subjects are summarized in Table 6. Space changes refers to the difference in C2-C7 disc space between before traction and during traction. The data was based on the three subjects that were tested in both devices. In general, there were significant changes for most of the angles in the inclined position (P < 0.05 for all except P = 0.054 at 20° anterior). In the sitting position, however, our results showed no statistically significant changes for all traction angles.

Table 6. Mean Changes of Intervertebral Disc Spaces in Inclined and Sitting Positions

Position (n = 3)	Traction Angle	Side	Space Change Mean (mm)	SD	Paired t-test P value
Inclined Position	10°	Anterior	2.53	0.27	< 0.05
		Posterior	2.03	0.16	< 0.05
	20°	Anterior	3.35	1.40	0.054
		Posterior	2.51	0.97	< 0.05
	30°	Anterior	4.56	1.46	< 0.05
		Posterior	3.76	0.79	< 0.05
	40°	Anterior	4.78	1.29	< 0.05
		Posterior	3.70	0.19	< 0.05
Sitting Position	10°	Anterior	0.74	0.89	0.193
		Posterior	0.70	0.81	0.183
	20°	Anterior	0.98	0.66	0.059
		Posterior	0.83	0.86	0.148
	30°	Anterior	1.12	1.20	0.158
		Posterior	1.13	1.25	0.169
	40°	Anterior	1.21	1.21	0.140
		Posterior	1.89	1.77	0.122

4.3.2　　Mean Changes of Intervertebral Separation
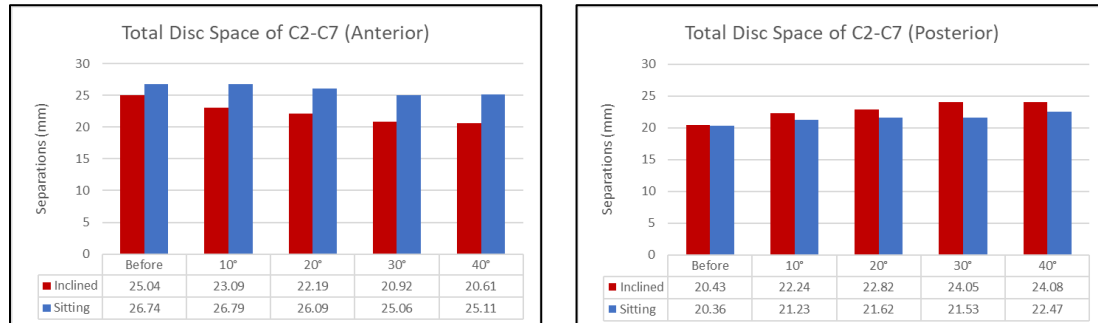
Figure 38. Total disc spaces of C2-C7 vs. traction angles (left: anterior, right: posterior)
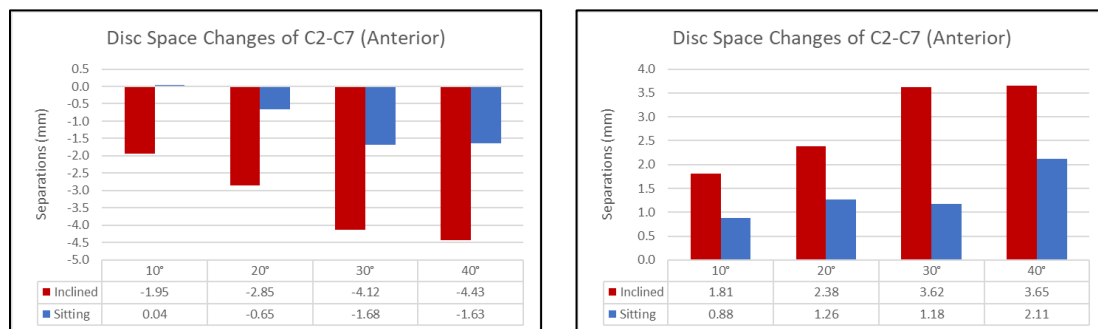
Figure 39. Disc space changes of C2-C7 vs. traction angles (left: anterior, right: posterior)

The data from all six subjects were combined to show the mean changes between the two traction positions. Figure 38 shows the total disc spaces (C2-C7) for each traction angle. Figure 39 shows the differences before traction and during traction. As illustrated in both figures, the inclined position yielded a larger change on both the anterior and posterior sides. In addition, the result also shows that sitting position at 30° behaved inconsistently compared to 20° and 40°.

4.3.3　　Posterior Changes in Cervical Segment

Since doctors and therapists often want to increase disc space only to a specific segment of the cervical spine, it is important to examine the segment changes in the experiment results. A traction technique that can accurately and reliably increase disc space at a specific segment, such as C4-C5, will be of great importance. The mean

intervertebral separations of each cervical segment for all six subjects are presented in Table 7 and Table 8. These figures represent the changes in disc space between before traction and during traction for each traction angle. Since the anterior side contains mostly compression, this section will focus on the posterior changes, which increase disc space.
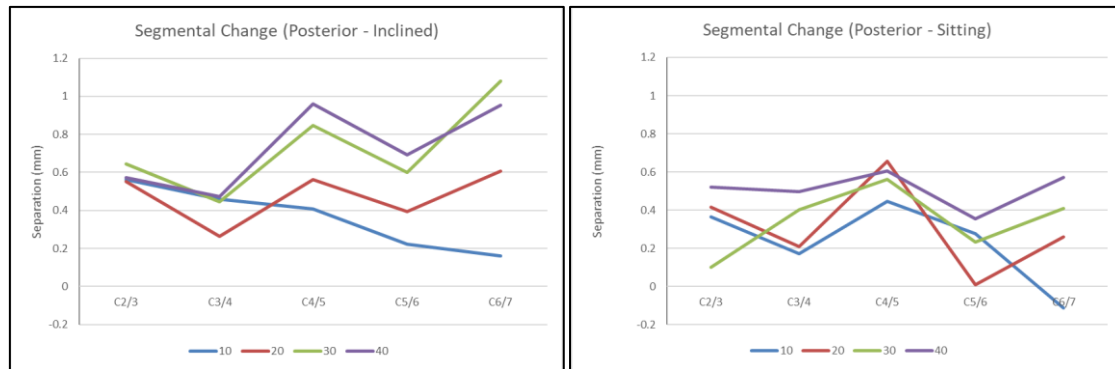
Figure 40. Posterior change by cervical segment (left: inclined, right: sitting)

Figure 40 illustrates the posterior data presented in Table 7 and Table 8. One can see that the overall changes in the sitting position is smaller than the ones in the inclined position. In the sitting position, the C45 segment always achieves the largest change regardless of the traction angles. On the other hand, the data in the inclined position exhibits two patterns based on the traction angles. With traction angle at 10°, the C23 segment achieves the largest changes, while the C67 segment achieves the smallest changes. Then at 20°/30°/40°, the trend reverses and the disc spaces extend proportionally to the traction angles. In a previous study, Ito et al. [15] examined the relationship between traction angles and cervical segment changes. Their work concluded that small traction angles (10°/20°) can extend posterior disc space in the upper spine, and large traction angles (30°/40°) can do the same for the lower spine. The data in the inclined position agrees with their results.

Table 7. Mean Segment Changes in Inclined Position

Side	Segment	Traction Angles			
		10°	20°	30°	40°
Anterior	C23	-0.33	-0.05	-0.44	-0.34
	C34	-0.69	-0.82	-0.84	-0.96
	C45	-0.80	-0.93	-1.09	-0.83
	C56	-0.22	-0.66	-0.96	-1.09
	C67	0.09	-0.40	-0.80	-1.21
	Total	-1.95	-2.85	-4.13	-4.43
Posterior	C23	0.56	0.55	0.65	0.57
	C34	0.46	0.27	0.44	0.47
	C45	0.41	0.56	0.85	0.96
	C56	0.22	0.40	0.60	0.69
	C67	0.16	0.61	1.08	0.95
	Total	1.81	2.38	3.62	3.65

Table 8. Mean Segment Changes in Sitting Position

Side	Segment	Traction Angles			
		10°	20°	30°	40°
Anterior	C23	0.08	0.18	-0.15	-0.20
	C34	0.05	0.00	-0.08	-0.01
	C45	0.16	0.09	-0.18	-0.39
	C56	0.10	-0.25	-0.33	-0.28
	C67	0.02	-0.36	-0.31	-0.42
	Total	0.39	-0.34	-1.06	-1.28
Posterior	C23	0.36	0.42	0.10	0.52
	C34	0.17	0.21	0.40	0.50
	C45	0.45	0.66	0.56	0.61
	C56	0.28	0.01	0.23	0.35
	C67	-0.11	0.26	0.41	0.57
	Total	1.15	1.55	1.70	2.55

4.3.4   Transformation of the Cervical Spine in Experiment

In this section, we compared the movement of the cervical spine during traction between the two positions. As illustrated in Figure 41 and Figure 42, the cervical spine underwent different transformations in the two positions. With the rotating chair mechanism in the inclined position, the outline of the radiographic images shows only a small movement. On the contrary, the transformation in the sitting position was comparatively larger, even though the sitting position yielded a smaller mean change in both anterior and posterior sides with all four traction angles. The relatively small transformation in the inclined position help to maintain stability and this may have contributed to the overall improvement in the intervertebral separations. When compared to the simulation result of Model 1, one can see that the transformations of the cervical spine agree between the model and the experiment result.
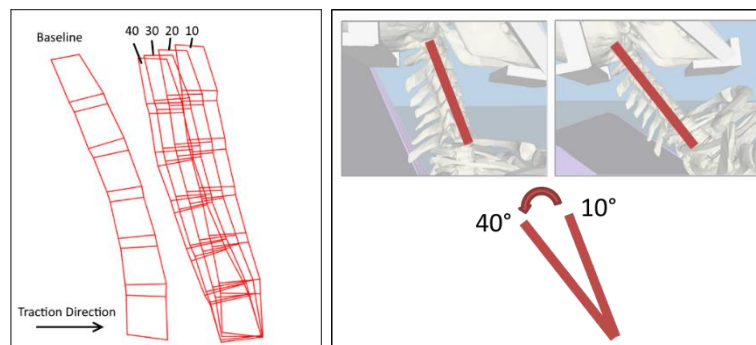
Figure 41. Cervical spine transformation in inclined position (left: experiment, right: Model 1)
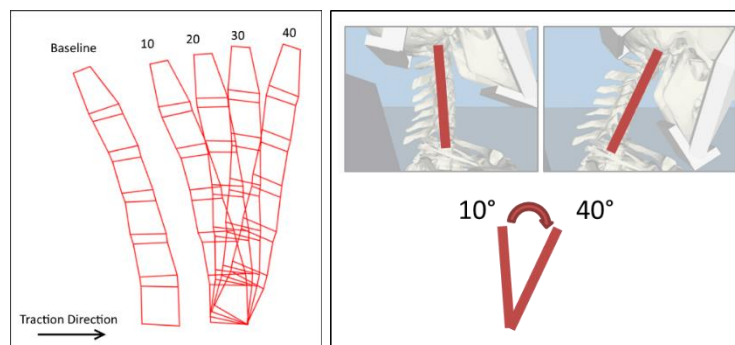
Figure 42. Cervical spine transformation in sitting position (left: experiment, right: Model 1)

4.3.5   Age Difference vs. Intervertebral Separation Changes

The six subjects were chosen such that their age differences in response to traction at various angles can be examined. Since intervertebral discs tend to lose water content in elderly subjects [48], it was expected that their intervertebral separations would be different from the ones in younger subjects. However, due to the limited sample size in the experiment, we were not able to observe a significant difference. Among the subjects using the inclined position, 60A has the largest compression and extension, while 30A recorded the smallest changes. Conversely, data from the sitting position did not yield any significant differences between older and younger subjects.

4.3.6   Disc Space Change Due to Traction Force and Angles
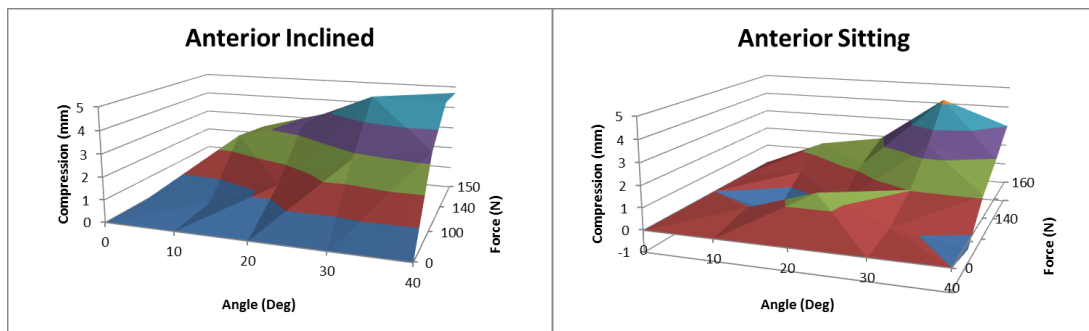
Figure 43. Anterior compression caused by traction force and traction angle
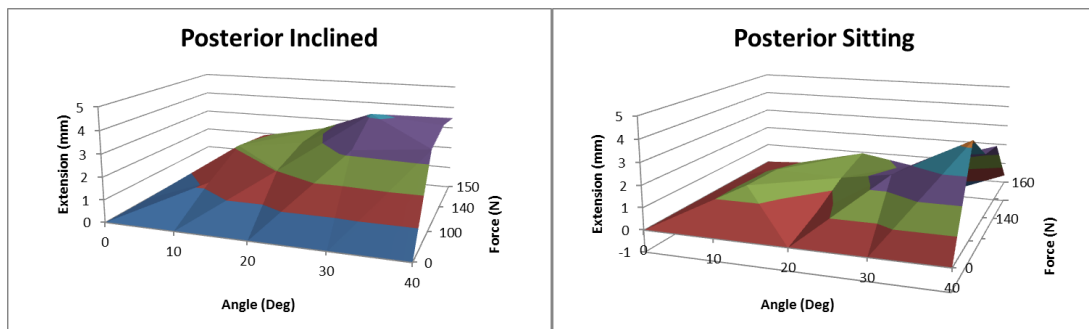
Figure 44. Posterior separation caused by traction force and traction angle

Figure 43 and Figure 44 illustrate the compression and separation of the intervertebral disc space due to traction force and angles. In the inclined position, both the anterior and

posterior sides exhibited a smooth transition as the force and angle increase. On the other hand, the transition was uneven for the sitting position on both sides. In fact, larger traction force actually resulted in smaller separation on the posterior side. It suggests that it is more difficult to control separations in the sitting position with traction force and angles.

4.4   Simulation Model of Cervical Traction Therapy

The cervical traction model, Model 1, is a multi-body simulation model consisted of a cervical spine, a skeleton body and two mechanical traction devices, representing the inclined and sitting positions respectively. Originally, it was developed using Vortex Dynamics, a commercial physics engine developed by CM Labs. Although the physics engine was capable of running the simulation described in Chapter 3, the software license was locked to the computer's hardware configuration. In addition, the outdated software often crashed when the simulation model became more complex. Since CM Labs no longer supported transferring the Vortex license to another computer, a decision was made to re-create the simulation model using an open source physics engine, the Bullet Physics Library [34]. This new engine was free and was capable of running the simulation on a more powerful computer. The development environment was also updated to Visual Studio 2015 on a Windows 7 computer (Windows 7 Enterprise, I7-3930K 3.2 GHz 32GB ram). The programming language is C++.

4.4.1   Cervical Spine and Skeleton Body Model

The cervical spine model developed in Chapter 3 [49] was re-modelled with the new physics engine for performance improvement. It consisted of a skull and seven pieces of rigid cervical vertebrae (C1-C7). The C2-C7 cervical vertebrae were attached to adjacent vertebrae by a pair of translational and rotational joint with separated stiffness and damping parameters to control its movement. The C7-T1 joint was fixed. In order to simplify the model, rotation and lateral flexion were disabled, leaving only vertical

movement, flexion and extension in each joint. The skeleton body model included the rest of the body below the cervical spine and was modelled as separated rigid bodies. All the 3D models used were retrieved from Anatomography/BodyParts3D [29]. The body segment mass ratio was configured based on the data from Zatsiorsky et al. [38]. The body model was set to be 1.74m and 73kg. The mass configuration was the same as the model used in Chapter 3. The starting values for stiffness and damping at each intervertebral joint were referenced from previous literatures [22][23].

4.4.2 Traction Device Models

The two traction device models were built using Visual Studio 2015, C++ and the Bullet Physics Library [34]. The dimensions and the mechanical movement of the device models followed the same traction devices [5][6] used in the radiographic experiment and they represented the inclined and sitting positions. Figure 45 shows the inclined and sitting position simulation models at 10° and 40° traction.
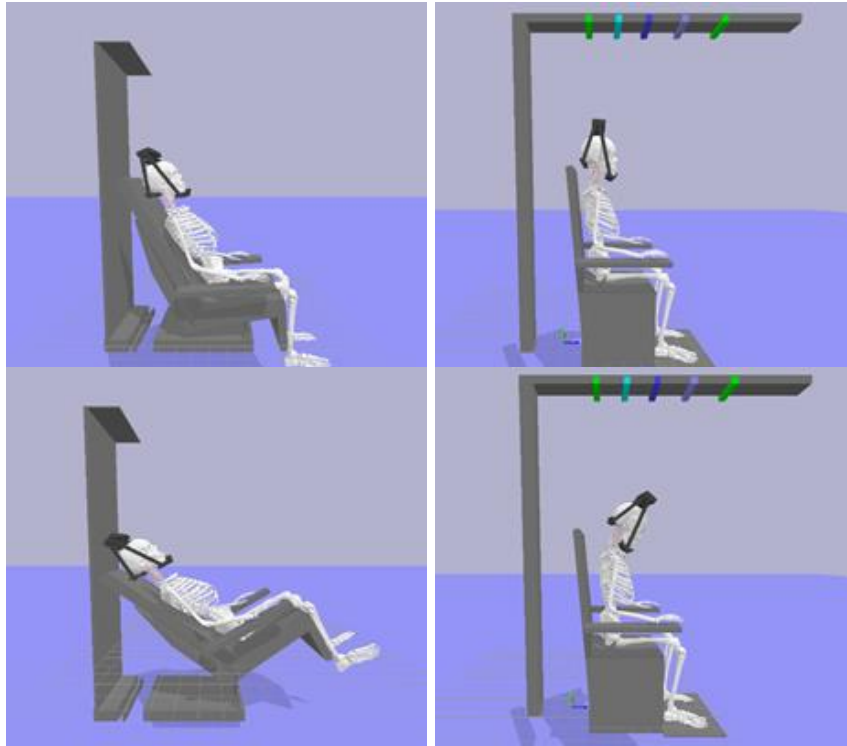
Figure 45. Cervical traction simulation models (Top-left: inclined 10°, top-right: sitting 10°, bottom-left: inclined 40°, bottom-right: sitting 40°).

4.4.3 Simulation Setup

Since the timing of the simulation model used in Chapter 3 was different from the experiment, the simulation result needs to be re-run in order to match the experiment setup. The traction force was applied incrementally as a ramping function from 0N to the target force within a period of 10 seconds and remain constant afterwards. The period of each simulation trial was 15 seconds. Since the original range of motion were limiting the movement of the are also relaxed as de

4.4.4   Simulation Results
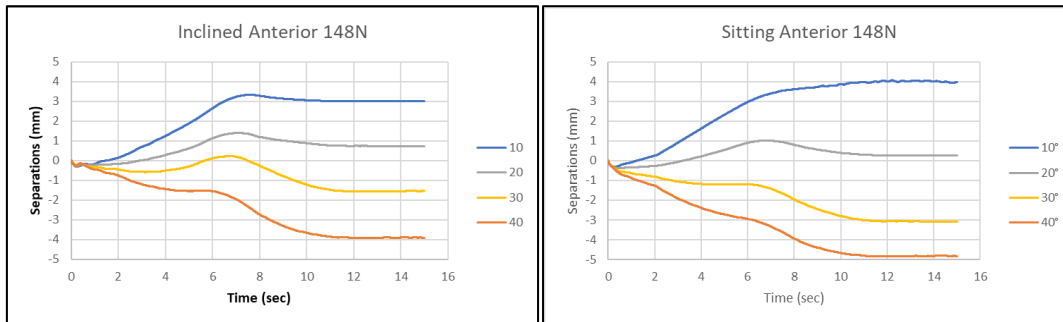
Figure 46. Changes of anterior separations at 148N in inclined (left) and sitting (right) positions
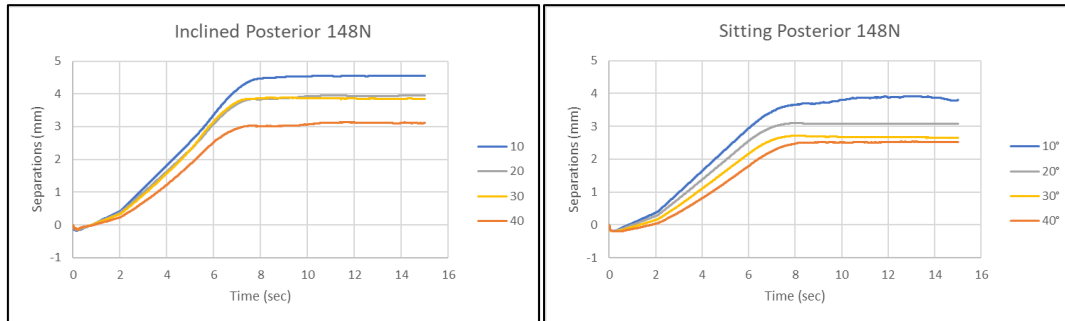
Figure 47. Changes of posterior separations at 148N in inclined (left) and sitting (right) positions

Figure 46 and Figure 47 show the time responses of the simulation results after the time adjustment. When compared to the experiment result, we can see that the simulation results showed different behaviour.
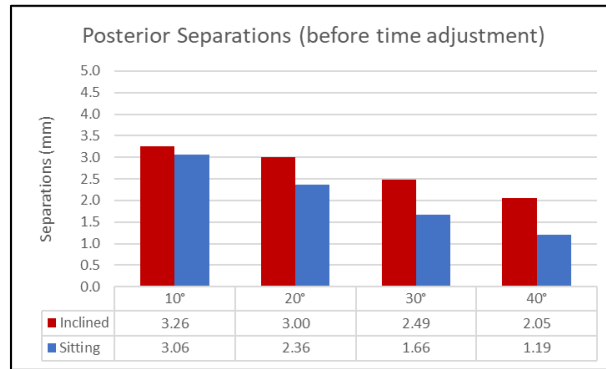
Figure 48. Posterior separations from simulation model (before time adjustment)
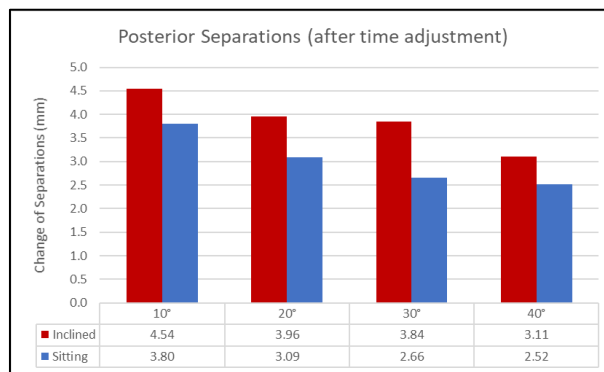
Figure 49. Posterior separations from simulation model (after time adjustment)
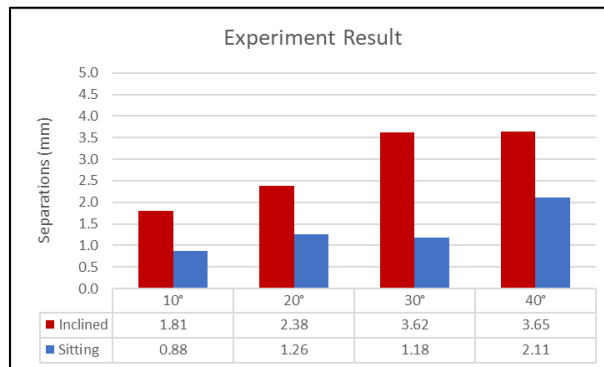
Figure 50. Posterior separations from experiment

Figure 48 and Figure 49 shows a comparison of the posterior separations from the simulation before and after time adjustment. With the application time of the traction force set to 10 seconds, the amount of posterior separations increased but the trend remains the same. The experiment data in Figure 50 shows that the posterior separations is the smallest when traction angle is at 10° and largest at 40° for both positions. That is,

the larger the traction angle, the greater the posterior separation. However, the simulation model shows the largest posterior separations at 10° and smallest at 40°.

4.4.5   Limited Intervertebral Separations in the Simulation Model

Upon examining Figure 21 and Figure 22, one can notice that the separations reached the maximum value before the traction force reached its target. One possible explanation is that the stiffness parameters was too small such that the vertebrae ran into the limit of the range of motion configured in the spring-damper constraints. In an attempt to investigate the behaviour, we increased the range of motions in the z-axis and re-ran the simulation. From Figure 51, we can see that the same amount of traction force is able to achieve even greater separations in the model. This behaviour could be observed in the inclined position.
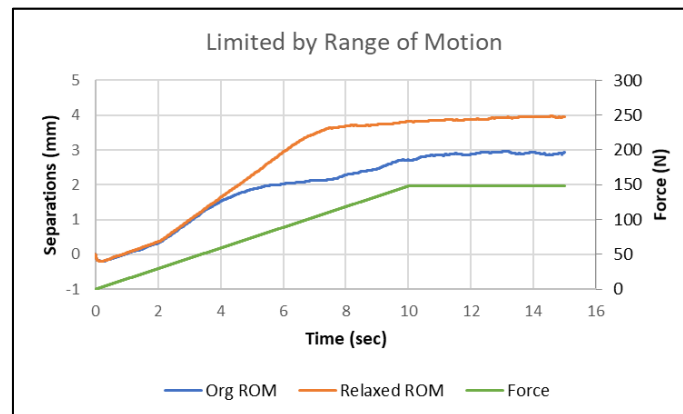
Figure 51. An example of separations limited by ROM

Although the simulation model was built with biomechanical parameters reference form published literatures, it is worth pointing out that the stiffness and damping parameters were derived from in vitro experiments, but the range of motion were in vivo parameters collected from volunteers [22]. As a result, it is likely that the in-vivo stiffness values are larger than the measured in-vitro stiffness, causing the cervical spine model to be too flexible. In order to address this problem, Jager's model [22] used the in vitro stiffness value as the starting parameters and later adjust the stiffness parameters with scaling factors when the simulation result was too flexible or too stiff during the

calibration stage. In future model, we will also consider to adopt this approach when calibrating the stiffness parameters. In this simulation, the ROMs were relaxed to allow the reduce the limitations.

4.4.6   Simulation Results with Modified parameters

Due to the different behavior revealed in the previous section, Model 1 was calibrated to match the measurements from the radiographic experiment. Since each cervical intervertebral joint was only represented by a pair of translational and rotational joints, the over-simplified structure made it difficult to calibrate to the experiment result. Extensive amount of time was spent to fine-tune the parameters of the model. The range of motion in the flexion/extension and tension/compression loading directions were changed to limit the separations. The translational and rotational stiffness parameters were also adjusted to promote posterior separation in the lower spine. The point of rotation of the rotational joints were also adjusted. Simulation trials were performed using the same traction angles, forces and positions as in the experiment. In each run, both the anterior and posterior intervertebral separations between C2-C7 vertebrae were measured. The traction force was set to be 20% of the subject, which yields 148N. The measured separations represent the changes of separation before and during traction applied. The simulation results are shown in Figure 52. The result shows a similar trend as the mean measurements from the experiment.
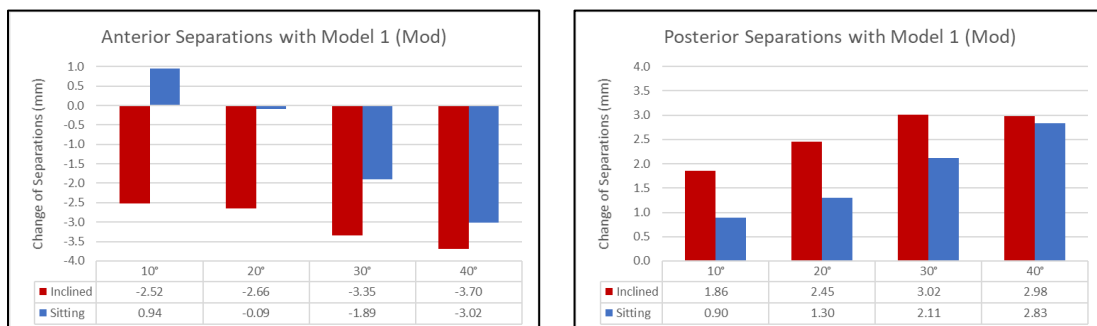
Figure 52. Simulation result of C2-C7 intervertebral separations. (Left: anterior, right: posterior)

4.5   Discussion

4.5.1   Forward Leaning Tendency in Sitting Position
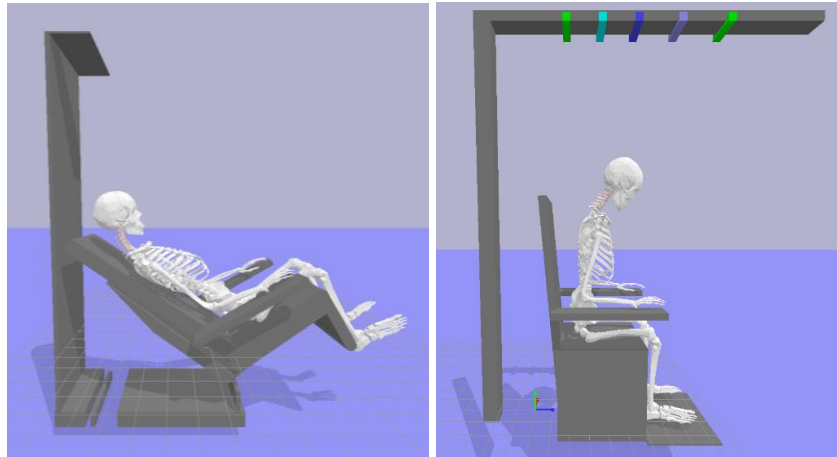
Figure 53. Subject leans forward at large traction angle (left: inclined, right: sitting)

In both the experiment and simulation with large traction angles, we observed that the subject in the sitting position always lean forward due to the pulling force as shown in Figure 53. This was not observed in the inclined position. Since the back of the skeleton body remained in contact with the back of the seat during the therapy, the inclined position was able to maintain the target traction angle throughout the session of the traction. This factor may help to explain the consistent and linear behaviour in the inclined position in the experiment data.

4.5.2   Discrepancy between the Simulation and Experiment result

The results of the Model 1 did not agree with the ones from the experiment. Although Model 1 was built using biomechanical parameters referenced from literatures and skeleton models based on anatomically correct 3D human models, it is possible that the over-simplified structure of the model may be the cause of the problem. Since each cervical intervertebral joint was only represented by a pair of translational and rotational joints, the structure of the model omitted the resistive force on the posterior side caused by the posterior ligaments. In addition, since the referenced stiffness and damping

parameters were in vitro measurements, they may be too flexible when compared to the actual stiffness and damping parameters in our subjects. Further investigation of the experiment and the current model will be described in the next chapter.

There were some limitations in this study. Due to time and resource constraints, it was necessary to finish the experiment in one day and only three individuals were able to receive tractions in both positions. With all individuals receiving traction at four angles within one day for one position, it was possible that the traction from the last angle left a residual effect on the next angle, causing larger than normal amount of separations. Since radiographic images were taken only before and during traction, we were not able to measure the transformation of the cervical spine at each cervical segment during the 10 seconds of pulling. For future work, it would also be beneficial to capture sequences of radiographic images during the entire traction cycle to investigate the transformation of the cervical segments. It would also be desirable to gather more clinical data over a larger population, which includes subjects from both genders and subjects at various age groups.

4.6 Summary

In the last chapter, Model 1 was developed to investigate the differences between the inclined and sitting traction positions. However, the lack of clinical data in the two positions prevented us from evaluating its accuracy. The work in this chapter aimed to address such problem by conducting a radiographic study to gather data of the intervertebral separations during cervical traction therapy. Six subjects participated in the experiment to receive cervical traction on two mechanical traction devices. Radiographic images of their cervical spines were taken before and during the therapy and the resulting intervertebral disc changes were analyzed.

The result of the experiment showed that the movement of the cervical spine during traction was smaller in the inclined position. For the three subjects who received cervical traction in both positions, the inclined position was able to achieve greater separations than the sitting position in all four traction angles. Both findings agreed with the

simulation result of Model 1 from the last chapter. The amount of change in posterior separations in response to traction angles was also examined. In the experimental result of the inclined position, we observed that increase in traction angle leads to larger posterior separations. The result of the sitting position showed similar but less consistent behavior. This suggested that using traction angle to control the amount of posterior separations becomes less reliable with the sitting position. In order to evaluate the behavior of Model 1, simulation result was re-generated based on the experiment setup conditions. The result of the simulation showed that the behavior of Model 1 was different from the ones in the experiment. While the posterior separations in the experiment increased with traction angles, posterior separations in Model 1 decreased with traction angles. In an attempt to modify the model to match with the experiment data, biomechanical parameters including the range of motion, stiffness and damping coefficients in Model 1 were modified. Although the modified model was able to match the behavior of the experiment result, the values of the parameters did not match with the ones reported by the reference literatures. As a result, it indicated that Model 1 was insufficient to accurately simulate the behavior of the cervical spine during cervical traction therapy. The next chapter will describe the development of a new simulation model and its difference from Model 1.

Chapter 5.

Improvement of Multi-body Simulation Model for Comparative Study of Cervical Traction Therapy

5.1 Introduction

In Chapter 3, Model 1 was developed to simulate the behavior of the cervical spine in cervical traction therapy. The model used only one pair of translational joint and rotational joint to represent the behavior of each intervertebral joint. After conducting a radiographic experiment and examining the cervical spine data from six subjects under cervical traction in the two traction positions as described in Chapter 4, however, it was shown that the behavior of Model 1 did not match with the experiment result. Attempts were made to calibrate the mechanical parameters in each joint in order to change Model 1's behavior, but the resulting parameters heavily deviated from the biomechanical parameters based on the reference literatures. Since the main problem in Model 1 was due to its over-simplified structure, it was deemed necessary to propose a new cervical spine model that can better represent the behavior of the cervical spine.

The objective of this chapter is to develop a new model, namely Model 2, to simulate the behavior of the cervical spine in cervical traction therapy. The new structure improved upon Model 1 with additional components to represent the non-linear viscoelastic behavior of the intervertebral joints and the resistive force of the posterior ligaments. The data collected from the radiographic experiment was used to evaluate the response of Model 2. The simulation results from the two models are also compared to demonstrate that Model 2 offers a more accurate response in the upper and lower cervical spine. Using Model 2, a parametric study was conducted to investigate the effects of the subject's body parameters on the intervertebral separations during cervical traction in the inclined and sitting positions.

5.2 Methods

5.2.1 Structure of Model 2

The cervical spine model, Model 2, used in this chapter was developed based on Model 1 used in Chapter 3 and Chapter 4. Model 1 represented each intervertebral disc in the cervical spine with only a pair of spring and damper in parallel for the translational and rotational movement respectively. However, the anterior and posterior stiffness was not modelled separately. In order to further improve the accuracy, Model 2 was developed.

Eight rigid bodies are used to represent the head and the seven pieces of the cervical vertebrae (C1-C7). Each intervertebral joint is modelled as non-linear viscoelastic material in flexion and extension. It is built as a "free joint" element in the simulation engine. The "free joint" element allows stiffness and damping properties to be assigned to the joint with required number of degrees of freedom of motion. Since traction force is applied symmetrically during cervical traction, lateral translation (as known as lateral shear) is not modelled in the simulation. Also, since the inclined and sitting positions do not cause axial rotation and lateral bending to the cervical spine, these two rotation directions are not modelled. In other words, only the anterior/posterior shear, tension/compression and flexion/extension are modelled in the simulation.

For the ligaments, one translational joint at the spinous process is used to represent the combined behavior of all the posterior ligaments, which includes the posterior longitudinal ligament (PLL), joint capsules (JC), ligamentum flavum (LF) and interspinous ligaments at each cervical level. The transitional joint is modelled as a translational joint with stiffness and damping parameters.

During cervical traction therapy, the subject is always asked to remain relaxed during the session. Thus, the resistive force of the active muscles should be minimal. The passive muscles at rest have some initial stress and may increase the stiffness of the spine. In Jager's global model [22] , the influence of the passive muscle was accounted for by scale factors to increase the joint stiffness. In Deng's model, the passive muscles were modelled as non-linear springs, but was shown to have only moderately influenced the responses.

And in Van der Horst's model [25], the influence of the passive muscle was also examined and was shown to have only little impacts to the response of the model. Thus, we determined to omit muscle components in Model 2. An overview of the cervical spine model is illustrated in Figure 54 and the detailed structure of each segment is illustrated in Figure 55. The structure of the intervertebral joint used in Model 1 is also shown in Figure 56 for comparison purpose.
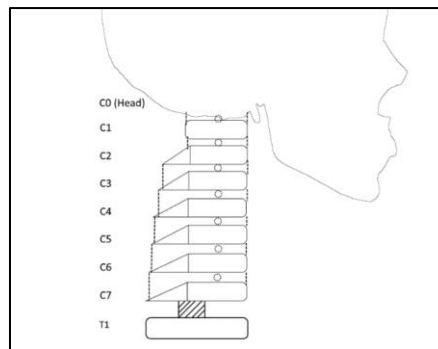
Figure 54. Overview of the Cervical Spine Model
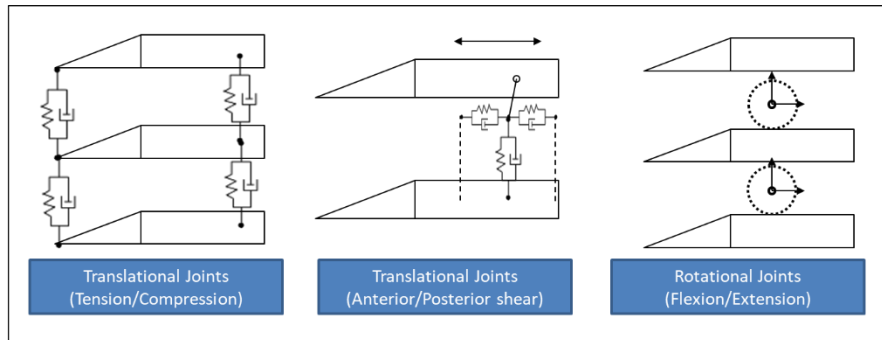
Figure 55. Detailed Structure of Each Cervical Segment in Model 2
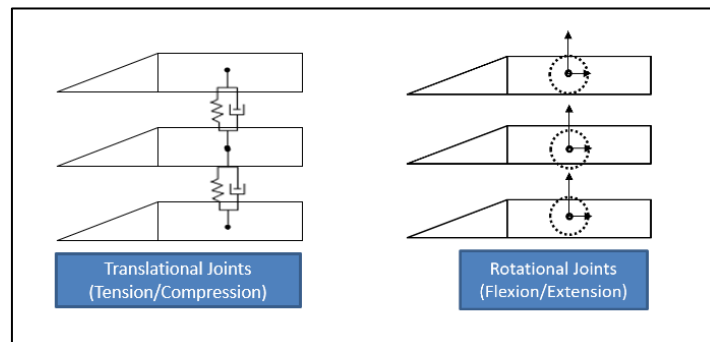
Figure 56. Detailed Structure of Each Cervical Segment in Model 1

5.2.2   Modifications in the Traction Position Models

In both traction device models, the vertex of the traction angle is set at a fixed point at the chair, at a position near the back of the first thoracic vertebra (T1) of the subject. In the simulation model, T1 connects the base of the cervical spine to the rest of the upper body. The upper limbs and forearm are modeled as rigid bodies and are connected to the shoulder with hinge joints. The hip joint is a rotational joint that connects to the thighs. Since the subject is heavy enough that the friction at the seat prevents the subject from sliding along the seat, the thighs and the rest of the lower body are modeled as fixed structure attached to the traction devices. This design allows the subject to remain stable during traction. It also matches the observed behavior of the human subjects in our radiographic experiment. The kinematic structure of the inclined and sitting models are illustrated in Figure 57.
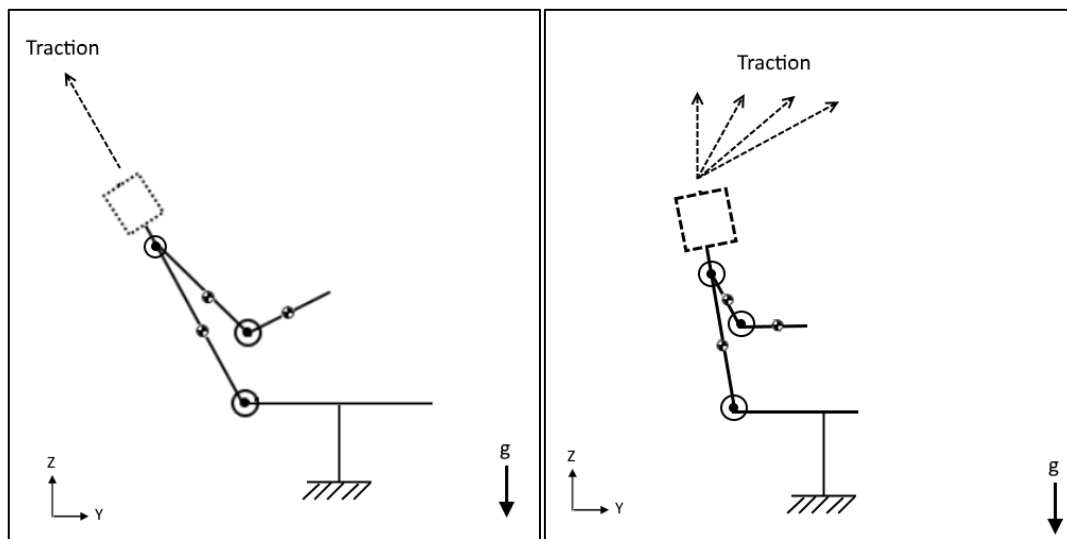
Figure 57. Kinematics overview of traction positions (left: inclined, right: sitting)

Since the model is designed for cervical traction therapy analysis, several assumptions were made. The model assumes that the traction force applied to the spine is symmetrical during cervical traction, thus it does not model lateral translations. Since the inclined and sitting positions do not cause axial rotation and lateral bending to the cervical spine, the

modelling of these two loading directions are not included in the structure of the model. In other literatures, some head-neck simulation models would include muscle in the simulation. In our study, we made the assumption that the subject is in a relaxed state during cervical traction and muscle activation in the cervical spine is minimal. Thus, it reduced the need to include muscle components in the model.

5.2.3   Biomechanical Parameters for Cervical Spine Model

All the rigid body 3D models used in the simulation were retrieved from BodyParts3D [29]. The skeleton model is scaled to be 174cm tall and weighs 73kg. The body segment mass ratio was calculated based on data from Zatsiorsky et al. [38]. The inertial and geometric data of the model are shown Table 9.

Table 9. Inertial and geometric data for the rigid bodies

Part Name	Mass (kg)	Moment of Inertia (kg*cm^2)			Origin (m)		
		x	y	z	x	y	z
C0 (head)	4.69	469.0	361.2	349.5	0.00	-0.13	1.30
C1	0.22	0.7	1.9	2.4	0.00	-0.18	1.24
C2	0.25	1.3	1.3	1.6	0.00	-0.18	1.23
C3	0.24	1.0	1.1	1.7	0.00	-0.18	1.21
C4	0.23	0.9	1.0	1.6	0.00	-0.18	1.19
C5	0.23	1.0	1.1	1.8	0.00	-0.18	1.17
C6	0.24	1.3	1.2	2.1	0.00	-0.19	1.16
C7	0.22	1.4	1.3	2.4	0.00	-0.19	1.14
Trunk & pelvis	31.72	12429.0	14090.8	4640.7	0.00	-0.17	0.95
Left upper limb	1.98	168.9	182.4	22.1	-0.19	-0.17	0.92
Right upper limb	1.98	168.9	182.4	22.1	0.20	-0.17	0.92
Left forearm	1.63	257.8	24.8	264.9	-0.22	0.04	0.74
Right forearm	1.63	257.8	24.8	264.9	0.22	0.04	0.74
Lower body*	-	-	-	-	0.0	0.0	0.0

*Lower body is fixed to the chair as one rigid body and served as the base

The biomechanical parameters for the cervical spine model are referenced from previous head-neck simulation model studies [22][23][25] and cadaver samples studies [26][27]. The range of motion at each cervical level is shown in Table 10. The range of motion represents the total amount of displacement that a motion segment can sustain without being damaged [22]. In the simulation model, the range of motion was used to limit the movement of each joint. The stiffness and damping parameters for the

intervertebral discs from C2 to C7 are listed in Table 11. Previous study [39] stated that there were very little vertical and horizontal translations at the C0-C1 and C1-C2 segments, thus the vertical and horizontal movement for these two joints are set to zero. The anterior/posterior shear movement are represented as horizontal translations along the y-axis. Tension and compression movement are represented as vertical translations along the z-axis. The flexion/extension movement are represented as rotation around the x-axis. Previous studies [40][41] measured the positions of the CORs for using static lateral X-ray images of the cervical spine of human subjects in full flexion and full extension. And in subsequent study conducted by Van Mameren et. al. [42] using X-ray recording at 4 frames/s, it was found that these CORs varied little during motion between full flexion and full extension. In our model, the CORs in our model are set to maintain a fixed distance with the upper vertebra. The center of rotation is set at the approximate center point of intervertebral space between the two adjacent vertebrae.

Table 10. Range of Motion of Cervical Vertebrae [22]

Loading Direction	Range of Motion of intervertebral joint						
	C0-C1	C1-C2	C2-C3	C3-C4	C4-C5	C5-C6	C6-C7
Flexion (deg)	12.5	10	5.5	8.3	11.1	11.1	9.4
Extension (deg)	12.5	10	4.5	6.7	8.9	8.9	7.6
Tension (mm)	0	0	1.1	1.1	1.1	1.1	1.1
Compression (mm)	0	0	0.7	0.7	0.7	0.7	0.7

Table 11. Stiffness and Damping Parameters for Intervertebral Discs [23][25]

Loading Direction	Stiffness (N/mm)					Damping ratio
	C2-C3	C3-C4	C4-C5	C5-C6	C6-C7	C2-C7
Anterior Shear	62	62	62	62	62	1.0
Posterior Shear	50	50	50	50	50	1.0
Tension	63.5	69.8	66.8	68	69	1.0
Compression	637.5	765.3	784.6	800.2	829.7	1.0

In order to model the non-linear viscoelastic behavior of the intervertebral joint during flexion and extension, the stiffness parameters in the rotational joints at each cervical level are dynamically updated based on the joint angle between adjacent vertebrae. The rotational stiffness and damping parameters referenced from previous literature [22] are illustrated in Figure 58 and Figure 59. The actual rotational stiffness parameters are linearly interpolated in every simulation step based on values of the current joint angle. The damping coefficient is 0.026 for all rotational joints [23].
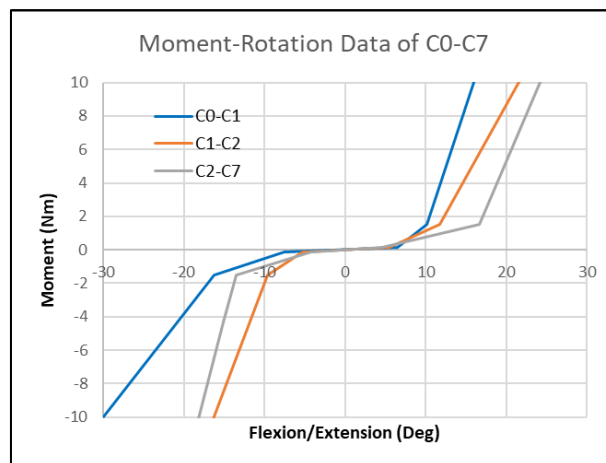
Figure 58. Moment-Rotation Data of C0-C7 (Flexion is positive)
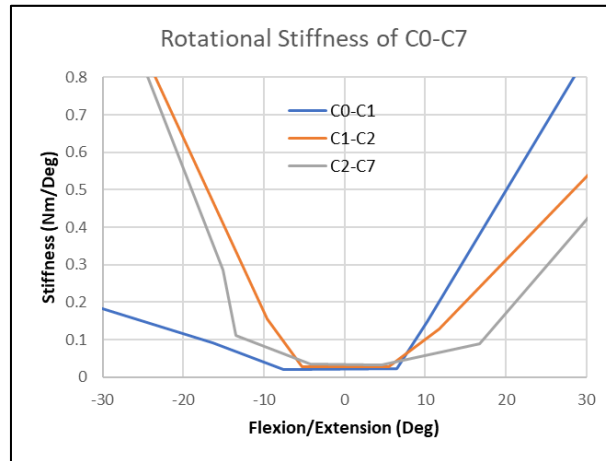
Figure 59. Non-linear Rotational Stiffness of C0-C7 (Flexion is positive)

The stiffness parameters for the posterior ligaments are based on published reference literature [28] and are listed in Table 12. The ligaments were modelled as one-directional spring element such that it only generates resistive force during tension. Stiffness is at zero during compression.

Table 12. Stiffness Parameters for Posterior Ligaments [24]

Ligament Type	Stiffness (N/mm)	
	C23/C34/C45	C56/C67
PLL	25.4	23.0
JC	33.6	36.9
LF	25.0	21.6
ISL	7.74	3.36
Combined Total	91.74	84.86

Model 2 was developed using C++ in Microsoft Visual Studio 2015. The Bullet physics library was used as the physics engine. Iterative constraint solver is used, with

78

the number of iteration count set to 5,000. The timestep was fixed at 1/360th second (~2.78ms). The period of each simulation trial was 15 seconds, with 10 seconds to apply traction force incrementally as a ramping function. The traction force remains constant in the last 5 seconds.

In early simulation trials, the cervical spine part was shown to be too flexible. As suggested in the reference literature [22], since the reported biomechanical parameters were gathered from in-vitro samples, it is possible that they are different from the actual stiffness in a human cervical spine. As a result, a scaling factor was introduced to calibrate the joint stiffness to calibrate the response to match our experiment result. The same approach has also been used in other head-neck models [22][25]. Such scaling factor is necessary to represent the difference between in-vitro stiffness and in-vivo stiffness. In particular, in order to account for the posterior ligamental resistive force that applies to the rotational movement, the dynamic rotational stiffness was increased by a factor of 10 to match the experiment values. Additionally, the ligament stiffness was scaled by 0.75 to match the experiment result.

5.2.4   Differences between the Model 1 and Model 2

Model 1 uses the same geometric data and range of motion parameters listed in Table 9 and Table 10, but it is different from Model 2 in several ways. In Model 1, each intervertebral joint between C2 and C7 was modelled by a "free joint" element but only the tension/compression and flexion/extension directions were modelled. In additional, the C0-C2 joints were fixed as one rigid body for simplification purpose. Model 1 does not dynamically update the rotational stiffness based on joint angle and it only uses tension stiffness parameter for vertical translational movement. The posterior ligaments were not modelled. The parameters for Model 1 are listed in Table 13. The damping coefficients were the same as Model 2.

Table 13. Stiffness and Damping Parameters used in Model 1 [22]

Parameters	Cervical Segment				
	C2-C3	C3-C4	C4-C5	C5-C6	C6-C7
Translational Stiffness (N/mm)	63.5	69.8	66.8	68	69
Rotational Stiffness (Nm/deg)	14	14	14	14	14
Translational Damping	1.0	1.0	1.0	1.0	1.0
Rotational Damping	0.026	0.026	0.026	0.026	0.026

5.3   Results

Model 2 was compared to the measurements collected from the radiographic experiment described in Chapter 4. In the experiment, the human subjects were seated in two types of mechanical traction devices, representing the inclined and sitting positions. The amount of traction force is set to equal to 20% of the subject's body weight. Among the six subjects, traction forces ranged between 100N and 160N were used. Traction angles from 10° to 40° were tested in each run. Each run lasted for around 60 seconds and radiographic images were taken before and during traction. The anterior and posterior separations in each image were measured. For the new simulation model, same traction parameters were applied. Traction force was set at 148N, which equals to 20% of the weight of the simulated subject.

5.3.1   Time Responses for Inclined and Sitting Positions

This section describes the time response of the cervical spine in the inclined and sitting positions for traction force at 148N. The traction force is applied in small increment during the first 10 seconds of the run (reached target amount at the 3600th step) and it

remains constant throughout the run. The total number of steps is 5400 steps, which equals to 15 seconds per run.
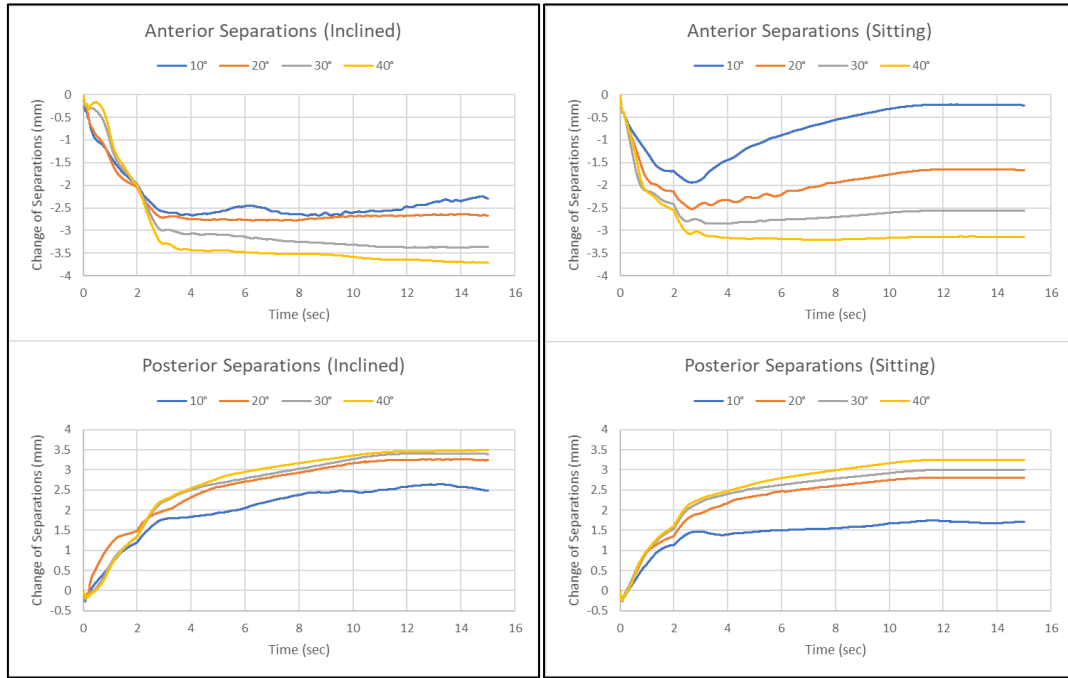
Figure 60. Time responses in inclined (left) and sitting (right) positions

Figure 60 shows the anterior and posterior time response of the inclined and sitting positions. The time response shows that both traction positions behave similarly, i.e., the posterior separation increases along with the traction angles. The main difference between the two positions can be observed in the anterior response. Although traction force is still being applied, the compression decreases rapidly in the sitting position. This decrease in compression reduces the posterior separations at 10° but does not affect the values in other traction angles. In fact, the combination of a decrease in anterior compression and a decrease in posterior separations at the same time indicates the occurrence of cervical extension. The timing response suggests that at the beginning of the simulation, when traction is being applied, the subject is starting to lose body balance and began to lean forward, thus creating a short period of cervical extension. Such behavior was not observed in the inclined position.

5.3.2 Transformation of Cervical Spine in Model 2
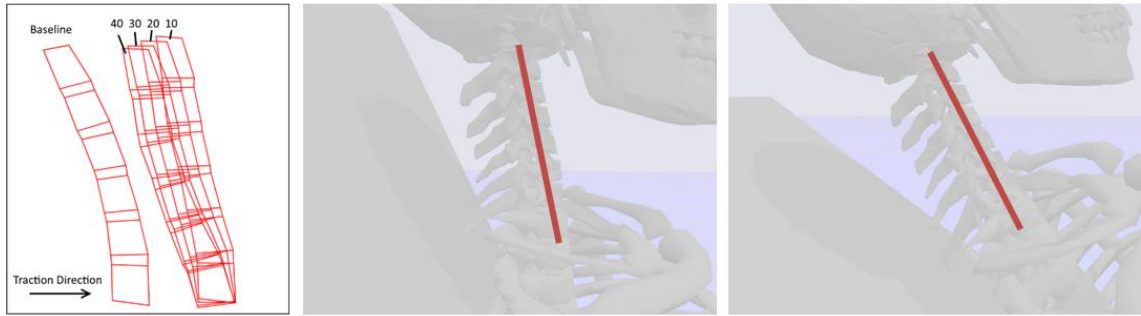
Figure 61. Transformation of cervical spine in inclined position
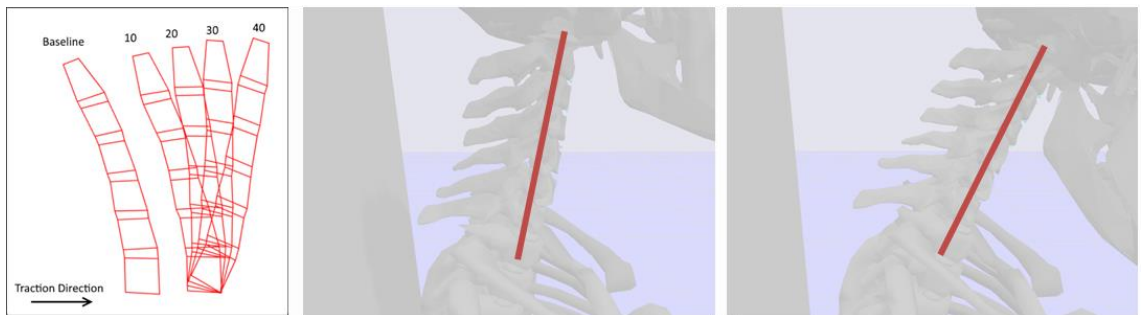
Figure 62. Transformation of cervical spine in sitting position

The transformation of the cervical spine in inclined and sitting positions are shown in Figure 61 and Figure 62 respectively. Similar to the experiment result, the simulation result shows that the cervical spine in the inclined position is more stable during traction. The movement of the sitting position is larger and thus potentially lead to larger variations in the intervertebral separations.

5.3.3 Validation using Changes of Separation in C2-C7

In this section, the change of separations in C2-C7 in the experiment is compared to the ones in the new simulation model. The values shown in the figures represent the combined amount of disc space changes in the intervertebral discs between C2 and C7, before and during traction, i.e. ΔC2-C7 = ΔC2-C3 + ΔC3-C4 + … + ΔC6-C7. The experiment values represent the mean changes of the six human subjects combined.
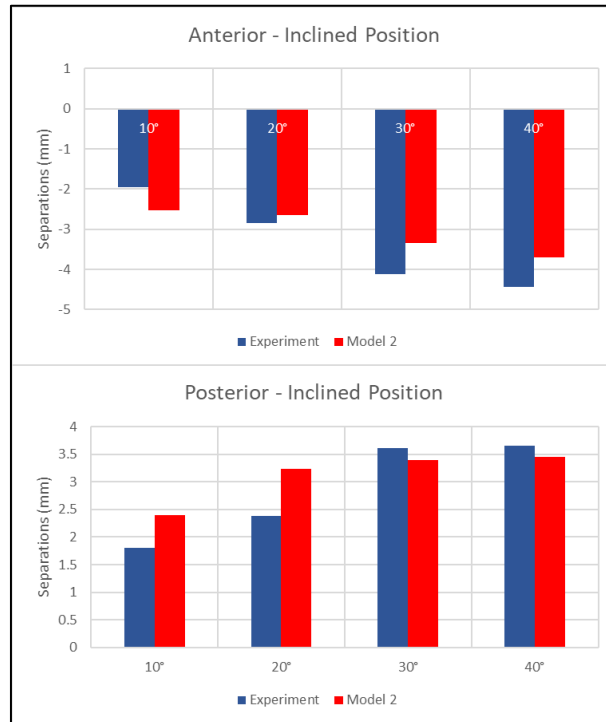
Figure 63. Experiment vs Simulation in Inclined Position

Figure 63 shows a comparison between the experiment and the simulation in inclined position. In the inclined position, the simulation model shows a similar trend as the experiment result. The amount of changes in separations in response to traction angles are also similar to the ones from the experiment. Both the simulation and the experiment show that changes in separations in C2-C7 increase with traction angles in the inclined position.
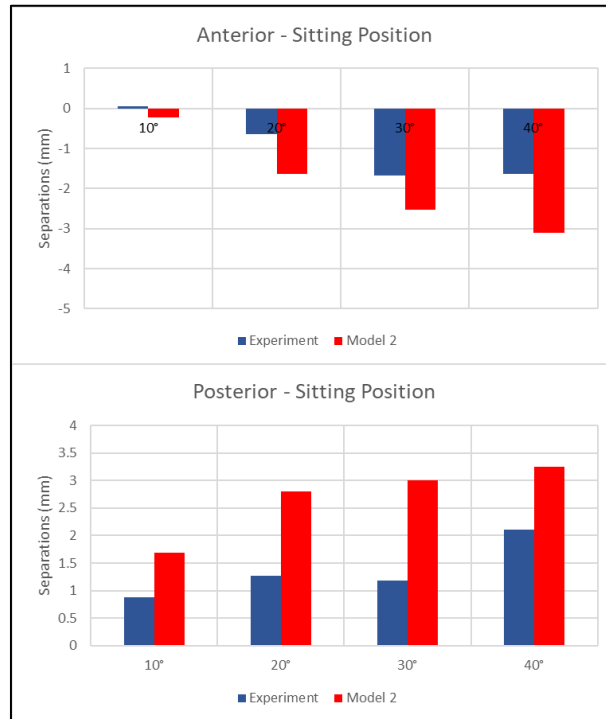
Figure 64. Experiment vs Simulation in Sitting Position

Figure 64 shows the comparison of the sitting position. In the sitting position, we can also see a similar trend between the experiment and the simulation, but the amount of changes is different. The sitting simulation shows larger values than the experiment, especially on the posterior side. One possible explanation for this large discrepancy is likely related to the individual measurements collected in the experiment and the small sample size. Table 14 shows the mean and standard deviation among three subjects (50A/50B/60A) that received traction in both positions. The subjects in the sitting traction shows a larger standard deviation. The sitting position has been shown in Chapter 4 that it cannot consistently maintain traction angles during traction. As a result, the discrepancy between the simulation and the experiment can be attributed to the inconsistent nature of the sitting position.

Table 14. Mean and SD% of Changes in Posterior Separations among Subjects

Traction Angle	Inclined		Sitting	
	Mean	SD %	Mean	SD %
10°	2.02	6.4%	1.26	16%
20°	2.50	31.7%	1.44	45%
30°	3.76	17.0%	1.73	41%
40°	3.70	4.3%	2.85	38%

Overall, the simulation result matches with the experiment result in that the inclined position achieved a greater amount of changes in separations in all four traction angles than the sitting position, though the actual amount of changes was different. It is important to note that since the experiment was conducted with a small sample size of six subjects, it is reasonable that the simulation model did not yield the exact same measurements as the mean values of the six subjects combined. The mean values should only be served as a reference when evaluating the performance of the two traction positions.

5.3.4   Validation using Changes of Separation in Upper and Lower Cervical Spine in Individual Subjects

This section examines the changes in separations in the upper and lower cervical spine. Instead of using the mean changes of all the subjects combined, individual measurements from three of the human subjects (50A/50B/60A) are used. Since the traction forces used for these three subjects were between 140N and 150N, we expect the amount of changes in separations to be similar to the simulation result, which uses 148N as traction force. The upper cervical spine refers to the combined changes between C2 and C4, while the lower cervical spine refers to the combined changes between C4 and C7. Similar to the analysis in Chapter 4, the comparison will focus on the posterior changes, since one of

the main objectives in cervical traction therapy is to increase the disc space on the posterior side.
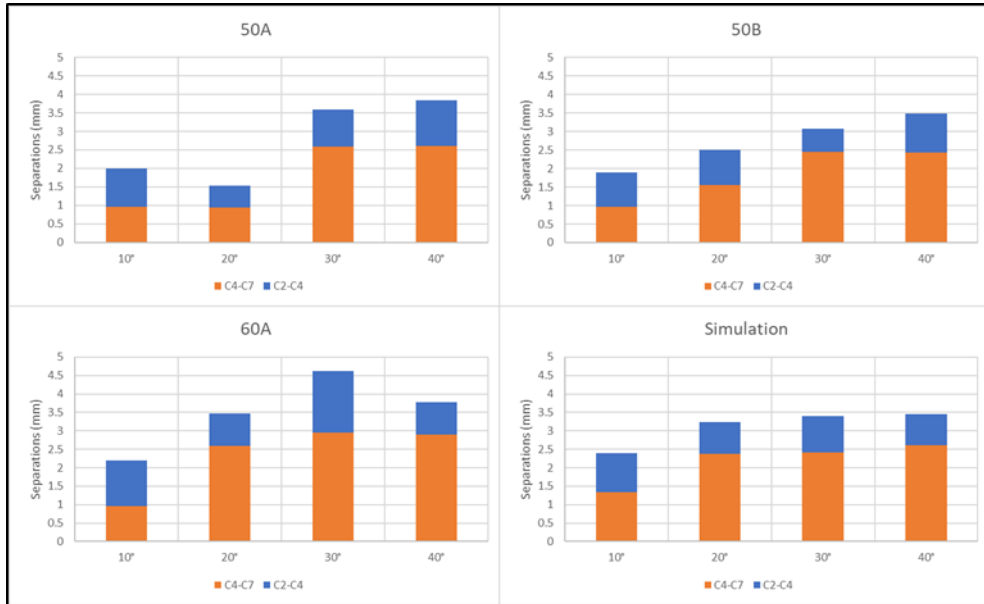
Figure 65. Posterior Change of Separations in Inclined Position (Individuals vs. Simulation)

Figure 65 compares the posterior measurement of each subject against the simulation result. In the inclined position, one can see that the data from the three subjects share similar trends with the simulation. In particular, when traction angle is at 10°, the upper spine and lower spine show similar amount of changes. For traction angles at 20/30/40°, the separations in lower spine increases proportionally along with traction angles, while the upper spine only increases slightly. Both the experiment and the simulation result demonstrate that changing the traction angles in the inclined position can alter the amount of posterior separations between the upper and lower spine.
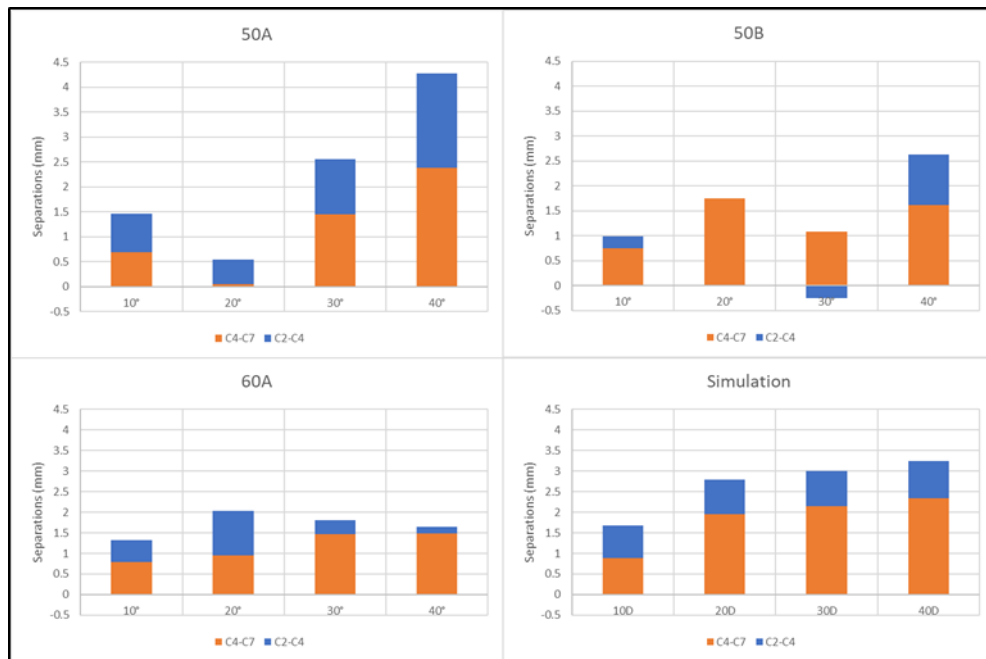
Figure 66. Posterior Changes of Separations in Sitting Position (Individuals vs. Simulation)

Figure 66 shows the same comparison in the sitting position. Upon examining the experiment result, one can see that the amount of changes in the upper and lower spine shows large differences among the three subjects. The changes also do not correspond to the increase in traction angles. As a result, a large discrepancy was shown between the experiment result and the simulation result. In Chapter 4, the sitting position was shown that it cannot consistently maintain proper traction angles during traction therapy. As a result, such discrepancy can be attributed to the inconsistent nature of the sitting position.

5.3.5   Comparison of Model 1 and Model 2

In this section, Model 1 is compared against Model 2 and the experiment result. Firstly, Model 1 with unmodified and modified parameters will be compared to Model 2 and the experiment. Then a comparison using the changes of separations in upper and lower spine will be presented.

5.3.5.1 Model 1 with Unmodified Parameters
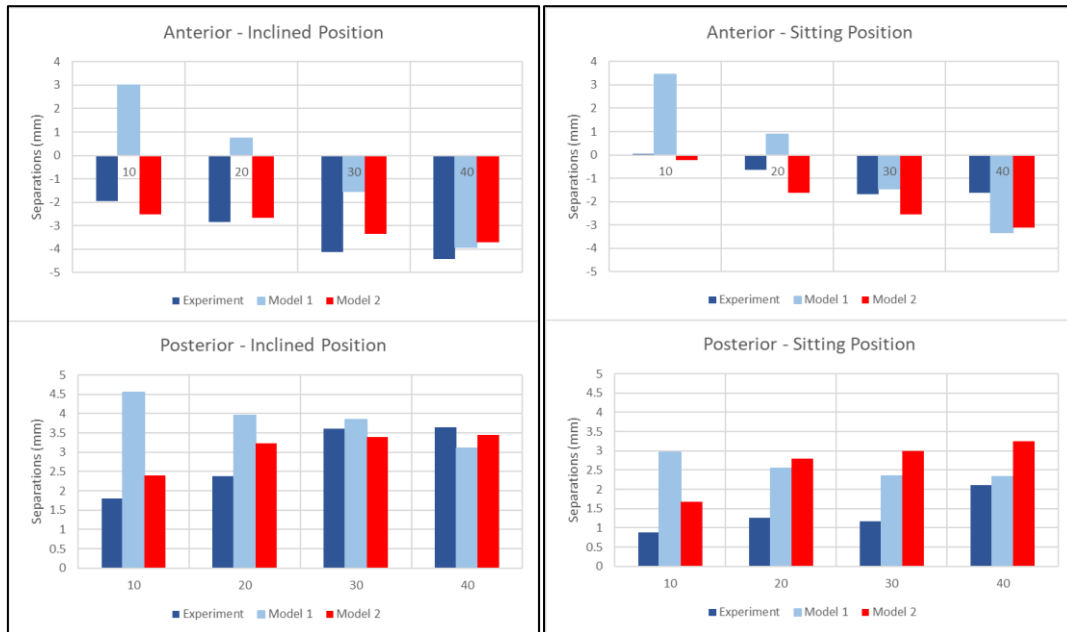
Figure 67. Experiment vs Model 1 vs Model 2 (left: inclined, right: sitting)

Figure 67 shows a comparison of the result from Model 1 with unmodified parameters, Model 2 and the experiment result in the sitting and inclined positions. One can see that Model 1 showed positive anterior separations at 10° and 20° and compression at other angles. On the posterior side, however, Model 1 shows opposite trend in all four angles in both positions. The posterior separations decrease as traction angle increases for both positions. It is apparent that the overall behavior of Model 1 differs from the results of experiment and Model 2.

5.3.5.2 Model 1 with Modified Parameters

In Chapter 4, we have attempted to modify Model 1 to match the experiment result by using specific ROM and stiffness values. The modified parameters used to adjust the result of Model 1 are listed in Table 15.

Table 15. Modified Parameters used to adjust Model 1

Parameters	C2-C3	C3-C4	C4-C5	C5-C6	C6-C7
Flexion ROM (Deg)	4.5	4.1	4.2	8.7	8.5
Extension ROM (Deg)	0	0	0	0	0
Tension ROM (mm)	2	1	1	2.5	3.5
Compression ROM (mm)	5	1	2	2	5.5
Translational Stiffness (N/mm)	80	75	67	35	26
Translational Damping Ratio	1.0	1.0	1.0	1.0	1.0
Rotational Stiffness (Nm/deg)	25	11.3	6.3	3.8	3.8
Rotational Damping Ratio	0.026	0.026	0.026	0.026	0.026

The modified parameters aimed to increase posterior tension and flexion movement in the lower spine and limit extension movement, in order to reverse the trend in the posterior separations. When compared the values to the ones in Table 10 and Table 11, one can see that all the flexion ROMs are reduced by several degrees. The ROM of extension is set to zero to prevent extension. The ROM of tension and compression were modified to be larger than the reference values to allow for larger separations. The rotational stiffness was set such that the lower spine rotates at larger angles. The translational stiffness was increased to reduce the separation in small traction angles. It was also reduced for the lower spine. In addition, the center of rotation was moved forward to increase the posterior separations.
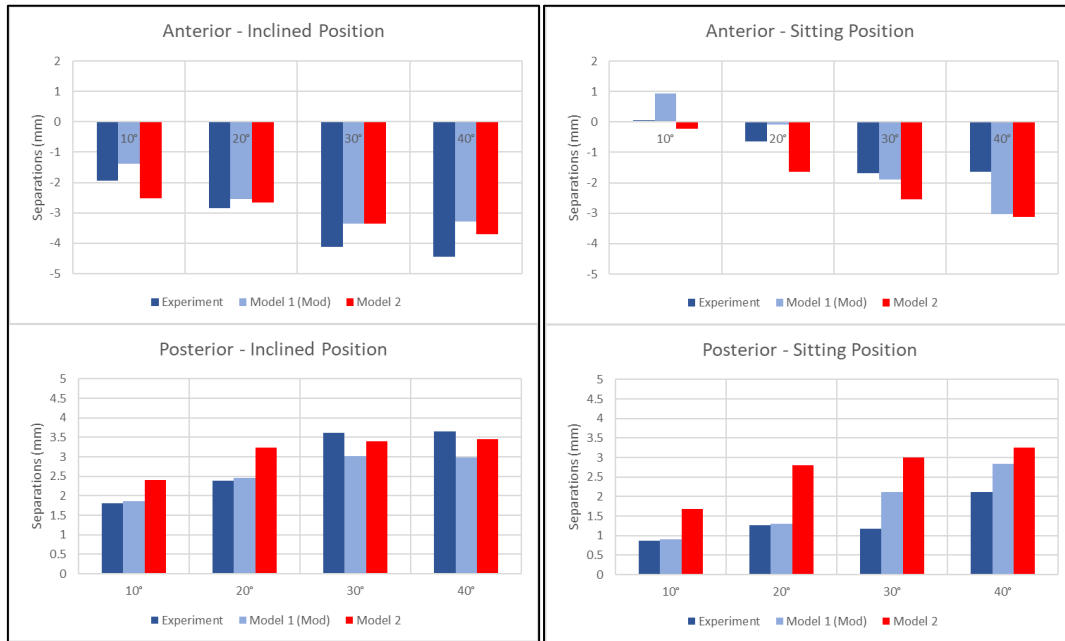
Figure 68. Model 1 with Modified Parameters (left: inclined, right: sitting)

Figure 68 shows the results after the adjustment. Although the modified parameters enable Model 1 to behave closer to the experiment result, the limitation in the ROM and tailor-made parameters deviates from the reported parameters from the reference literatures. Since the objective of the cervical traction simulation model is to investigate the various parametric changes in cervical traction, it would be necessary to develop a new model that can represent more loading directions and can adopt to the biomechanical parameters acquired from reference literatures with minimal adjustment. In fact, Model 2 follows the biomechanical parameters based on the reference literatures with some scaling adjustment, as described in Section 5.2.3, to reflect the differences between in-vitro and in-vivo parameters. As a result, we determined that the structural modification (adding posterior ligaments) in Model 2 is essential to improve its accuracy.
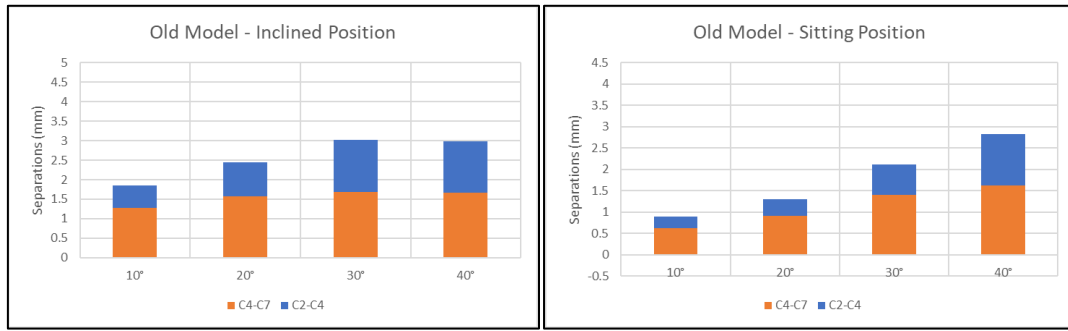
Figure 69. Posterior Separations in Upper and Lower Spine in Model 1 with Modified Parameters

Figure 69 shows the changes of posterior separations in upper and lower spine using Model 1 with modified parameters. Compared to Figure 65 and Figure 66 in section 5.3.4, we can see that the behavior of this model does not match with the experiment values. In the inclined position, as traction angle increases, the separations in upper spine increases but the separations in the lower spine remains the same. This does not match with the behavior of the experiment data. The separations in the sitting position also behaves differently from the experiment data. Therefore, the upper and lower spine behavior of Model 1 with modified parameters failed to match the experiment results.

5.4 Parametric Studies of Body Parameters

In the previous section, we can see from the experiment data in Figure 66 that individual subjects in sitting position show large variations in the result, while the same subjects in inclined position was able to show a more consistent result in Figure 65. In order to investigate this large difference in consistency, we used Model 2 to conduct parametric studies on the effects of hip joint stiffness and the stiffness parameters in the anterior and posterior shear, tension compression and rotational loading directions.

5.4.1 Effect of Hip Joint Stiffness in Traction Response

Since both positions require the subject to be seated while traction is applied, it is possible that the upper body can be pulled away from the seat. When the back of the

subject is no longer in contact with the seat, the desired traction angle changed and thus affects the resulting intervertebral separation. In the simulation model, the rotational stiffness parameter for the hip joint was set to 10 Nm/rad [50]. Under this setting, the subject in sitting position leans forward especially at large traction angles. By adjusting the rotational stiffness at the hip joint, we investigated how it affects the resulting separations in the upper and lower cervical spine.
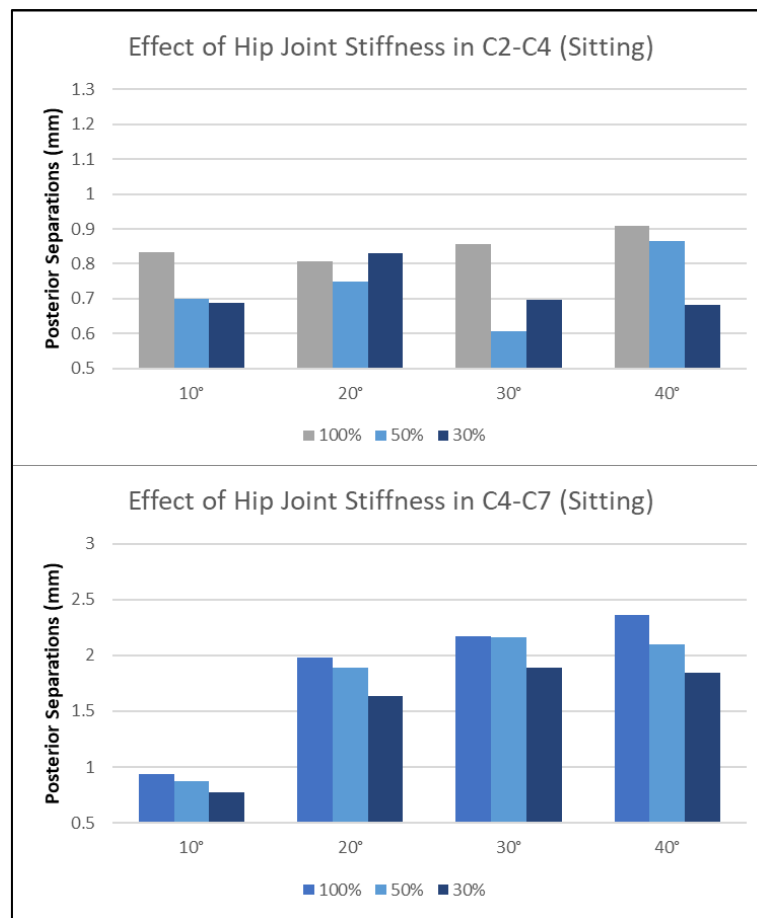
Figure 70. Effect of Hip Joint Stiffness in Sitting Position

Figure 70 shows the posterior separations with hip joint rotational stiffness set at 30/50/100% in the sitting position. We can see that a loose hip joint not only reduces separation, it also affects the distribution of separations between the upper and lower cervical spine. It is thus possible that the inconsistent result in the human experiment in Figure 66 is caused by the forward-leaning problem in the sitting position. Since the sitting position does not provide frontal support to the subject, the subject has to spend extra effort to maintain balance during traction. The same parameters were tested using

the inclined position. The result in Figure 71 shows that the inclined position is less affected by variation in hip joint stiffness. As the subject is always seated at an inclined angle, the subject's own weight helps to stabilize the body during traction. The hip joint stiffness can also vary in actual therapy session. It can depend on factors such as age, muscle resistance and whether the subject has the intention to maintain body balance. As a result, the forward-leaning problem not only leads to reduced intervertebral separations, it also adds inconsistency to the result of the sitting position.
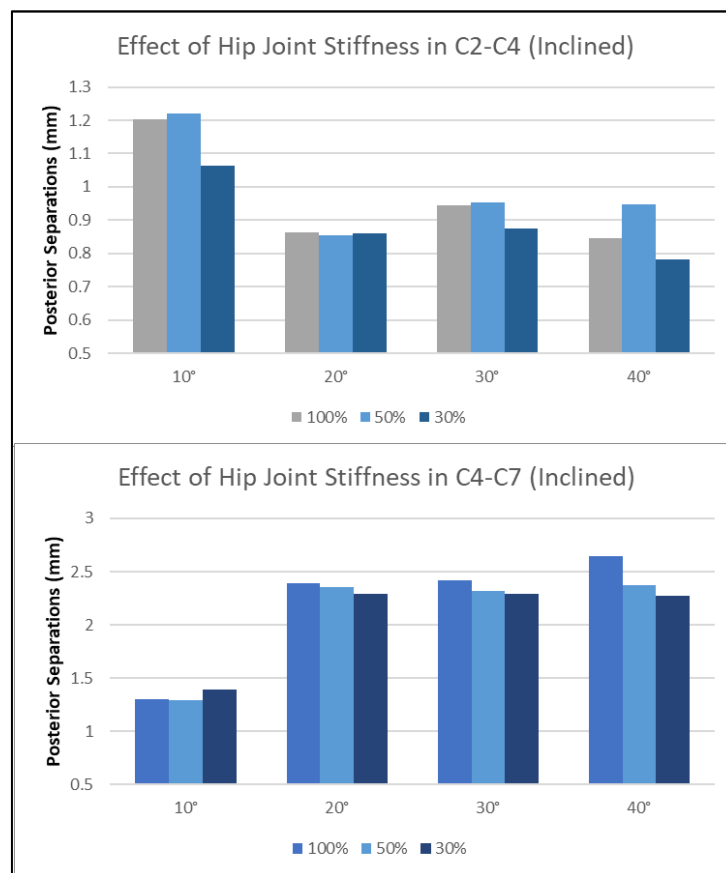
Figure 71. Effect of Hip Joint Stiffness in Inclined Position

5.4.2　Effect of Stiffness Parameters in Traction Response

The initial stiffness parameters used in the model were based on previous literatures that examined the biomechanical properties of cervical spine from cadaver samples. Depending on the quality of the samples and measurement methods, these parameters can

vary. For instance, in Moroney's study based on 38 specimens [27], the measured stiffness for compression, anterior/posterior shear, flexion/extension had a range of S.D. between 40% and 120%. This suggests that the stiffness parameters can vary greatly due to individual differences. In this section, in order to investigate the effects of stiffness parameters in cervical traction, the stiffness parameters for compression/tension, flexion/extension and anterior/posterior shear at each cervical level were modified to +/- 30% of the initial values.

Figure 72 shows the change in posterior separations when the overall stiffness parameters are set to 70% and 130% of the initial values. With the stiffness parameters set at 70%, the cervical spine is more relaxed and stretchable, thus allowing larger posteriorly separations in both positions. The average increase is 17.1% for the inclined position and 17.9% for the sitting position. When the stiffness parameters are increased to 130%, the separations were reduced by an average of 12.0% in the inclined position and 10.5% in the sitting position. The result of the effect of stiffness parameters are listed in Table 16 and Table 17.
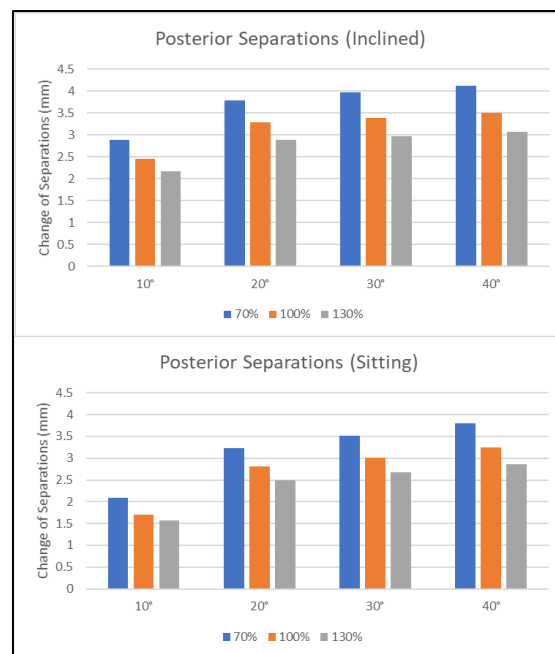
Figure 72. Effect of Stiffness Parameters in Posterior Separations

Table 16. Effect of Stiffness Parameters in Inclined Position

Inclined Position	Change	Anterior	Posterior		
			C2-C7	C24	C47
Rotational Stiffness	+30%	-2.0%	-3.0%	1.7%	-5.7%
	-30%	12.0%	4.0%	2.1%	3.9%
Tension/Compression	+30%	12.7%	-8.4%	-16.6%	-7.2%
	-30%	-11.3%	11.7%	18.6%	8.2%
Anterior/Posterior Shear	+30%	0.3%	-1.4%	5.9%	-6.1%
	-30%	0.4%	0.4%	14.9%	-8.0%
All Stiffness	+30%	4.5%	-12.0%	-24.1%	-8.6%
	-30%	-2.0%	17.1%	28.0%	11.6%

Table 17. Effect of Stiffness Parameters in Sitting Position

Sitting Position	Change	Anterior	Posterior		
			C2-C7	C24	C47
Rotational Stiffness	+30%	-11.0%	-3.0%	-6.3%	-2.4%
	-30%	7.0%	3.0%	3.8%	2.7%
Tension/Compression	+30%	21.6%	-7.3%	-28.0%	0.7%
	-30%	-52.2%	13.8%	15.7%	12.8%
Anterior/Posterior Shear	+30%	-1.8%	-1.6%	-1.6%	-1.6%
	-30%	-2.0%	0.2%	1.0%	0.3%
All Stiffness	+30%	18.9%	-10.5%	-32.1%	-1.9%
	-30%	-48.1%	17.9%	21.3%	15.9%

5.5 Discussion

In order to match the Model 1 to the experiment data, we tried to limit the range of motion and adjusted the stiffness parameters at each cervical segment level. The process involved a lot of trial-and-error and was very time-consuming. Although the end result looked similar to the total separations in the experiment data, the changes in the upper and lower spine were not matched as shown in section 5.3.5. it showed that just modifying the parameters was not enough to compensate for the structural problem in Model 1. A structural change was required and thus developing a new model was necessary. Model 2 takes into account of the resistance in the posterior side of the spine and the shear directions. These changes helped to allow Model 2 to better represent the behavior of the cervical spine.

Using Model 2, parametric studies related to the subject's body parameters were conducted. Since both traction positions require the subject to be seated and the traction angles were pre-determined, it is possible that the variations in the subject's body parameters can alter the desired traction angles and the resulting separations. The effects of the hip joint stiffness and variations in cervical spine stiffness were investigated. Due to the design of the sitting position, the results showed that variation in the hip joint stiffness affects the resulting intervertebral separations. When the hip joint stiffness is low, i.e. the subject does not resist the traction force, the subject can be pulled forward during the traction, thus affecting the separations in the upper and lower spine. The tendency of the leaning forward was less apparent in the inclined position, suggesting that the inclined position can provide more consistent result.

Although the initial stiffness parameters were acquired from literatures that are often cited in head-neck simulation model studies, it is important to point out that they only represent the average values of all the sampled specimen. Since these parameters can vary by 40% – 120% to the mean values, we conducted a parametric study to investigate the effects of each parameter in the shear, tension/compression, flexion/extension loading directions. The result shows that the stiffness parameters in the tension/compression directions have the strongest effect on the resulting separation. It would be important for

future studies to investigate various factors, such as aging, injuries and fatigue, that affect the stiffness of tension/compression in the cervical spine.

As the technology of mechanical traction device advances in the future, it will be essential to develop patient-specific, customizable device that can apply traction to injured area with precision. For future work, it is important to further analyze the mechanism of the cervical traction therapy by gathering more data on patients. While the present study focuses on evaluating the difference between the inclined position and sitting position, future studies can make use of this simulation model to evaluate and explore other traction positions.

5.6 Summary

In this chapter, Model 2 was developed to analyze the behavior of the cervical spine during cervical traction therapy. New components were added to the intervertebral joint to represent the tension/compression movement, anterior/posterior shear and flexion/extension rotational movement. The behavior of Model 2 was evaluated using experimental data. The simulation result showed that the movement of the cervical spine is smaller in the inclined position. This result agreed with the experiment that the inclined position can achieve more stable traction than the sitting position. Also, the behavior of Model 2 was shown to match the overall behavior of the experiment result such that an increase in the traction angles leads to larger posterior separations.

The posterior separations in the upper and lower spine were also compared between the inclined and sitting positions. In the experiment result of the inclined position, it was found that increase in traction angle leads to larger posterior separation only in the lower spine. The amount of posterior separations in the upper spine remains similar regardless of traction angle. This shows that when cervical traction is conducted in the inclined position, traction angle can be used to control the amount of posterior separations distributed between the upper and lower spine. On the other hand, such behavior was not observed in the sitting position. The behavior of the upper and lower spine in Model 1

and Model 2 were compared against the experiment result. While Model 1, even with the modified parameters, failed to match the behaviour, Model 2 was shown to match the behaviour of the upper and lower spine in the experiment.

Using Model 2, parametric studies were conducted to investigate the effects of body parameters on intervertebral separations. The result suggested that the sitting position is more sensitive to variation in hip joint stiffness. The position tends to cause the subject to lose balance, thus leading to undesired changes to the receiving traction angles. In contrast, the inclined position is less sensitive to variations in hip joint stiffness and the stiffness level at each cervical segment. This may explain why individual subjects in the experiment shows similar results and consistent increase of separations along with traction angles in the inclined position. Among the anterior/posterior shear stiffness, tension/compression stiffness and rotational stiffness, variations in the tension/compression stiffness were shown to cause the largest changes in intervertebral separations during traction.

Chapter 6.
Conclusion

6.1 Conclusion

Cervical traction therapy has been widely employed in clinical situations and rehabilitation as a non-surgical treatment for the cervical spine. However, due to the complex structure of the cervical spine and the traction parameters, such as traction force, angle and position, involved in the treatment, the mechanism of cervical traction therapy has not been fully understood. Traction force and angle refer to the magnitude and the direction of the pulling force. Traction position refers to the posture of the subject during cervical traction. This research aimed to compare the differences between two traction positions, namely the sitting and inclined positions, and their abilities to achieve intervertebral separations at specific part of the cervical spine in cervical traction therapy. The sitting position is a common position and the inclined position is a new position proposed to improve therapy result. In order to better understand the mechanism of the two positions, three studies were performed.

In the first study, we developed a simple cervical traction simulation model which consisted of a cervical spine and two cervical traction devices, each representing the inclined and sitting positions respectively. This model, named Model 1, was used to simulate cervical traction using different amount of traction force and traction angles in the inclined and sitting positions. The result showed that the inclined position was able to achieve greater posterior separations than the sitting position in all four traction angles when given the same amount of traction force. Also, the overall movement of the cervical spine was shown to be smaller in the inclined position during traction, thus suggesting a more stable traction in the inclined position.

In order to evaluate the accuracy of Model 1, the second study conducted a radiographic experiment with human subjects receiving cervical tractions in the two positions. The result of the experiment agreed with the simulation result of Model 1 that the inclined position creates greater intervertebral separations than the sitting position

under the same amount of traction forces. The movement of the cervical spine also agreed with the simulation that the inclined position causes smaller movement than the sitting position during traction. However, it was found that the behavior of Model 1 in response to traction angles was different from the experiment. While the posterior separations in the experiment increased with traction angles in both positions, posterior separations in Model 1 decreased with traction angles. In an attempt to modify the model to match with the experiment data, biomechanical parameters including the range of motion, stiffness and damping coefficients in the model were modified. Although the modified model was able to match the behavior of the experiment result, the values of the parameters did not match with the ones reported by the reference literatures. As a result, it indicated that Model 1 was insufficient to accurately simulate the behavior of the cervical spine during cervical traction therapy.

Consequently, a new simulation model, Model 2, with additional components was developed. Anterior and posterior horizontal shear movement of the intervertebral discs were added to the model. Two translational joints were used to represent the anterior and posterior vertical movement separately, with the posterior vertical movement representing the resistance force of the posterior ligaments. The behavior of Model 2 was evaluated using experimental data. The simulation result showed that the movement of the cervical spine is smaller in the inclined position. This result agreed with the experiment that the inclined position can achieve more stable traction than the sitting position. Also, the behavior of Model 2 was shown to match the overall behavior of the experiment result such that an increase in the traction angles leads to larger posterior separations. The posterior separations in the upper and lower spine were also compared between the inclined and sitting positions. In the experiment result of the inclined position, it was found that increase in traction angle leads to larger posterior separation only in the lower spine. The amount of posterior separations in the upper spine remains similar regardless of traction angle. On the other hand, such behavior was not observed in the sitting position. The behavior of the upper and lower spine in Model 1 and Model 2 were compared against the experiment result. While Model 1, even with the modified parameters, failed to match the behaviour, Model 2 was shown to match the behaviour of the upper and lower spine in the experiment. Next, a parametric study was conducted to

investigate the effects of body parameters on intervertebral separations. The result suggested that the sitting position is more sensitive to variation in hip joint stiffness, since it tends to cause the subject to lose balance and leads to undesired changes to the actual receiving traction angles. In contrast, the inclined position is less sensitive to variations in hip joint stiffness and the stiffness level at each cervical segment. Among the anterior/posterior shear stiffness, tension/compression stiffness and rotational stiffness, the stiffness level in the tension/compression was shown to affect the resulting separations the most.

Based on the results of the simulation and experiment, we concluded that the inclined position is more effective than the sitting position in several aspects. Firstly, the inclined position is able to achieve a greater amount of separation than the sitting position, when given the same amount of the traction force. The movement of the cervical spine is more stable in the inclined position during traction, thus leading to a more stable traction. Also, the relationship between traction angles and the amount of separations is more consistent when using the inclined position. It was demonstrated that with the inclined position, traction angle could be used to increase the amount of posterior separations in the lower spine, while keeping the amount of posterior separations constant in the upper spine. Finally, the result of parametric study shows that the resulting intervertebral separations in the sitting position is more susceptible to variations in the body parameters of the subjects, causing subject to lose balance and altering the resulting traction angle. The inclined position, in contrast, is less sensitive to such variations and is able to provide a more reliable and predictable traction result.

6.2   Future Work

Future work of the study should focus on gathering more clinical data in the inclined and sitting positions. It would be important to capture radiographic videos of the cervical spine during traction to measure the transformation of each intervertebral discs, since such data will be necessary to validate the timing responses of the present simulation models. The effects of body parameters, gender and age of cervical traction patients

should be further investigated. By collecting more clinical data regarding the patients, the simulation model can be improved to estimate the intervertebral separations based on patient-specific data. It will help to identify the necessary traction parameters to achieve customized traction in the future. Furthermore, it may be worthwhile to add other traction positions to the simulation model for analysis. We hope to use this simulation model to help others to gain insight in the understanding of the cervical traction therapy.

References

[1] A. A. Harte, G. D. Baxter, and J. H. Gracey, "The efficacy of traction for back pain: a systematic review of randomized controlled trials.," *Arch Phys Med Rehabil*, vol. 84, no. October, pp. 1542–1553, 2003.

[2] T. T. Chiu, J. K.-F. Ng, B. Walther-Zhang, R. J. Lin, L. Ortelli, and S. K. Chua, "A randomized controlled trial on the efficacy of intermittent cervical traction for patients with chronic neck pain," *Clin. Rehabil.*, vol. 25, no. 9, pp. 814–822, Sep. 2011.

[3] S. R. I. Bukhari, S. Shakil-ur-Rehamn, S. Ahmad, and A. Naeem, "Comparison between effectiveness of mechanical and manual traction combined with mobilization and exercise therapy in patients with Cervical Radiculopathy," *Pakistan J. Med. Sci.*, vol. 32, no. 1, pp. 31–34, 2016.

[4] A. Jellad, Z. Ben Salah, S. Boudokhane, H. Migaou, I. Bahri, and N. Rejeb, "The value of intermittent cervical traction in recent cervical radiculopathy.," *Ann. Phys. Rehabil. Med.*, vol. 52, no. 9, pp. 638–52, 2009.

[5] Tractizer Model TC-30D, Minato Medical Science, Japan. Available: http://www.minato-med.co.jp/medical/products/physical/tc.php

[6] Tractizer Model TC-C1, Minato Medical Science, Japan. Available: http://www.minato-med.co.jp/medical/products/physical/tcc1.php

[7] C. T. Chung *et al.*, "Comparison of the intervertebral disc spaces between axial and anterior lean cervical traction," *Eur. Spine J.*, vol. 18, no. 11, pp. 1669–76, 2009.

[8] G. J. van der Heijden, a J. Beurskens, B. W. Koes, W. J. Assendelft, H. C. de Vet, and L. M. Bouter, "The efficacy of traction for back and neck pain: a systematic, blinded review of randomized clinical trial methods.," *Phys. Ther.*, vol. 75, no. 2, pp. 93–104, Feb. 1995.

[9] D. M. Daniel, "Non-surgical spinal decompression therapy: does the scientific literature support efficacy claims made in the advertising media?," *Chiropr. Osteopat.*, vol. 15, p. 7, Jan. 2007.

[10] R. Zylbergold and M. Piper, "Cervical spine disorders: a comparison of three types of traction," *Spine (Phila. Pa. 1976).*, vol. 10, no. 10, pp. 867–871, 1985.

[11] C. Savva and G. Giakas, "The effect of cervical traction combined with neural mobilization on pain and disability in cervical radiculopathy. A case report.," *Man.*

Ther., vol. 18, no. 5, pp. 443–6, Oct. 2013.

[12] P. R. Harris, "Cervical traction. Review of literature and treatment guidelines," *Phys Ther*, vol. 57, no. 8, pp. 910–914, 1977.

[13] M. J. Murphy, "Effects of cervical traction on muscle activity.," *J. Orthop. Sports Phys. Ther.*, vol. 13, no. 5, pp. 220–225, 1991.

[14] A. Wong, C. Leong, and C. Chen, "The traction angle and cervical intervertebral separation," *Spine (Phila. Pa. 1976).*, vol. 17, no. 2, pp. 136–138, 1992.

[15] F. Ito and T. Kiyama, "Angular Factor in Intermittent Cervical Traction," *Sogo Rehabil.*, vol. 13, no. 3, pp. 213–218, 1985.

[16] D. C. W. Fater and T. W. Kernozek, "Comparison of cervical vertebral separation in the supine and seated positions using home traction units.," *Physiother. Theory Pract.*, vol. 24, no. 6, pp. 430–6, 2008.

[17] S. Akinbo, I. Danesi, and M. Abudu, "Comparison Of Supine And Sitting Positions Cervical Traction On Cardiovascular Parameters, Pain And Neck Mobility In Patients With Cervical Spondylosis.," *Internet J. Rheumatol.*, vol. 8, no. 1, pp. 1–11, 2013.

[18] M. M. Panjabi, "Cervical spine models for biomechanical research.," *Spine (Phila. Pa. 1976).*, vol. 23, no. 24, pp. 2684–2700, 1998.

[19] M. J. Fagan, S. Julian, and A. M. Mohsen, "Finite element analysis in spine research," *Proc. Inst. Mech. Eng. Part H J. Eng. Med.*, vol. 216, no. 5, pp. 281–298, 2002.

[20] M. G. Coutinho, "Dynamic Simulations of Multibody Systems". New York, NY: Springer; 2001.

[21] T. Merrill, W. Goldsmith, and Y. C. Deng, "Three-dimensional response of a lumped parameter head-neck model due to impact and impulsive loading," *J. Biomech.*, vol. 17, no. 2, pp. 81–95, 1984.

[22] M. de Jager, "Mathematical Head-Neck Models for Acceleration Impacts," *Thesis, Eindhoven Univ. Technol.*, p. 144, 1996.

[23] D. W. van Lopik and M. Acar, "Development of a multi-body computational model of human head and neck," Proc. Inst. Mech. Eng. Part K J. Multi-body Dyn., vol. 221, no. 2, pp. 175–197, 2007.

[24] H. Ahn and D. DiAngelo, "A biomechanical study of artificial cervical discs using computer simulation," *Spine (Phila. Pa. 1976).*, vol. 33, no. 8, pp. 883–892, 2008.

[25] M. J. van der Horst, Human Head Neck Response in Frontal, Lateral and Rear End

Impact Loading - modelling and validation -. 2002.

[26] N. Yoganandan, P. R. Walsh, and F. A. Pintar, "Human head-neck biomechanics under axial tension," vol. 1, no. 4, pp. 289–294, 1996.

[27] S. P. Moroney, A. B. Schultz, J. A. A. Miller, and G. B. J. Andersson, "Load-displacement properties of lower cervical spine motion segments," J. Biomech., vol. 21, no. 9, pp. 769–779, 1988.

[28] N. Yoganandan, S. Kumaresan, and F. A. Pintar, "Geometric and Mechanical Properties of Human Cervical Spine Ligaments," J. Biomechanical Eng., vol. 122, no. December, pp. 623–629, 2000.

[29] Anatomography/BodyParts3D. Copyright 2008. The Database Center for Life Science licensed under CC Attribution-Share Alike 2.1 Japan

[30] M. Nordin and V. H. Frankel, *Basic Biomechanics of the Musculoskeletal System*, 4th ed. Lippincott Williams & Wilkins, 2012.

[31] Herniated Disc Image. By Edave (Own work) [CC-BY-SA-3.0], Retrieved from http://commons.wikimedia.org/wiki/File:L4-l5-disc-herniation.png

[32] L. J. Haughie, I. M. Fiebert, and K. E. Roach, "Relationship of Forward Head Posture and Cervical Backward Bending to Neck Pain," *J. Man. Manip. Ther.*, vol. 3, no. 3, pp. 91–97, Jan. 1995.

[33] H. Gray and C. Clemente, *Anatomy of the human body*. Philadelphia: Lea & Febiger, 1985.

[34] Bullet Physics Library. Available: http://bulletphysics.org/

[35] Blender. Available: http://www.blender.org/

[36] E. Catto, "Modeling and Solving Constraints", 2009. Available: http://twvideo01.ubm-us.net/o1/vault/gdc09/slides/04-GDC09_Catto_Erin_Solver.pdf

[37] Vortex Dynamics (3.0) by CM LABS. Available: http://www.vxsim.com/

[38] P. De Leva, "[38]s to Zatsiorsky-Seluyanov's segment inertia parameters," *J. Biomech.*, vol. 29, no. 9, pp. 1223–1230, 1996.

[39] White III, A.A. and M.M. Panjabi. Clinical Biomechanics of the Spine. J.B. Lippincott Company, 2nd edition, 1990.

[40] L. Penning, "Functional anatomy of joints and discs," Cerv. Spine, pp. 33–56, 1989.

[41] J. Dvorak, M. M. Panjabi, J. E. Novotny, and J. A. Antinnes, "In vivo flexion/extension of the normal cervical spine," J. Orthop. Res., vol. 9, no. 6, pp. 828–834, 1991.

[42] H. van Mameren, H. Sanches, J. Beursgens, and J. Drukker, "Cervical Spine Motion in the Sagittal Plane II: Position of Segmental Averaged Instantaneous Centers of Rotation -A Cineradiographic Study," Spine (Phila. Pa. 1976)., vol. 17, no. 5, 1992.

[43] C. Dong, C. C. Loy, K. He, and X. Tang, "Image Super-Resolution Using Deep Convolutional Networks," *IEEE Trans. Pattern Anal. Mach. Intell.*, vol. 38, no. 2, pp. 295–307, 2014.

[44] V. M. Dabbs and L. G. Dabbs, "Correlation Between Disc Height Narrowing and Low-Back Pain," *Spine (Phila. Pa. 1976).*, vol. 15, no. 12, pp. 1366–9, 1990.

[45] D. E. Martins *et al.*, "Correlations between radiographic, magnetic resonance and histological examinations on the degeneration of human lumbar intervertebral discs," *Sao Paulo Med. J.*, vol. 128, no. 2, pp. 63–8, 2010.

[46] ImageJ 1.51. Available: https://imagej.nih.gov/ij/

[47] Inkscape 0.91. Available: https://inkscape.org/en/

[48] S. J. Ferguson and T. Steffen, "Biomechanics of the aging spine," *Eur. Spine J.*, vol. 12, no. Suppl. 2, pp. S97–S103, 2003.

[49] L. K. F. Wong, Z. Luo, and N. Kurusu, "Dynamic simulation of cervical traction therapy: Comparison between sitting and inclined positions," in *2014 IEEE International Conference on Robotics and Biomimetics, ROBIO 2014*, 2014, pp. 167–172.

[50] D. X. Leite, J. M. M. Vieira, V. O. C. Carvalhais, V. L. Araújo, P. L. P. Silva, and S. T. Fonseca, "Relationship between joint passive stiffness and hip lateral rotator concentric torque.," Rev. Bras. Fisioter., vol. 16, no. 5, pp. 414–21, 2012.

Publications

L. K. F. Wong, Z. Luo, and N. Kurusu, "Dynamic simulation of cervical traction therapy: Comparison between sitting and inclined positions," in *2014 IEEE International Conference on Robotics and Biomimetics, ROBIO 2014*, 2014, pp. 167–172.

L. K. F. Wong, Z. Luo, N. Kurusu, and K. Fujino, "Comparative experiment and dynamic simulation on cervical traction therapy," in *2016 IEEE International Conference on Robotics and Biomimetics, ROBIO 2016*, 2016, pp. 39–44.

L. K. F. Wong, Z. Luo, and N. Kurusu, "The Effect of Traction Position in Cervical Traction Therapy Based on Dynamic Simulation Models," *J. Biomed. Sci. Eng.*, vol. 10, no. 5, pp. 243–256, 2017.

L. K. F. Wong, Z. Luo, N. Kurusu, and K. Fujino, "Experiment and Dynamic Simulation of Cervical Tractions in Inclined and Sitting Positions," *Open J. Ther. Rehabil.*, vol. 5, no. 3, pp. 83–97, 2017.

L. K. F. Wong, Z. Luo, N. Kurusu, and K. Fujino, "Improvement of Multi-body Simulation Model for Comparative Study of Cervical Traction Therapy – Comparison between Inclined and Sitting Traction," in *2018 IEEE International Conference on Robotics and Biomimetics, ROBIO 2018*, 2018, pp. 150–155.

L. K. F. Wong, Z. Luo, N. Kurusu, and K. Fujino, "A multi-body model for comparative study of cervical traction simulation – development, improvement and validation (part 1)," (submitted to Computer Methods in Biomechanics and Biomedical Engineering, under review)

L. K. F. Wong, Z. Luo, N. Kurusu, and K. Fujino, "A multi-body model for comparative study of cervical traction simulation – comparison between inclined

and sitting traction (part 2)," (submitted to Computer Methods in Biomechanics and Biomedical Engineering, under review)

Acknowledgements

I would like to thank my academic advisor, Professor Zhiwei Luo for giving me the opportunity to work on this project and for his guidance and encouragement through the learning process of my study in Kobe University. I would like to express my gratitude to Professor Akira Kageyama and Professor Makoto Tsubokura for their valuable advices in the review process.

I would also like to express my gratitude to Mr. Nobuyuki Kurusu and his team of engineers from Minato Medical Science Co. Ltd. and Dr. Keiji Fujino from Fujino Orthopedics Hospital for their tremendous support and advices along the way.

Finally, I would like to thank my parents, who have always supported me over the years, by keeping me harmonious and helping me putting pieces together. Above all, I would like to express my most appreciation to my wife for her tremendous love, support and understanding throughout the years.

Doctor Thesis, Kobe University

"Multi-body Simulation of Cervical Traction Therapy", 109 pages

Submitted on January, 21, 2019

The date of publication is printed in cover of repository version published in Kobe University Repository Kernel.